STUDY OF NONLINEAR EVOLUTION EQUATIONS WITH VARIABLE COEFFICIENTS FOR SOLITARY WAVE SOLUTIONS

A THESIS

Submitted to the

FACULTY OF SCIENCE

PANJAB UNIVERSITY, CHANDIGARH

for the degree of

DOCTOR OF PHILOSOPHY

2013

AMIT GOYAL

DEPARTMENT OF PHYSICS

CENTRE OF ADVANCED STUDY IN PHYSICS

PANJAB UNIVERSITY

CHANDIGARH, INDIA

This thesis is dedicated to my family,
friends & teachers
for their love, endless support
and encouragement.

Acknowledgements

First and foremost, I would like to express my gratitude to my supervisors Prof. C. Nagaraja Kumar and Dr. Sunita Srivastava, Department of Physics, Panjab University, Chandigarh for being such an inspiration to me. I am extremely grateful to Prof. C. Nagaraja Kumar for his continuous encouragement, generous and expert guidance throughout the course of my research work. I am indebted to Prof. P. K. Panigrahi and Dr. T. Soloman Raju for useful suggestions and cooperation throughout this work.

I express my thanks to the Chairman, Department of Physics, Panjab University for providing me the required facilities in the department. I am highly grateful to Prof. Manjit Kaur, Prof. D. Mehta, Prof. K. Tankeshwar, Dr. Kuldip Kumar and Dr. Samarjit Sihotra for their cooperation and help as and when required. I am also thankful to all the staff members of Department of Physics, Panjab University for all type of help during this work.

I am fortunate to have the company and help of my lab members Alka, Jasvinder, Rama, Vivek, Shally, Harleen, Kanchan for completion of various research projects. I am thankful to Rama for enlightening discussions and useful suggestions on different aspects of my research problems. I am grateful for the generous funding provided by the CSIR, Govt. of India over the period of my research work.

I would like to thank my friends for keeping me sane and happy. I am privileged for having the company of Surender, Gurjeet, Gurpreet, Vicky, Jasvinder, Vishal, Gurjot, Vipen, Raman, Janpreet, Bharti, Rohit, Ranjeet and Sandeep who have provided a joyful environment during all these years in Panjab University. Special thanks go to Kaushal for the trekking trip of a lifetime, Amitoj and Maneesh for making sure my weekends were not squandered on work, and Shivank, Nitin, Ashish, Atul, Sumali, Richa for long and entertaining discussions.

I am deeply indebted to my parents for all the achievements in my life. I am grateful to my parents for all their blessings and bhabhi Nidhi and Deepti, nephew Tanishq for their constant affection and care. I would like to say an extra-special thankyou to my brothers Neeraj and Bhupesh for being my companion down the years. Finally, I would like to acknowledge all the people, whoever helped me directly or indirectly in successful completion of my Ph.D. thesis work.

Date: **(Amit Goyal)**

Abstract

This thesis deals with the investigation of solitary wave or soliton-like solutions for nonlinear evolutions equations of physical interest. In general, the nonlinear evolution equations possess spatially and/or temporally varying coefficients because most of physical and biological systems are inhomogeneous due to fluctuations in environmental conditions and non-uniform media.

There has been considerable interest, experimentally as well as theoretically, in the use of tapered graded index waveguides in optical communication systems, as it helps in maximizing light coupled into optical waveguides. We investigate the effects of modulated tapering profiles on the intensity of self-similar waves, including bright and dark similaritons, self-similar Akhmediev breathers and self-similar rogue waves, propagating through tapered graded index waveguide. In this regard, we present a systematic analytical approach, invoking isospectral Hamiltonian technique, which enables us to identify a large manifold of allowed tapering profiles. It finds that the intensity of self-similar waves can be made very large for specific choice of tapering profile and thus paving the way for experimental realization of highly energetic waves in nonlinear optics.

Two photon absorption (TPA) is an area of research that has been attracting scientific interest over several decades. It is a nonlinear process which is accompanied by an enhanced nonlinear absorption coefficient of the material and thus finds applications in all-optical processes. This thesis shows results of the effect of TPA on soliton propagation in a nonlinear optical medium. We find that localized gain exactly balance the losses due to TPA and results into chirped optical solitons for arbitrary value of TPA coefficient.

We study a prototype model for the reaction, diffusion and convection processes with inhomogeneous coefficients. Employing auxiliary equation method, the kink-type solitary wave solutions have been found for variable coefficient Burgers- Fisher and Newell-Whitehead-Segel equations. The soliton-like solutions of complex Ginzburg-Landau equation can be stabilized either by adding quintic term to it or by using a external ac-source. We consider the complex Ginzburg-Landau equation driven by external source and solved it to obtain exact periodic and soliton solutions. The reported soliton solutions are necessarily of the kink-type and Lorentzian-type containing hyperbolic and pure cnoidal functions.

Contents

List of Figures

Chapter 1

Introduction

In past few decades, modern theories of nonlinear science have been widely developed to understand the challenging aspects of nonlinear nature of the systems. The nonlinear science has evolved as a dynamic tool to study the mysteries of complex natural phenomena. In general, nonlinear science is not a new subject or branch of science, although it delivers significantly a new set of concepts and remarkable results. Unlike quantum physics and relativity, it encompasses systems of different scale and objects moving with any velocity. Hence, due to feasibility of nonlinear science on every scale, it is possible to study same nonlinear phenomena in very distinct systems with the corresponding experimental tools. The whole field of nonlinear science can be divided into six categories, viz., fractals, chaos, solitons, pattern formation, cellular automata, and complex systems. The general theme underlying the study of nonlinear systems is nonlinearity present in the system.

Nonlinearity is exciting characteristic of nature which plays an important role in dynamics of various physical phenomena [1, 2], such as in nonlinear mechanical vibrations, population dynamics, electronic circuits, laser physics, astrophysics (e.g planetary motions), heart beat, nonlinear diffusion, plasma physics, chemical reactions in solutions, nonlinear wave motions, time-delay processes etc. A system is called nonlinear if its output is not proportional to its input. For example, a dielectric material behaves nonlinearly if the output field intensity is no longer pro-

portional to the input field intensity. For most of the real systems, nonlinearity is more regular feature as compared to the linearity. In general, all natural and social systems behave nonlinearly if the input is large enough. For example, the behavior of a spring and a simple pendulum is linear for small displacements. But for large displacements both of them act as nonlinear systems. A system has a very different dynamics mechanism in its linear and nonlinear regimes.

Most of the nonlinear phenomena are modelled by nonlinear evolution equations (NLEEs) having complex structures due to linear and nonlinear effects. The advancement of high-speed computers, and new techniques in mathematical softwares and analytical methods to study NLEEs with experimental support has stimulated the theoretical and experimental research in this area. The investigation of the exact solutions, like solitary wave and periodic, of NLEEs play a vital role in description of nonlinear physical phenomena. The wave propagation in fluid dynamics, plasma, optical and elastic media are generally modelled by bell-shaped and kink-shaped solitary wave solutions. The existence of exact solutions, if available, to NLEEs help in verification of numerical analysis and are useful in the study of stability analysis of solutions. Moreover, the search of exact solitary wave solutions led to the discovery of new concepts, such as solitons, rogue waves, vortices, dispersion-managed solitons, similaritons, supercontinuum generation, modulation instability, complete integrability, etc.

1.1 Solitary waves and solitons: Properties and applications

Solitary wave: A solitary wave is a non-singular and localized wave which propagates without change of its properties (shape, velocity etc.). It arises due to delicate balance between nonlinear and dispersion effects of a medium.

Soliton: A soliton is a self-reinforcing solitary wave solution of a NLEE which

- represents a wave of permanent form.

- is localized, so that it decays or approaches a constant value at infinity.
- is stable against mutual collisions with other solitons and retains its identity.

Physically it can be seen as, if two solitons with different amplitudes (hence with different speeds) are kept far apart such that the taller (faster) wave is on left of the shorter (slower) wave. After some time, the taller one ultimately catches up the shorter one and crosses it. When this happens, both of them undergo a nonlinear interaction and evolve from interaction absolutely preserving their shape and speed, as shown in Fig. 1.1.

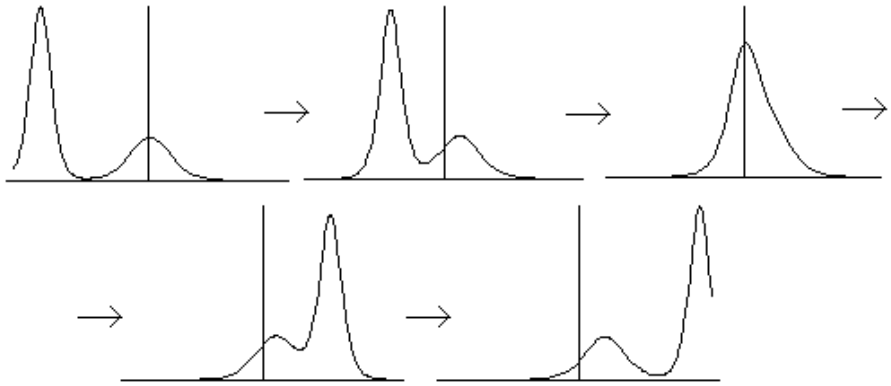

Figure 1.1: Collision of solitons

History

The concept of solitary wave was first introduced in the field of hydrodynamics by Scottish Engineer John Scott Russell in 1834. He observed a peculiar water wave in the narrow union canal near Edinburgh while he was conducting experiments to determine the most efficient design for canal boats. He called it as a "wave of translation" which propagates for miles before losing in the meanders of the canal. Subsequently, Russell performed experiments in his laboratory to study this phenomena more carefully and he made two key discoveries

1. The existence of solitary waves which are long and shallow water waves of permanent form.

2. The speed of propagation, v, of solitary wave in a channel is given by

$$v = \sqrt{g(h+\eta)},$$

where η is the amplitude of wave, h is the depth of channel and g is the force due to gravity.

In 1844, Russell published his work on wave of translation, latter known as solitary wave, in "British Association Reports". This phenomena attracted a considerable attention of other scientists including Airy (1845), Stokes (1847) and Boussinesq (1871, 1872). But the theoretical basis for this phenomenon was given by two Dutch physicists, Korteweg and de Vries in 1895, who presented a nonlinear evolution equation, known as KdV equation, for the evolution of long waves in a shallow one-dimensional water channel which admits solitary wave solution. In 1965, Zabusky and Kruskal [3] solved the KdV equation numerically as a model for nonlinear lattice and found that solitary wave solutions interacted elastically with each other. Due to this particle-like property, they termed these solitary wave solutions as solitons.

After that, the concept of soliton was accepted in general and soon Gardner *et al.* in 1967 reported the existence of multi-soliton solutions of KdV equation using inverse scattering method [4]. One year later, Lax generalized these results and proposed the concept of Lax pair [5]. Zakharov and Shabat [6] used the same method to obtain exact solutions for nonlinear Schrödinger equation. Hirota [7] introduced a new method, known as Hirota direct method, to solve the KdV equation for exact solutions for multiple collision of solitons. In 1974, Ablowitz *et al.* [8] showed that inverse scattering method is analog of the Fourier transform and used it to solve a wide range of new equations, such as the modified KdV equation, the nonlinear Schrödinger equation, and the classical sine-Gordon equation. These techniques stimulated the study of soliton theory in various fields such as optical communications, molecular biology, chemical reactions, oceanography etc.

Properties of solitons

Solitons have various interesting features, some of which are given below:

- ***Integrability***: Before the concept of soliton, it was believed that a nonlinear partial differential equation can not be solved exactly. But with the progress of soliton theory, multi-solitons have been found for NLEEs using inverse scattering transform, Lax pair, or Hirota techniques, which assures the integrability of NLEEs. Integrability is a mathematical property which can be used to obtain more predictive power and qualitative information to understand the dynamics of system locally and globally because for integrable systems, governing equation of motion is exactly solvable in terms of elementary functions which are analytic. So, nature of system is known at every instant of time and globally. Hence, it gives us a tremendous "window" into what is possible in nonlinearity.

- ***Particle-like behavior***: Solitons are localized waves which propagate without spreading. They retain their shape after collisions and are also robustly stable against the perturbations. This particle-like behavior of solitons has applications in explaining various nonlinear systems. However, there is no general well developed quantum theory which considers particle as soliton. But on macroscopic scale, the theory of propagation of waves in optics communications and in oceans are well defined using the concept of solitons.

- ***Nonlinear superposition***: For linear equations, new solutions could be found from the known solutions using superposition principle, according to which the linear combination of two or more solutions is again a solution of the considered equation. However, for NLEEs there was no analogue of this principle until the solitons had been discovered. But, the existence of multi-soliton solutions can be viewed as asymptotic (nonlinear) superposition of separated solitary waves. Hence, it leads to a recognition that there is a nonlinear superposition principle as well.

Applications

Solitons have various practical applications due to their interesting properties. Solitons and solitary waves appear in almost all branches of physics, such as hydrodynamics, plasma physics, nonlinear optics, condensed matter physics, nuclear physics, particle physics, low temperature physics, biophysics and astrophysics. Some of their applications are described below:

- ***Fluid dynamics***: Solitary waves are very useful to study the fluid dynamical problems. Russell's "wave of translation" was a water-wave soliton, and Korteweg and de Vries presented the KdV equation to study the propagation of shallow water waves. Zakharov [9] proposed another nonlinear model, known as nonlinear Schrödinger equation (NLSE), to study the occurrence of solitary waves in deep water oceans. Then, with the advent of rational solutions to NLSE, it was proposed that large amplitude freak waves (or rogue waves) also behave as solitary waves [10]. In plasma physics, the propagation of waves has been modeled similar to the solitons on a liquid surface [11]. Washimi and Taniuti [12] studied the transmission of ion-acoustic waves in cold plasma by using the KdV model. Afterwards, a large variety of soliton solutions have been studied in plasma physics [13], which are useful in the description of different models of strong turbulence theory.

- ***Nonlinear optics***: Solitons have much importance in the study of optical communication through the optical fiber because soliton pulses can be used as the digital information carrying 'bits' in optical fibers. The main prospects of optical soliton communication is that it can propagate without distortion over long distances and it enables high speed communication [14]. The concept of optical solitons originated in 1973 and was experimentally verified in 1980. They are formed due to dynamic balance between group velocity dispersion and the nonlinearity due to Kerr effect [15]. Apart from communications, optical solitons are also found useful in the construction of optical switches, logic gates, fiber lasers and pulse compression or amplification processes.

- ***Bose-Einstein condensates***: The process of Bose-Einstein condensation was first predicted by Bose and Einstein in 1924. It was shown that, at very low temperatures, a finite fraction of particles in a dilute boson gas condenses into the same quantum (ground) state, known as the Bose-Einstein condensate (BEC). In 1995, BECs were realized experimentally when atoms of dilute alkali vapors were confined in a magnetic trap and cooled down to extremely low temperature, of the scale of fractions of microkelvins [16, 17]. In BECs, nonlinearity arises due to the interatomic interactions which describes the existence of nonlinear waves, such as solitons and vortices. Hence, these matter-wave solitons can be viewed as nonlinear excitations of BECs [18]. Recently, the existence of matter rogue waves has also been predicted analytically in BECs [19].

- ***Josephson junctions***: A Josephson junction is an electronic circuit which is made up of two weakly coupled superconductors, separated by a non-conducting layer thin enough to permit passage of electrons through this insulating barrier. In Josephson junction, solitary wave theory can be studied as the propagation of electromagnetic wave between the two strips of superconductors [20, 21]. Solitons in long Josephson junction are called fluxons because each soliton contains one quantum of magnetic flux. Such junctions are found to be useful in the production of quantum-mechanical circuits such as superconducting quantum interference devices (SQUIDs).

- ***Biophysics***: Solitary wave formulation is also useful in explaining various biophysical processes. The Davydov soliton acts as a energy carrier in hydrogen-bonded spines which stabilize protein α-helices [22]. These soliton structures show the excited states of amide-I and connected hydrogen bond distortions. Solitary waves also arise in the study of nonlinear dynamics of DNA [23] and play an important role in the explanation of various processes undergone by the DNA double helix, such as transcription, duplication and denaturation [24].

- ***Field theory***: Solitons and their relative, such as instantons, play a vital role in understanding of both classical and quantum field theory [25]. Various forms of topological solitons such as monopoles, kinks, vortices, and skyrmions are important in the study of field theory. In quantum field theory, topological solitons of the sine-Gordon equation can be considered as fundamental excitations of the Thirring model.

1.2 Nonlinear evolution equations

Nonlinear evolution equations (NLEEs) arise throughout the nonlinear sciences as a dynamical description (both in time and space dimensions) to the nonlinear systems. NLEEs are very useful to describe various nonlinear phenomena of physics, chemistry, biology and ecology, such as fluid dynamics, wave propagation, population dynamics, nonlinear dispersion, pattern formation etc. Hence, NLEEs evolved as a useful tool to investigate the natural phenomena of science and technology. A NLEE is represented by a nonlinear partial differential equation (PDE) which contains a dependent variable (the unknown function) and its partial derivatives with respect to the independent variables. In literature, there are many NLEEs to describe various physical phenomena. Some of the well-known NLEEs which are of great interest are given below:

- ***KdV equation***: The KdV type equations have been the most important class of NLEE's, with numerous application in physical sciences and engineering. The KdV equation is given by

$$u_t + \alpha u u_x + u_{xxx} = 0. \tag{1.1}$$

  This equation was introduced by Korteweg and de Vries to study the propagation of shallow water waves. It represents the longtime evolution of wave phenomena in which the steepening effect of nonlinear term is counterbalanced by broadening effect of dispersion. KdV equation can be used to understand

the properties of many physical systems which are weekly nonlinear and weakly dispersive, e.g., nonlinear electric lines, blood pressure waves, internal waves in oceanography, ion-acoustic solitons in plasma etc.

- ***Nonlinear Schrödinger equation***: The nonlinear Schrödinger equation (NLSE) is very important in many branches of physics and is represented by

$$iu_t + u_{xx} + k|u|^2 u = 0. \tag{1.2}$$

This equation has been used to describe the wave propagation in nonlinear optics and quantum electronics, Langmuir waves in plasma, deep water waves, and propagation of heat pulses in solids. In $(1 + 1)$ dimensions, NLSE with nonlinear gain and spectral filtering is related to the complex Ginzburg-Landau equation (CGLE) which appear in the phenomenon of superconductivity.

- ***Sine-Gordon equation***: The sine-Gordon equation is a nonlinear hyperbolic partial differential equation. It was introduced by Frenkel and Kontorova in 1939 in the study of crystal dislocations. A mechanical model of the sine-Gordon equation consists of a chain of heavy pendula coupled to each other through a spring and constrained to rotate around a horizontal axis [20]. The equation reads

$$u_{tt} - u_{xx} = \sin u. \tag{1.3}$$

The sine-Gordon equation arises in many fields, such as propagation of dislocations in crystal lattices, Bloch wall motion of magnetic crystals, a unitary theory of elementary particles, nonlinear dynamics of DNA, in studying properties of Josephson junctions, charge density waves, liquid helium etc.

- ***Nonlinear reaction diffusion equation***: Reaction diffusion equations are the mathematical models of those physical or biological systems in which the concentration of one or more substances distributed in space varies under the effect of two processes: reaction and diffusion. Nonlinear reaction diffusion equations (NLRD), with convective term or without it, have attracted con-

siderable attention, as it can be used to model the evolution systems in real world. The general form of NLRD type equations is

$$u_t + vu^m u_x = Du_{xx} + \alpha u - \beta u^n. \tag{1.4}$$

NLRD equations plays an important role in the qualitative description of many phenomena such as flow in porous media, heat conduction in plasma, chemical reactions, population genetics, image processing and liquid evaporation.

1.3 Inhomogeneous nonlinear evolution equations

In the study of NLEEs as a model to an actual physical system, it is generally essential to consider the factors causing deviation from the actual system, originating due to the dissipation, environmental fluctuations, spatial modulations and other forces. In order to consider some or all of these factors, it is necessary to add the appropriate perturbing terms in NLEEs. Hence, inhomogeneous NLEEs are more realistic to study the dynamics of physical systems.

1.3.1 NLEEs with variable coefficients

The physical phenomena in which NLEEs with constant coefficients arise tend to be highly idealized. But for most of the real systems, the media may be inhomogeneous and the boundaries may be nonuniform, e.g., in plasmas, superconductors, optical fiber communications, blood vessels and Bose-Einstein condensates. Therefore, the NLEEs with variable coefficients are supposed to be more realistic than their constant-coefficient counterparts in describing a large variety of real nonlinear physical systems. Some phenomena which are governed by variable coefficient NLEEs, are given as

- In a real optical fiber transmission system, there always exist some nonuniformities due to the diverse factors that include the variation in the lattice parameters of the fiber media and fluctuations of the fiber's diameter. There-

fore, in real optical fiber, the transmission of soliton is described by the NLSE with variable coefficients [26]. Sometimes, the optical waveguide is tapered along the waveguide axis to improve the coupling efficiency between fibers and waveguides in order to reduce the reflection losses and mode mismatch. The propagation of beam through tapered graded-index nonlinear waveguides is governed by the inhomogeneous NLSE [27].

- The evolution equation for the propagation of weakly nonlinear waves in shallow water channels of variable depth and width and also in plasmas having inhomogeneous properties of media, is obtained as a variable coefficient KdV equation [28, 29].

- The dynamics of the matter wave solitons in BEC can be controlled through artificially inducing the inhomogeneities in system [30]. It has been achieved by varying the space distribution of the atomic two-body scattering length using optical methods, such as the optically induced Feshbach resonance [31]. The dynamical behavior of inhomogeneous BEC is described by the variable coefficient Gross-Pitaevskii equation also known as generalized nonlinear Schrödinger equation (GNLSE).

- Generally, the NLRD systems are inhomogeneous due to fluctuations in environmental conditions and nonuniform media. It makes the relevant parameters space or time dependent because external factors make the density and/or temperature change in space or time [32, 33].

- To describe waves in an energetically open system with a monotonically varying external field, sine-Gordon equation with dissipation and variable coefficient on the nonlinear term is considered [34].

1.3.2 NLEEs in the presence of external source

To control the dynamics of a nonlinear system, it is essential to investigate the effects of dissipation, noise and external force on the system. Dissipation leads to loss

of energy and hence affects the dynamics of system under consideration, whereas the external tunable driving acts as a source of energy and helps in stabilizing the dynamical system. Barashenkov *et al.* [35] considered the parametrically driven damped NLSE and showed the existence of stable solitons only if the strength of the driving force would be more than the damping constant. The studies of ac-driven NLSE date back to the works of Malomed *et al.* [36, 37] and Cohen [38]. Recently, works on forced NLSE is attracting much attention [39, 40, 41, 42], as it arises in many physical problems, such as the plasmas driven by rf-fields, pulse propagation in twin-core fibers, charge density waves with external electric field, double-layer quantum Hall (pseudo) ferromagnets, etc. (see [39], and references therein). The ac-driven sine-Gordon equation which arises in the study of DNA dynamics and Josephson junction under external field has been studied analytically and numerically (see [43], and references therein). The external feedback also helps in controlling the diffusion induced amplitude and phase turbulence (or spatiotemporal) in CGLE systems [44, 45, 46].

1.4 Outline of thesis

The layout of the thesis is as follows.

In Chapter 2, the discussion begins with the derivation of NLSE followed by introduction of generalized NLSE for wave propagation in tapered graded-index waveguides and a short overview of isospectral Hamiltonian approach. We present a large family of self-similar waves by tailoring the tapering function, through Riccati parameter, in a tapered graded-index nonlinear waveguide amplifier. It has been achieved using a systematic analytical approach which provides a handle to find analytically a wide class of tapering function and thus enabling one to control the self-similar wave structure. This analysis has been done for the sech^2-type tapering profile in the presence of only cubic nonlinearity and also for cubic-quintic nonlinearity. Further, we show the existence of bright and dark similaritons in a parametrically controlled parabolic tapered waveguide.

Chapter 3 deals with the effect of two-photon absorption (TPA) on soliton propagation in a nonlinear optical medium. It is demonstrated that nonlinear losses due to TPA are exactly balanced by localized gain and induces the optical solitons in nonlinear optical medium. We present a class of chirped soliton solutions in different parameter regimes with corresponding chirp and gain profiles.

Chapter 4 shows the existence of solitary wave solutions for two nonlinear systems in the presence of inhomogeneous conditions. In first section, we consider the nonlinear reaction diffusion type equations with variable coefficients and obtain propagating kink-type solitary wave solutions by using the auxiliary equation method. The second section of this chapter deals with the study of dynamics of the complex Ginzburg-Landau equation (CGLE) in the presence of ac-source. We consider that external force is out of phase with the complex field and present Lorentzian-type and kink-type soliton solutions for this model.

In conclusion, Chapter 5 discusses the results obtained in the preceding chapters and provides a summary of key findings.

Bibliography

[1] S Strogatz. *Nonlinear dynamics and chaos: With applications to physics, biology, chemistry and engineering.* Perseus Books Group, 2001.

[2] M Lakshmanan and S Rajaseekar. *Nonlinear dynamics: Integrability, chaos and patterns.* Springer, 2003.

[3] NJ Zabusky and MD Kruskal. Interaction of "solitons" in a collisionless plasma and the recurrence of initial states. *Physical Review Letters*, 15(6):240, 1965.

[4] CS Gardner, JM Greene, MD Kruskal, and RM Miura. Method for solving the Korteweg-de Vries equation. *Physical Review Letters*, 19:1095–1097, 1967.

[5] PD Lax. Integrals of nonlinear equations of evolution and solitary waves. *Communications on Pure and Applied Mathematics*, 21(5):467–490, 1968.

[6] AB Shabat and VE Zakharov. Exact theory of two-dimensional self-focusing and one-dimensional self-modulation of waves in nonlinear media. *Soviet Physics JETP*, 34:62–69, 1972.

[7] R Hirota. Exact solution of the Kortewegde Vries equation for multiple collisions of solitons. *Physical Review Letters*, 27(18):1192–1194, 1971.

[8] MJ Ablowitz, DJ Kaup, AC Newell, and H Segur. The inverse scattering transform-fourier analysis for nonlinear problems. *Studies in Applied Mathematics*, 53:249–315, 1974.

[9] VE Zakharov. Stability of periodic waves of finite amplitude on the surface of a deep fluid. *Journal of Applied Mechanics and Technical Physics*, 9(2):190–194, 1968.

[10] DH Peregrine. Water waves, nonlinear Schrödinger equations and their solutions. *The Journal of the Australian Mathematical Society*, 25(01):16–43, 1983.

[11] RZ Sagdeev. Cooperative phenomena and shock waves in collisionless plasmas. *Reviews of Plasma Physics*, 4:23, 1966.

[12] H Washimi and T Taniuti. Propagation of ion-acoustic solitary waves of small amplitude. *Physical Review Letters*, 17(19):996, 1966.

[13] EA Kuznetsov, AM Rubenchik, and VE Zakharov. Soliton stability in plasmas and hydrodynamics. *Physics Reports*, 142(3):103–165, 1986.

[14] A Hasegawa. An historical review of application of optical solitons for high speed communications. *Chaos: An Interdisciplinary Journal of Nonlinear Science*, 10(3):475–485, 2000.

[15] YS Kivshar and GP Agrawal. *Optical solitons: from fibers to photonic crystals*. Academic Press, London, 2003.

[16] MH Anderson, JR Ensher, MR Matthews, CE Wieman, and EA Cornell. Observation of Bose–Einstein condensation in a dilute atomic vapor. *Science*, 269(5221):198–201, 1995.

[17] KB Davis, MO Mewes, MR Van Andrews, NJ Van Druten, DS Durfee, DM Kurn, and W Ketterle. Bose-Einstein condensation in a gas of sodium atoms. *Physical Review Letters*, 75(22):3969, 1995.

[18] R Carretero-González, DJ Frantzeskakis, and PG Kevrekidis. Nonlinear waves in Bose–Einstein condensates: Physical relevance and mathematical techniques. *Nonlinearity*, 21(7):R139, 2008.

[19] YV Bludov, VV Konotop, and N Akhmediev. Matter rogue waves. *Physical Review A*, 80(3):033610, 2009.

[20] A Barone, F Esposito, CJ Magee, and AC Scott. Theory and applications of the sine-Gordon equation. *La Rivista del Nuovo Cimento*, 1(2):227–267, 1971.

[21] DK Campbell, S Flach, and YS Kivshar. Localizing energy through nonlinearity and discreteness. *Physics Today*, 57(1):43–49, 2004.

[22] A Scott. Davydov's soliton. *Physics Reports*, 217(1):1–67, 1992.

[23] W Alka, A Goyal, and CN Kumar. Nonlinear dynamics of DNA–Riccati generalized solitary wave solutions. *Physics Letters A*, 375(3):480–483, 2011.

[24] M Peyrard. Nonlinear dynamics and statistical physics of DNA. *Nonlinearity*, 17(2):R1, 2004.

[25] R Rajaraman. *Solitons and instantons: an introduction to solitons and instantons in quantum field theory*. North-Holland Amsterdam, 1982.

[26] VI Kruglov, AC Peacock, and JD Harvey. Exact self-similar solutions of the generalized nonlinear Schrödinger equation with distributed coefficients. *Physical Review Letters*, 90(11):113902, 2003.

[27] SA Ponomarenko and GP Agrawal. Optical similaritons in nonlinear waveguides. *Optics Letters*, 32(12):1659–1661, 2007.

[28] ZZ Nong. On the KdV-type equation with variable coefficients. *Journal of Physics A: Mathematical and General*, 28(19):5673, 1995.

[29] W Hong and YD Jung. Auto–Bäcklund transformation and analytic solutions for general variable-coefficient KdV equation. *Physics Letters A*, 257(3):149–152, 1999.

[30] FK Abdullaev, A Gammal, and L Tomio. Dynamics of bright matter-wave solitons in a Bose–Einstein condensate with inhomogeneous scattering length. *Journal of Physics B: Atomic, Molecular and Optical Physics*, 37(3):635, 2004.

[31] FK Fatemi, KM Jones, and PD Lett. Observation of optically induced feshbach resonances in collisions of cold atoms. *Physical Review Letters*, 85(21):4462, 2000.

[32] KI Nakamura, H Matano, D Hilhorst, and R Schätzle. Singular limit of a reaction-diffusion equation with a spatially inhomogeneous reaction term. *Journal of Statistical Physics*, 95(5-6):1165–1185, 1999.

[33] C Sophocleous. Further transformation properties of generalised inhomogeneous nonlinear diffusion equations with variable coefficients. *Physica A: Statistical Mechanics and its Applications*, 345(3):457–471, 2005.

[34] EL Aero. Dynamic problems for the sine-Gordon equation with variable coefficients: Exact solutions. *Journal of Applied Mathematics and Mechanics*, 66(1):99–105, 2002.

[35] IV Barashenkov, MM Bogdan, and VI Korobov. Stability diagram of the phase-locked solitons in the parametrically driven, damped nonlinear Schrödinger equation. *Europhysics Letters*, 15(2):113, 1991.

[36] D Cai, AR Bishop, N Grønbech-Jensen, and BA Malomed. Bound solitons in the ac-driven, damped nonlinear Schrödinger equation. *Physical Review E*, 49(2):1677, 1994.

[37] BA Malomed. Bound solitons in a nonlinear optical coupler. *Physical Review E*, 51(2):R864, 1995.

[38] G Cohen. Soliton interaction with an external traveling wave. *Physical Review E*, 61(1):874, 2000.

[39] IV Barashenkov and EV Zemlyanaya. Travelling solitons in the externally driven nonlinear Schrödinger equation. *Journal of Physics A: Mathematical and Theoretical*, 44(46):465211, 2011.

[40] TS Raju and PK Panigrahi. Optical similaritons in a tapered graded-index nonlinear-fiber amplifier with an external source. *Physical Review A*, 84(3):033807, 2011.

[41] F Cooper, A Khare, NR Quintero, FG Mertens, and A Saxena. Forced nonlinear Schrödinger equation with arbitrary nonlinearity. *Physical Review E*, 85(4):046607, 2012.

[42] FG Mertens, NR Quintero, and AR Bishop. Nonlinear Schrödinger solitons oscillate under a constant external force. *Physical Review E*, 87(3):032917, 2013.

[43] NR Quintero and A Sánchez. ac driven sine-Gordon solitons: dynamics and stability. *The European Physical Journal B-Condensed Matter and Complex Systems*, 6(1):133–142, 1998.

[44] D Battogtokh and A Mikhailov. Controlling turbulence in the complex Ginzburg-Landau equation. *Physica D: Nonlinear Phenomena*, 90(1):84–95, 1996.

[45] TS Raju and K Porsezian. On solitary wave solutions of ac-driven complex Ginzburg–Landau equation. *Journal of Physics A: Mathematical and General*, 39(8):1853, 2006.

[46] JBG Tafo, L Nana, and TC Kofane. Time-delay autosynchronization control of defect turbulence in the cubic-quintic complex Ginzburg-Landau equation. *Physical Review E*, 88(3):32911, 2013.

Chapter 2

Controlled self-similar waves in tapered graded-index waveguides

2.1 Introduction

There has been considerable interest, experimentally as well as theoretically, in the use of tapered graded-index waveguides in optical communication systems. The reason behind this is the potential applications achievable through the tapering effect. It helps in maximizing light coupled into optical fibers, and integrated-optic devices and waveguides by reducing the reflection losses and mode mismatch. Nowadays work is being done on the study of the propagation of the self-similar waves in the tapered graded-index waveguides. Self-similar waves are the waves which maintain their shape but the amplitude and width changes with the modulating system parameters such as dispersion, nonlinearity, and gain. Hence, these waves are of interest for various applications in ultra fast optics.

In this chapter, a large family of self-similar waves is presented by tailoring the tapering function, through Riccati parameter, in a tapered graded-index nonlinear waveguide amplifier. It has been achieved using a analytical approach, known as isospectral Hamiltonian approach, which provides a handle to find analytically a

wide class of tapering function and thus enabling one to control the self-similar wave structure. First this analysis is done for bright and dark similaritons, and also for self-similar Akhmediev breathers and rogue waves in a cubic nonlinear medium. Then this formalism is extended to cubic-quintic nonlinear medium by presenting the double-kink and Lorentzian-type similaritons. The discussion begins with the wave propagation equation in optical waveguides, referred as nonlinear Schrödinger equation (NLSE), which is followed by wave propagation in tapered waveguides and also self-similar solutions for generalized NLSE. Then a short introduction of isospectral Hamiltonian approach is given before presenting the main work.

2.2 Wave propagation in optical waveguides

In recent years, a lot of work has been done in the field of nonlinear optics for the advancement of optical technologies like telecommunications, information storage etc.. For a better understanding of nonlinear optical systems, it is necessary to study the propagation of electromagnetic waves in optical waveguides. An optical waveguide is a general structure in which a high refractive index region is surrounded by a low refractive index dielectric material and the light propagates through the high refractive index region by total internal reflection. The nonlinear equation governing the light wave propagation in optical waveguide is the famous nonlinear Schrödinger equation (NLSE) for the complex envelope of the light field. The NLSE in ideal Kerr nonlinear medium is completely integrable using the inverse scattering theory and hence all solitary wave solutions to NLSE are called as solitons. In most nonlinear systems of physical interest, we have non-Kerr or other types of nonlinearities and hence can be modelled by non-integrable generalized NLSE. The wave solutions for non-integrable equations are generally referred as optical solitary waves to distinguish them from solitons in integrable systems. But in recent literature on nonlinear optics, there is no nomenclature distinction and all solitary wave solutions in optics are referred as optical solitons.

2.2.1 Optical solitons

In nonlinear optics, the term soliton represents a light field which does not change during propagation in an optical medium. The optical solitons have been the subject of intense theoretical and experimental studies because of their practical applications in the field of fiber-optic communications. These solitons evolve from a nonlinear change in the refractive index of a material induced by the light field. This phenomenon of change in the refractive index of a material due to an applied field is known as optical Kerr effect. The Kerr effect, i.e. the intensity dependence of the refractive index, leads to nonlinear effects responsible for soliton formation in an optical medium [1].

The optical solitons can be further classified as being spatial or temporal depending upon the confinement of light in space or time during propagation. The spatial self-focusing (or self-defocusing) of optical beams and temporal self-phase modulation (SPM) of pulses are the nonlinear effects responsible for the evolution of spatial and temporal solitons in a nonlinear optical medium. When self-focusing of an optical beam exactly compensate the spreading due to diffraction, it results into the formation of spatial soliton, and a temporal soliton is formed when SPM balances the effect of dispersion-induced broadening of an optical pulse. For both soliton solutions, the wave propagates without change in its shape and is known as self-trapped. Self-trapping of a continuous-wave (CW) optical beam was first discovered in a nonlinear medium in 1964 [2]. But, these self-trapped beams were not said to be spatial solitons due to their unstable nature. First stable spatial soliton was observed in 1980 in an optical medium in which diffraction spreading was confined in only one transverse direction [3]. The first observation of the temporal soliton is linked to the nonlinear phenomenon of self-induced trapping of optical pulses in a resonant nonlinear medium [4]. Later, temporal solitons was found in an optical fiber both theoretically [5] and experimentally [6].

2.2.2 Nonlinear Schrödinger equation: Derivation and solutions

The basic equation governing the propagation of light field in optical waveguide is known as the nonlinear Schrödinger equation (NLSE) [1], whose general form is

$$i\frac{\partial\psi}{\partial z} + a_1\frac{\partial^2\psi}{\partial x^2} + a_2|\psi|^2\psi = 0. \tag{2.1}$$

where $\psi(z, x)$ is the complex envelope of the electric field, a_1 is the parameter of group velocity dispersion, a_2 represents cubic nonlinearity. As its name suggests, Eq. (2.1) is similar to the well-known Schrödinger equation of quantum mechanics. Here, of course, it has nothing to do with quantum mechanics. Rather, it is just Maxwells equations, adapted to study the field propagation in optical medium. However, the analogy with quantum mechanics can be made by considering the nonlinear term as analogous to a negative potential energy, which allows the possibility of self-focused solutions.

The solutions represented by $\psi(z, x)$ of Eq. (2.1) directly yield the spatial/temporal form of the field as seen by an observer at the location z. The second term in the equation, the second derivative of $\psi(z, x)$, represents the effects of dispersion, whereas the third term in the equation corresponds to the nonlinear term. The nonlinearity is based on the fact that the index of refraction is dependent on the light intensity.

Derivation

The propagation of light wave in optical medium can be studied by using the unified theory of electric and magnetic fields given by James Clerk Maxwell in 1860s. He gave the set of four equations, known as Maxwell's equations, to describe the relationship between four field vectors such as the electric field **E**, the electric displacement **D**, the magnetic field **H** and the magnetic flux density **B**. Maxwell's

equations in vector forms are

$$\nabla \times \mathbf{E} = -\frac{\partial \mathbf{B}}{\partial t}, \tag{2.2}$$

$$\nabla \times \mathbf{H} = \mathbf{J} + \frac{\partial \mathbf{D}}{\partial t}, \tag{2.3}$$

$$\nabla . \mathbf{D} = \rho, \tag{2.4}$$

$$\nabla . \mathbf{B} = 0, \tag{2.5}$$

where $\mathbf{J}$ and ρ are free current and charge densities, respectively. In a non-magnetic medium, such as dielectric material, the free charge in a medium is equal to zero, that is $\mathbf{J} = 0$ and $\rho = 0$, and the flux densities have the form

$$\mathbf{D} = \epsilon_0 \mathbf{E} + \mathbf{P}, \tag{2.6}$$

$$\mathbf{B} = \mu_0 H, \tag{2.7}$$

where $\mathbf{P}$ is the induced electric polarization in the medium, ϵ_0 and μ_0 are the permittivity and permeability of free space, respectively.

The wave equation for the electric field associated with an optical wave propagating into the medium can be derived by first taking the curl of Eq. (2.2) and using the other relations:

$$\nabla^2 \mathbf{E} - \frac{1}{c^2}\frac{\partial^2 \mathbf{E}}{\partial t^2} = \frac{1}{\epsilon_0 c^2}\frac{\partial^2 \mathbf{P}}{\partial t^2}, \tag{2.8}$$

where c is the speed of light in vacuum and $c^2 = \frac{1}{\epsilon_0 \mu_0}$.

The electric polarization is a vector field that represents the density of permanent or induced electric dipole moments in a dielectric material. The polarization induced in a dielectric material, when a material is placed in an external electric field and its molecules gain electric dipole moment. This induced electric dipole moment per unit volume of the dielectric material is known as the electric polarization of the dielectric. Hence, the induced polarization in a nonlinear dielectric medium is

related to the electric field by the following expression

$$\mathbf{P} = \epsilon_0 \left[\chi^{(1)} \,.\, \mathbf{E} + \chi^{(2)} \,.\, \mathbf{EE} + \chi^{(3)} \,.\, \mathbf{EEE} + ...\right], \tag{2.9}$$

where $\chi^{(i)}$ is the i-th order susceptibility tensor. For linear dielectric materials, only $\chi^{(1)}$ contributes significantly as $\chi^{(1)} = n^2 - 1$, where n is the refractive index of material. The second order susceptibility tensor $\chi^{(2)}$ is responsible for the second harmonic generation and nonlinear wave mixing processes. But, we consider the isotropic optical materials, that is a centrosymmetric material, for which $\chi^{(2)} = 0$. The third order susceptibility tensor $\chi^{(3)}$ is the lowest-order nonlinear effect which give rise to very important nonlinear effect of intensity dependent refractive index and other nonlinear phenomena such as third-order harmonic generation, four-wave mixing.

Now assuming that the electric field is polarized in the y-axis, confined in the x-axis and propagating along z-axis, the general solution of Eq. (2.8) can be written as

$$\mathbf{E} = \frac{1}{2} \left\{u(z,x) \exp[i(\beta_0 z - \omega_0 t)] + \ c.c.\right\} \ \hat{x} \tag{2.10}$$

where β_0 is the propagation constant given by $\beta_0 = k_0 n_0 = \frac{2\pi n_0}{\lambda}$ such that λ is optical wavelength and ω_0 is carrier frequency. Substituting Eq. (2.10) into the Eq. (2.9), the induced polarization will take the form

$$P = \epsilon_0 \left(\chi^{(1)} + \frac{3}{4}\chi^{(3)}|E|^2\right) E. \tag{2.11}$$

Now susceptibility $\chi = \chi_l + \chi_{nl}$ can be considered as combination of linear and nonlinear contribution to polarization given by $\chi_l = \chi^{(1)}$ and $\chi_{nl} = \frac{3}{4}\chi^{(3)}|E|^2$. Hence, due to this the refractive index of an optical material also depends on the intensity of wave as

$$n = n_0 + n_2|E|^2, \tag{2.12}$$

where n_0 is the linear coefficient of refractive index and n_2 is the nonlinear or Kerr coefficient of refractive index. For high light intensities, the refractive index deviates

from linear dependance of intensity and in general can be written as

$$n = n_0 + n_{nl}(I), \tag{2.13}$$

where $n_{nl}(I)$ represents the variation in the refractive index due to the light intensity $I = |E|^2$. For Kerr medium, $n_{nl}(I) = n_2 I$ and for cubic-quintic medium $n_{nl}(I) = n_2 I + n_4 I^2$.

Substituting Eq. (2.10) into Eq. (2.8), and assuming the slowly varying envelope approximation (SVEA), the Eq. (2.8) reduces to NLSE

$$i\frac{\partial u}{\partial z} + \frac{1}{2\beta_0}\frac{\partial^2 u}{\partial x^2} + k_0|u|^2 u = 0. \tag{2.14}$$

Introducing the dimensionless variables

$$X = \frac{x}{w_0}, \quad Z = \frac{z}{L_D}, \quad U = (k_0|n_2|L_D)^{1/2}u, \tag{2.15}$$

where $L_D = \beta_0\, w_0^2$ is the diffraction length, the dimensionless form of NLSE reads [1]

$$i\frac{\partial U}{\partial Z} + \frac{1}{2}\frac{\partial^2 U}{\partial X^2} \pm |U|^2 U = 0, \tag{2.16}$$

where the sign ($\pm$) depends on the type of nonlinearity, the negative sign for self-defocusing case (i.e. for $n_2 < 0$) and positive sign for self-focusing case (i.e. for $n_2 > 0$).

Solutions

In standard form, the NLSE can be written as

$$i\frac{\partial \psi}{\partial z} + \frac{1}{2}\frac{\partial^2 \psi}{\partial x^2} \pm |\psi|^2 \psi = 0, \tag{2.17}$$

where sign + (-) corresponds to self-focusing (self-defocusing) nonlinearity. In 1971, Zakharov and Shabat [7] showed that NLSE is completely integrable through the inverse scattering transform. The NLSE has a class of exact localized solutions which

have applications not only in nonlinear optics but also in the fields of hydrodynamics, plasma studies, electromagnetism and many more. Here we have given expressions of some localized solutions of NLSE which have been used further in this thesis.

(a) Bright and dark solitons

The NLSE has bright and dark solitons depending upon the sign of nonlinearity. For self-focusing case, the NLSE admits bright solitons which decay to background state at infinity. The general form of bright soliton for NLSE is given as [7]

$$\psi(z,x) = a \text{ sech}\left[a(x-vz)\right] \; e^{i(vx+(a^2-v^2)z/2)}, \tag{2.18}$$

where a represents the amplitude of soliton and v gives the transverse velocity of propagating soliton. The intensity expression for bright soliton will take the form

$$\begin{aligned} I_B &= |\psi(z,x)|^2 \\ &= a^2 \text{ sech}^2\left[a(x-vz)\right]. \end{aligned} \tag{2.19}$$

The evolution of bright soliton for NLSE is shown in Fig. 2.1 for typical values of a and v.

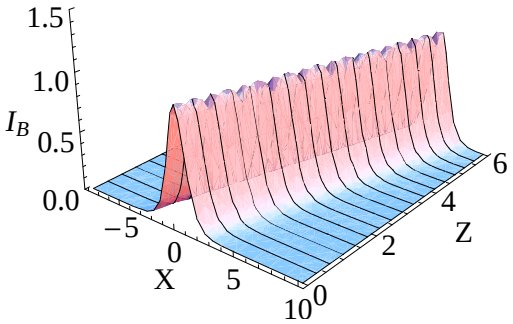

Figure 2.1: Evolution of bright soliton of the NLSE for $a = 1$ and $v = 1$.

For self-defocusing case, the NLSE have soliton solutions which do not vanish at infinity called dark solitons. These solitons have a nontrivial background and, as

name suggests, exist in the form of intensity dips on the CW background [8]. The fundamental dark soliton for NLSE has the following general form [9]

$$\psi(z,x) = u_0 \left[B \ \tanh(u_0 B(x - Au_0 z)) + iA\right] \ e^{-iu_0^2 z}, \tag{2.20}$$

where u_0 is CW background, and A and B satisfy the realation $A^2 + B^2 = 1$. Introducing a single parameter ϕ, we have $A = \sin\phi$ and $B = \cos\phi$ such that angle 2ϕ gives the total phase shift across the dark soliton. The intensity expression for dark soliton will take the form

$$I_D = u_0^2 \left[\cos^2\phi \ \tanh^2(u_0 \cos\phi(x - u_0 \sin\phi \ z)) + \sin^2\phi\right]. \tag{2.21}$$

Hence, $u_0 \sin\phi$ represents the velocity of the dark soliton and $\cos^2\phi$ gives the magnitude of the dip at the center. The evolution of dark soliton for NLSE is shown in Fig. 2.2 (a) for typical values of u_0 and ϕ. For $\phi = 0$, the velocity of dark soliton is zero i.e. it is a stationary soliton and at the dip center intensity also drops to zero (shown in Fig. 2.2 (b)), and hence it is called as black soliton. For other values of ϕ, the intensity of soliton does not drop to zero and these are referred as gray solitons.

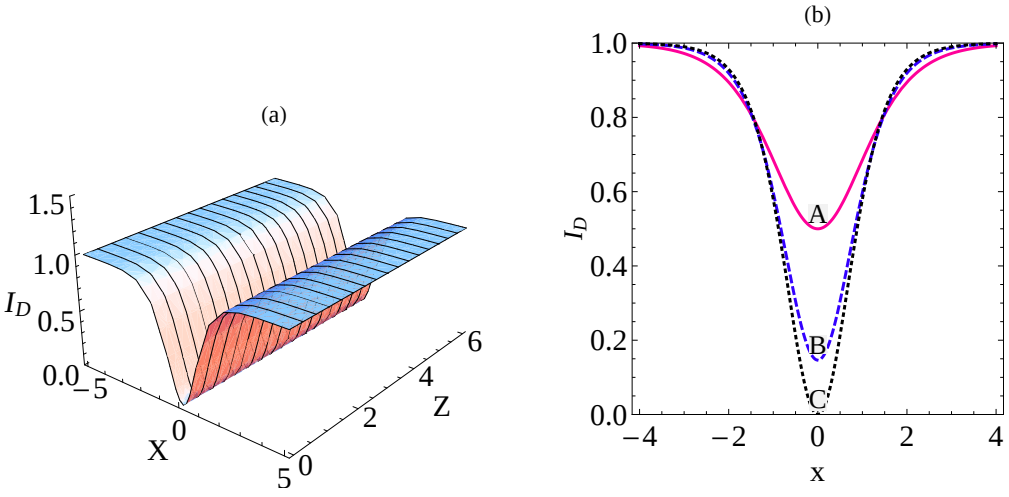

Figure 2.2: (a) Evolution of dark soliton of the NLSE for $u_0 = 1$ and $\phi = 0$. (b) Intensity plots at $z = 0$ for different values of ϕ. Curves A,B and C correspond to $\phi = \pi/4, \pi/8$ and 0 respectively.

(b) Rational solutions

Apart from bell-shaped (bright) and kink-shaped (dark) solitons, the NLSE also admits rational solutions which are localized in both x and Z directions. These rational solutions play an important role in the field of hydrodynamics as the self-focusing NLSE also applicable to the theory of ocean waves. These solutions are also known by the name of "rogue waves","freak waves","killer waves" related to the giant single waves appearing in the ocean, with amplitude significantly larger than those of the surrounding waves. They manifest from nowhere, are extremely rare, and disappear without a trace [10]. In recent years, apart from hydrodynamics the study of rogue waves has been extended to other physical systems, such as nonlinear fiber optics [11, 12, 13] and Bose-Einstein condensates [14, 15]. In particular, the study of rogue waves has gained fundamental significance in nonlinear optical systems, because it opens the possibility of producing high intensity optical pulses. The first observation of optical rogue solitons (the optical equivalent of oceanic rogue waves) in nonlinear optical systems was reported by Solli *et al.* in 2007 [11]. The role of optical rogue solitons in supercontinuum generation in fibers [16] and in the context of optical turbulence [17] has been recently investigated.

The fundamental cause of rogue wave formation is modulation instability, which makes the small amplitude waves grow into higher amplitude ones, resulting in the formation of Akhmediev breathers (ABs) [18]. Subsequently, double and triple collisions of these breathers lead to the creation of rogue waves, whose amplitudes are two to three times higher than that of the average wave crest. ABs are the spatially periodic solutions of the NLSE which consist of an evolving train of ultra-short pulses. The AB solution of the NLSE is given by [10]

$$\psi(z,x) = \frac{(1-4a)\cosh(\beta z) + \sqrt{2a}\cos(px) + i\beta\sinh(\beta z)}{\sqrt{2a}\cos(px) - \cosh(\beta z)}\, e^{iz}, \tag{2.22}$$

where a is a free parameter, and the coefficients β and p are related to a by: $\beta = \sqrt{8a(1-2a)}$ and $p = 2\sqrt{1-2a}$. The characteristics of AB depends on the modulation parameter a. As the value of a increases, the separation between adja-

cent peaks increases and the width of each individual peak decreases, as shown in Fig. 2.3.

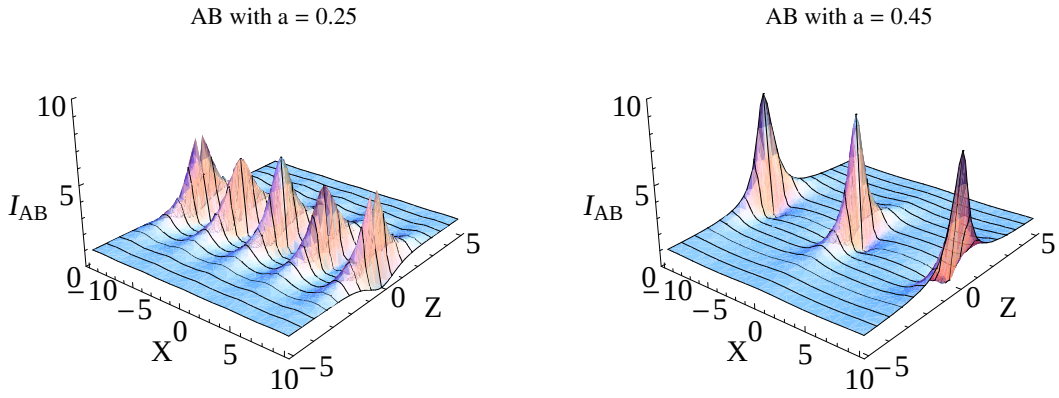

Figure 2.3: (a) Intensity profiles for ABs of the NLSE for modulation parameter: $a = 0.25$ and $a = 0.45$, respectively.

For the limiting case $a \to 1/2$, the AB solution reduces to the rational solution known as rogue wave solution, first given by Peregrine [19] in 1983. The next-order rational solution was proposed by Akhmediev *et al.* [10] in 2009, which gives the possible explanation for the existence of high amplitude rogue waves. Indeed, here is a hierarchy of rational solutions of the self-focusing NLSE with progressively increasing central amplitude [20]. The basic structure of these rational solutions is given by

$$\psi(z,x) = \left[1 - \frac{K + iH}{D}\right] e^{iz}, \tag{2.23}$$

where K, H and D are the polynomials in z and x. For first-order rogue wave solution, obtained by taking the limiting case $a \to 1/2$ in AB solution, one can obtain $K = 4$, $H = 8z$ and $D = 1 + 4z^2 + 4x^2$. Thus the full solution reads

$$\psi(z,x) = \left[1 - 4\frac{1 + 2iz}{1 + 4z^2 + 4x^2}\right] e^{iz}. \tag{2.24}$$

The intensity expression for first-order rogue wave is given by

$$I_{R_1} = 1 + 8\frac{1 + 4z^2 - 4x^2}{(1 + 4z^2 + 4x^2)^2}. \tag{2.25}$$

The second-order rogue wave solution has the form given by Eq. (2.23) with K, H and D given by

$$\begin{aligned} K &= \left(\chi^2+\zeta^2+\frac{3}{4}\right)\left(\chi^2+5\zeta^2+\frac{3}{4}\right)-\frac{3}{4}, \\ H &= \zeta\left(\zeta^2-3\chi^2+2(\chi^2+\zeta^2)^2-\frac{15}{8}\right), \\ D &= \frac{1}{3}\left(\chi^2+\zeta^2\right)^3+\frac{1}{4}\left(\chi^2-3\zeta^2\right)^2+\frac{3}{64}\left(12\chi^2+44\zeta^2+1\right), \end{aligned} \tag{2.26}$$

And, the intensity expression for second-order rogue waves will take the form

$$I_{R_2} = \left(\frac{D-K}{D}\right)^2+\left(\frac{H}{D}\right)^2. \tag{2.27}$$

The intensity plots for first- and second-order rogue waves are shown in the Fig. 2.4.

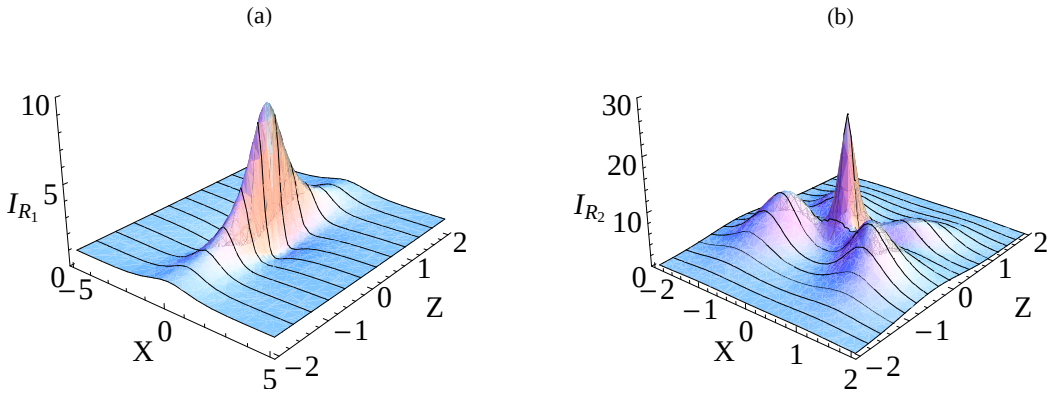

Figure 2.4: Intensity profiles for (a) first-order, and (b) second-order rogue waves of the NLSE, respectively.

2.2.3 Tapered waveguides - Generalized NLSE

In recent years, the design and properties of the tapered optical waveguides have been studied extensively both theoretically as well as experimentally [21]. The reason behind this is the potential applications achievable through the tapering effect. It helps in improving the coupling efficiency between fibers and waveguides by reduc-

ing the reflection losses and mode mismatch [22]. Tapering also finds applications for the phenomena which require longitudinally varying waveguide properties, for instance, in highly efficient Raman amplification [23] and extended broadband supercontinuum generation [24].

The refractive index distribution inside the tapered graded index waveguide can be written as [21]

$$n(x,z) = n_0 + n_1 F(z) x^2 + n_2 |u|^2, \tag{2.28}$$

where the first two terms correspond to the linear part of refractive index and the last term is Kerr-type nonlinearity. The function $F(z)$ describes the geometry of tapered waveguide along the waveguide axis. The quadratic variation of the refractive index in transverse direction is a good approximation to the true refractive index distribution, and is often known as lens-like medium. Such waveguides have applications in image-transmitting processes because they possess a very wide bandwidth. The shape of a taper i.e. $F(z)$ can be modelled appropriately depending upon the practical requirements. A taper can be made by heating of one or more fibers up to the material softening point and then stretching it until a desired shape has been obtained. Here, we have studied the propagation of similaritons in two types of tapered waveguides (a) sech^2-type taper, and (b) parabolic taper. The parabolic taper waveguide, given by $F(z) = F_0(1 + \gamma z^2)$ [25, 26], is the optimum shape for fiber couplers which can be fabricated by the use of Ag-ion exchange in soda-lime glass [27]. Recently, authors [21, 28, 13] have also worked on the wave propagation through sech^2-type tapered waveguide by considering the lowest-order mode of sech^2-profile waveguide [29].

The propagation of beam through tapered graded-index nonlinear waveguide amplifier is governed by generalized nonlinear Schrödinger equation (GNLSE)

$$i\frac{\partial u}{\partial z} + \frac{1}{2k_0}\frac{\partial^2 u}{\partial x^2} + \frac{1}{2}k_0 n_1 F(z) x^2 u - \frac{i(g(z) - \alpha(z))}{2}u + k_0 n_2 |u|^2 u = 0, \tag{2.29}$$

where $u(x,z)$ is the complex envelope of the electrical field, g and α account for

linear gain and loss, respectively, $k_0 = 2\pi n_0/\lambda$, λ being the wavelength of the optical source generating the beam, n_1 is the linear defocusing parameter ($n_1 > 0$), and n_2 represents Kerr-type nonlinearity. The dimensionless profile function $F(z)$ can be negative or positive, depending on whether the graded-index medium acts as a focusing or defocusing linear lens. Introducing the normalized variables $X = x/w_0$, $Z = z/L_D$, $G = [g(z) - \alpha(z)]L_D$, and $U = (k_0|n_2|L_D)^{1/2}u$, where $L_D = k_0 w_0^2$ is the diffraction length associated with the characteristic transverse scale $w_0 = (k_0^2 n_1)^{-1/4}$, Eq. (2.29) can be rewritten in a dimensionless form [21, 13],

$$i\frac{\partial U}{\partial Z} + \frac{1}{2}\frac{\partial^2 U}{\partial X^2} + F(Z)\frac{X^2}{2}U - \frac{i}{2}G(Z)U \pm |U|^2 U = 0. \tag{2.30}$$

2.2.4 Self-similar waves

In some cases, the underlying equations governing the wave propagation in a physical system are mathematically integrable and can be solved directly to obtain solitary wave-type solutions, e.g. NLSE, KdV equation etc.. However, in the presence of non-uniformities and gain/loss in the system, the evolution equations are more complicated and can not be solved directly using integrable techniques. Recently, a new mathematical technique, known as "symmetry reduction", has been introduced to obtain solutions of complex differential equations. In particular, the evolution of a physical system often exhibits some form of symmetry such that the dynamics of system at one time can be mapped onto its dynamics at some other time using a suitable scaling transformation, known as "similarity transformation". This transformation led to the discovery of a new class of solutions called self-similar solutions. These solutions obey relatively some scaling laws in such a way that their evolution can be regarded as self-similar [30]. These self-similar solutions corresponds to the self-similar waves propagation in a highly nonlinear medium which maintain their shape but the amplitude and width changes with the modulating system parameters such as dispersion, nonlinearity, and gain [31, 32]. Their temporal and spectral

profile is independent of the input pulse profile, but are determined with the input pulse energy and amplifier parameter. In comparison to optical solitons which become unstable at high power, self-similar waves are most robust with increasing intensity [33].

Although the study on self-similarity techniques is very common in the fields involving nonlinear physical phenomena such as hydrodynamics and plasma physics, but yet these techniques has not been used widespread in the field of optics. Recently, there has been a lot of interest in self-similar effects in the study of nonlinear wave propagation in optical waveguide amplifiers [21, 31, 34, 35]. Waveguide amplifiers play an important role in optical communications systems and high-power ultrafast transmission. The first experimental observation of self-similar pulses, known as similaritons, was reported by Fermann *et al.* in a nonlinear fiber amplifier [34]. By analogy with the soliton behavior of solitary wave solutions, these self-similar solutions are known as similaritons. Apart from fundamental interest in self-similar waves (as they provide a new set of solutions to the NLSE with gain), it is expected that these solutions will also find applications in optical systems in both the laboratory and in industry.

Mathematical approach

The functional form of the self-similar solution is invariant such that the solution at one stage can be found from a solution at another stage using a similarity transformation. Mathematically, self-similar solutions can be obtained by reformulating the differential equation in terms of a certain combinations of the original variables, known as a similarity variable [36]. It helps to solve a complicated partial differential equation by recasting it into a reduced system of differential equations which can be simplified easily. Exactly how this technique is carried out, depends on the specific problem.

2.3 An introduction to isospectral Hamiltonian approach

From supersymmetric (SUSY) quantum mechanics, it is known that for a given ground state wave function and energy, isospectral deformation of the Hamiltonian can always be done [37]. For two isospectral Hamiltonians, the energy eigenvalue spectrum is exactly same whereas the wave functions and their dependent quantities are different. The fact that such Hamiltonians exist has been known for a long time from Gefland-Levitan approach or the Darboux procedure, but these methods are much complicated in comparison to isospectral Hamiltonian approach of SUSY quantum mechanics. Thus, starting from an one-dimensional potential, one can construct an one-parameter family of strictly isospectral potentials, that is the potentials which have same eigenvalues, reflection and transmission coefficients as of those for original potential. Before the advent of SUSY quantum mechanics, this aspect was discussed by Infeld and Hull [38] and also by Mielnik [39] to construct new potentials from a given potential. This formalism has been proved to be advantageous in various physical situations [40, 41, 42, 43]. Recently this approach has been used to control the dynamical behavior of rogue waves in nonlinear fiber optics [13, 44] and in BEC's [15] .

Formalism

A single particle quantum Hamiltonian can be written as

$$H_1 = -\frac{d^2}{dx^2} + V_1(x), \tag{2.31}$$

for $\hbar = 2m = 1$. Choosing ground state energy to be zero, the Schrödinger equation for the ground state wavefunction $\psi_0(x)$ is

$$-\frac{d^2\psi_0(x)}{dx^2} + V_1(x)\psi_0(x) = 0, \tag{2.32}$$

so that potential $V_1(x)$ is of the form

$$V_1(x) = \frac{1}{\psi_0(x)} \frac{d^2\psi_0(x)}{dx^2}. \tag{2.33}$$

We can factorize the Hamiltonian, given by Eq. (2.31), as follows

$$H_1 = A^\dagger A, \tag{2.34}$$

where $A = \frac{d}{dx} + \Lambda(x)$ and $A^\dagger = -\frac{d}{dx} + \Lambda(x)$. Here, A and $A^\dagger$ are the SUSY operators and $\Lambda(x)$ is the superpotential given by

$$\Lambda(x) = -\frac{d}{dx} \left[\ln \psi_0(x)\right]. \tag{2.35}$$

It allows us to identify $V_1(x)$ as

$$V_1(x) = \Lambda^2(x) - \frac{d\Lambda(x)}{dx}. \tag{2.36}$$

In SUSY theory, a SUSY partner Hamiltonian can be generated by reversing the order of A and $A^\dagger$ in H_1, that is $H_2 = AA^\dagger$. The new potential $V_2(x)$ corresponding to SUSY partner Hamiltonian

$$H_2 = -\frac{d^2}{dx^2} + V_1(x), \tag{2.37}$$

is

$$V_2(x) = \Lambda^2(x) + \frac{d\Lambda(x)}{dx}. \tag{2.38}$$

The potentials $V_1(x)$ and $V_2(x)$ are known as SUSY partner potentials.

Now, following Mielnik [39], question can arise whether the factorization $H_2 = AA^\dagger$ is unique or not, in the definition of the partner potential $V_2(x)$. Suppose H_2 has another factorization as $H_2 = BB^\dagger$, where $B = \frac{d}{dx} + \widehat{\Lambda}(x)$ and $B^\dagger = -\frac{d}{dx} + \widehat{\Lambda}(x)$.

For superpotential $\widehat{\Lambda}(x)$, the partner potential reads

$$V_2(x) = \widehat{\Lambda}^2(x) + \frac{d\widehat{\Lambda}(x)}{dx}. \tag{2.39}$$

Comparing it with Eq. (2.38), the particular solution is $\widehat{\Lambda}(x) = \Lambda(x)$. But, in order to find the most general solution, let

$$\widehat{\Lambda}(x) = \Lambda(x) + \phi(x), \tag{2.40}$$

which yields

$$\frac{d\phi(x)}{dx} + 2\Lambda(x)\phi(x) + \phi^2(x) = 0. \tag{2.41}$$

This is a Riccati equation whose solution is

$$\phi(x) = \frac{{\psi_0}^2(x)}{c + \int_{-\infty}^{x} {\psi_0}^2(x')dx'}, \tag{2.42}$$

where c is constant of integration, known as Riccati parameter, and chosen in such a way that $\phi(x)$ is non-singular.

Thus, the most general $\widehat{\Lambda}(x)$ satisfying the Eq. (2.39) is

$$\widehat{\Lambda}(x) = \Lambda(x) + \frac{{\psi_0}^2(x)}{c + \int_{-\infty}^{x} {\psi_0}^2(x')dx'}. \tag{2.43}$$

Hence, $H_2 = AA^\dagger = BB^\dagger$ but $H = B^\dagger B$ is not equal to $A^\dagger A$ rather it defines a new class of isospectral Hamiltonians which have same energy spectrum as H_1. The corresponding one parameter family of isospectral potentials is given as

$$\widehat{V}_1(x) = V_1(x) - 2\frac{d}{dx}\left(\frac{{\psi_0}^2(x)}{c + \int_{-\infty}^{x} {\psi_0}^2(x')dx'}\right), \tag{2.44}$$

which have the same SUSY partner potential $V_2(x)$. The normalized ground state

wavefunction corresponding to the potential $\widehat{V}_1(x)$ reads

$$\widehat{\psi}_0(x) = \frac{\sqrt{c(c+1)}\psi_0(x)}{c + \int_{-\infty}^{x} {\psi_0}^2(x')dx'}. \tag{2.45}$$

Thus, we have a class of potentials $\widehat{V}_1(x)$ which have exactly same energy spectrum as that of $V_1(x)$.

2.4 Riccati parameterized self-similar waves in sech^2-type tapered waveguide

In this section, we have studied the GNLSE given by Eq. (2.30) and obtained a class of self-similar solutions for sech^2-type tapered waveguides. Serkin and his collaborators, in a series of papers [45, 46], considered the GNLSE arising in the context of Bose-Einstein condensates (BEC) and fiber optics, and obtained nonautonomous 1- and 2-soliton solutions using inverse scattering technique. Control of solitons in BEC has been demonstrated in Ref. [47]. Ponomarenko and Agrawal [21] studied the paraxial wave evolution in the tapered, graded-index nonlinear waveguide amplifier and obtained optical similaritons by reducing the GNLSE to standard NLSE using similarity transformation. Later, Raju and Panigrahi [28] solved this equation in the presence of external source which describes the similariton propagation through asymmetric twin-core fiber amplifiers. Recently, the self-similar rogue wave solutions have also been explored for the GNLSE using similarity transformation [15, 48, 49].

Here, we demonstrate that the intensity of self-similar waves can be made significantly large, creating the possibility to produce highly energetic optical waves for practical applications. This has been achieved by making use of the observation that the mathematical structure of the equation governing the width of the self-similar wave is similar to the Schrödinger equation of quantum mechanics, with a tapering function as the potential. It enables one to analytically identify a large manifold

of allowed tapering profiles with compatible gain functions. The allowed profiles are governed by a free Riccati parameter c, which provides a control for tuning the self-similar wave amplitude and width. The choice of its value changes the intensity of the optical wave quite intensively from that of the original one.

2.4.1 Self-similar transformation

The propagation of beam through tapered graded-index nonlinear waveguide amplifier is governed by GNLSE [50]

$$i\frac{\partial U}{\partial Z} + \frac{1}{2}\frac{\partial^2 U}{\partial X^2} + F(Z)\frac{X^2}{2}U - \frac{i}{2}G(Z)U \pm |U|^2 U = 0. \tag{2.46}$$

Eq. (2.46) has been solved for self-similar solutions by transforming it into standard homogeneous NLSE, using the gauge and similarity transformation, together with a generalized scaling with respect to the Z variable [21, 48],

$$U(X,Z) = A(Z)\Psi\left[\frac{X - X_c(Z)}{W(Z)}, \zeta(Z)\right] e^{i\Phi(X,Z)}, \tag{2.47}$$

where A, W and X_c are the dimensionless amplitude, width and center position of the self-similar wave. The phase is given by

$$\Phi(X,Z) = C_1(Z)\frac{X^2}{2} + C_2(Z)X + C_3(Z), \tag{2.48}$$

where $C_1(Z)$, $C_2(Z)$ and $C_3(Z)$ are, the parameters related to the phase-front curvature, the frequency shift, and the phase offset, respectively, to be determined. Now substituting Eqs. (2.47) and (2.48) into Eq. (2.46), one obtains the NLSE

$$i\frac{\partial \Psi}{\partial \zeta} + \frac{1}{2}\frac{\partial^2 \Psi}{\partial \chi^2} \pm |\Psi|^2 \Psi = 0. \tag{2.49}$$

Here the amplitude, effective propagation distance, similarity variable, guiding-

center position and phase are given respectively as

$$A(Z) = \frac{1}{W(Z)}, \qquad \zeta(Z) = \zeta_0 + \int_0^Z \frac{dS}{W^2(S)},$$

$$\chi(X,Z) = \frac{X - X_c(Z)}{W(Z)}, \quad X_c(Z) = W(Z)\left(X_0 + C_{02}\int_0^Z \frac{dS}{W^2(S)}\right),$$

$$\Phi(X,Z) = \frac{X^2}{2W}\frac{dW}{dZ} + \frac{C_{02}X}{W} - \frac{C_{02}^2}{2}\int_0^Z \frac{dS}{W^2(S)}, \tag{2.50}$$

where $C_2(0) = C_{02},\ X_c(0) = X_0$, and we choose $W(0) = 1$. Further, the tapering function, gain and similariton width $W(Z)$ are related as

$$d^2W/dZ^2 - F(Z)W = 0, \tag{2.51}$$

$$G(Z) = -d[\ln W(Z)]/dZ. \tag{2.52}$$

Interestingly, Eq. (2.51) can be observed as Schrödinger eigenvalue problem, by identifying $F(Z)$ as potential and $W(Z)$ as corresponding wave function with zero energy. As Schrödinger equation is exactly solvable for a variety of potentials, so this identification enables us to study Eq. (2.46) for a variety of tapering profiles. Moreover, using the fact that for a given ground state wave function and energy, isospectral deformation of the Hamiltonian can always be done, as described in Section 2.3, one can write a class of width and tapering functions using Eqs. (2.44) and (2.45) as

$$\widehat{W}(Z) = \frac{\sqrt{c(c+1)}\ W(Z)}{c + \int_{-\infty}^{Z} W^2(S)dS}, \tag{2.53}$$

$$\widehat{F}(Z) = F(Z) - 2\frac{d}{dZ}\left(\frac{W^2(Z)}{c + \int_{-\infty}^{Z} W^2(S)dS}\right), \tag{2.54}$$

where c is an integration constant, known as Riccati parameter, which is to be chosen in a way so as to avoid singularities. Hence, the modified gain function becomes

$$\widehat{G}(Z) = -d[\ln \widehat{W}(Z)]/dZ. \tag{2.55}$$

As stated earlier, transformation (2.47) reduces Eq. (2.46) to the exactly integrable homogeneous NLSE, so for all the solutions of NLSE the self-similar solutions of GNLSE can be obtained.

2.4.2 Bright and dark similaritons

The exact form of the bright and dark solitons for Eq. (2.49) with +ve and -ve signs of Kerr nonlinearity, respectvely, can be found from the Eqs. (2.19) and (2.21). Hence, the intensity expression of the bright similariton for GNLSE (with +ve Kerr nonlinearity in Eq. (2.46)) is given by

$$I_B = \frac{a^2}{W^2}\mathrm{sech}^2[a(\chi - v\zeta)], \tag{2.56}$$

where a and v are the soliton amplitude and velocity. In the similar way, the intensity expression of the dark similariton for GNLSE with -ve sign of Kerr nonlinearity is given by

$$I_D = \frac{u_0^2}{W^2}[\cos^2(\phi)\tanh^2(\Theta) + \sin^2(\phi)], \tag{2.57}$$

where u_0 is the background amplitude and ϕ governs the grayness and speed of the dark soliton. The soliton phase Θ is given as

$$\Theta(Z, X) = u_0\cos(\phi)[\chi - u_0\zeta\sin(\phi)]. \tag{2.58}$$

The intensity profiles of bright and dark similaritons is studied by Ponomarenko *et al.* [21] for sech^2-type tapered waveguide. The main theme of this work is to study the controlling of these similaritons through modified tapering given by Eq. (2.54). Hence, armed with the modified functions $\widehat{F}(Z)$, $\widehat{W}(Z)$ and $\widehat{G}(Z)$, one can discuss the effect of these new functions on the intensity profiles of the bright and dark similaritons given by Eqs. (2.56) and (2.57), respectively, taking an explicit example of sech^2-type tapering.

For general form of sech^2-type tapering, given by

$$F(Z) = n^2 - n(n+1)\ \mathrm{sech}^2 Z, \tag{2.59}$$

where n is a positive integer, the width and gain profiles from Eqs. (2.51) and (2.52) are

$$W(Z) = \mathrm{sech}^n Z, \tag{2.60}$$

$$G(Z) = n\ \tanh Z. \tag{2.61}$$

For the present analysis, the work has been done for two cases $n = 1$ and 2.

Case (i) : For $n = 1$, Eqs. (2.59)-(2.61) reads

$$F(Z) = 1 - 2\ \mathrm{sech}^2 Z, \quad W(Z) = \mathrm{sech}\ Z, \quad G(Z) = \tanh Z. \tag{2.62}$$

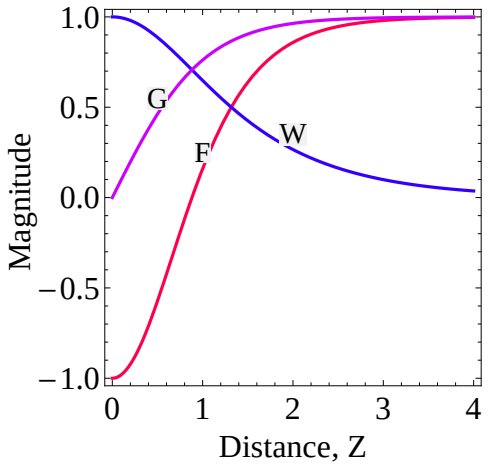

Figure 2.5: Profiles of tapering, width and gain, respectively, for $n = 1$.

In Fig. 2.5, the profiles for tapering, width and gain is shown for the expressions given by Eq. (2.62). For this choice of tapering, the evolution of bright and dark similaritons is shown in Fig. 2.6 [32].

Now, using Eq. (2.62) in Eq. (2.53), a class of width profile $\widehat{W}(Z)$ correspond-

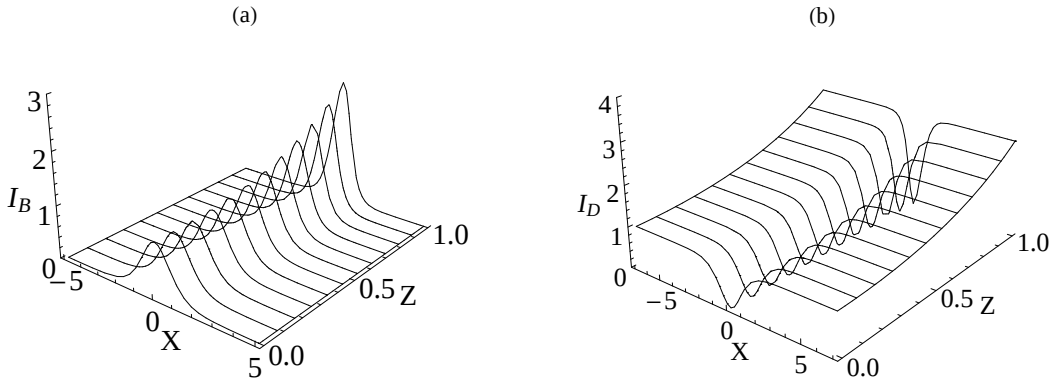

Figure 2.6: Evolution of bright and dark similaritons for tapering profile given by Eq. (2.62). The parameters used in the plots are $C_{02} = 0.3, X_0 = 0, \zeta_0 = 0, v = 0.3, a = 1, u_0 = 1$ and $\phi = 0$.

ing to generalized tapering profiles can be written as

$$\widehat{W}(Z) = \frac{\sqrt{c(c+1)}\ \text{sech}\ Z}{c + (1 + \tanh Z)}. \tag{2.63}$$

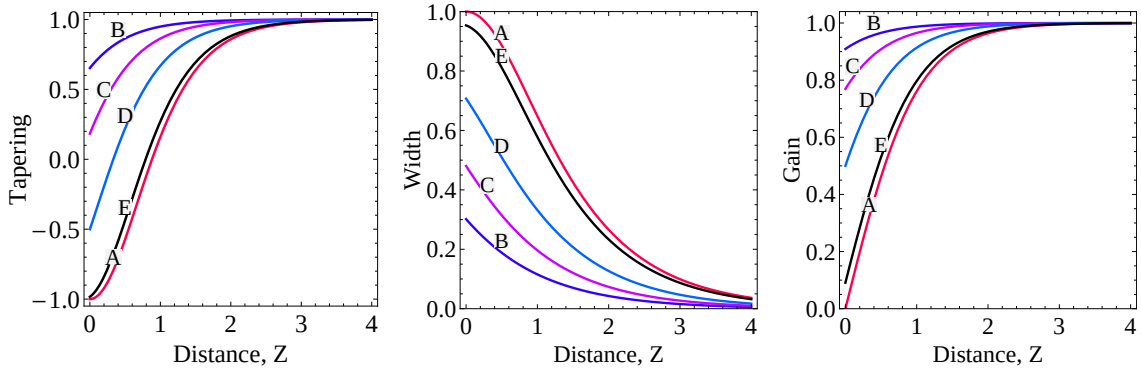

Figure 2.7: Profiles of tapering, width and gain, respectively, for $n = 1$. Curve A corresponds to profile given by Eq. (2.62) and curves B, C, D, E correspond to generalized class for different values of c; $c = 0.1$, $c = 0.3$, $c = 1$, $c = 10$ respectively.

In the similar way, $\widehat{F}(Z)$ and $\widehat{G}(Z)$ can also be found from Eqs. (2.54) and (2.55). In order to see the effect of c, we have plotted $\widehat{F}(Z)$, $\widehat{W}(Z)$ and $\widehat{G}(Z)$ for different values of c (see Fig. 2.7). It can be seen from the figure that for large value of Riccati parameter the generalized profiles, of all the three functions, approach to the profiles given by Eq. (2.62). For $c = 1$ and $c = 10$, the tapering function $\widehat{F}(Z)$

is initially negative and crosses zero at some value of Z, implying that the linear inhomogeneity of the waveguide is changing from focusing to defocusing type. But for $c < 0.414$, $\widehat{F}(Z)$ is always positive which means the linear inhomogeneity of the waveguide is of the defocusing type. This effect is shown in Fig. 2.7 for $c = 0.3$ and $c = 0.1$. The similariton width increases with increase in c. The amplitude of the required normalized gain is found to be inversely proportional to the Riccati parameter and tends to unity asymptotically.

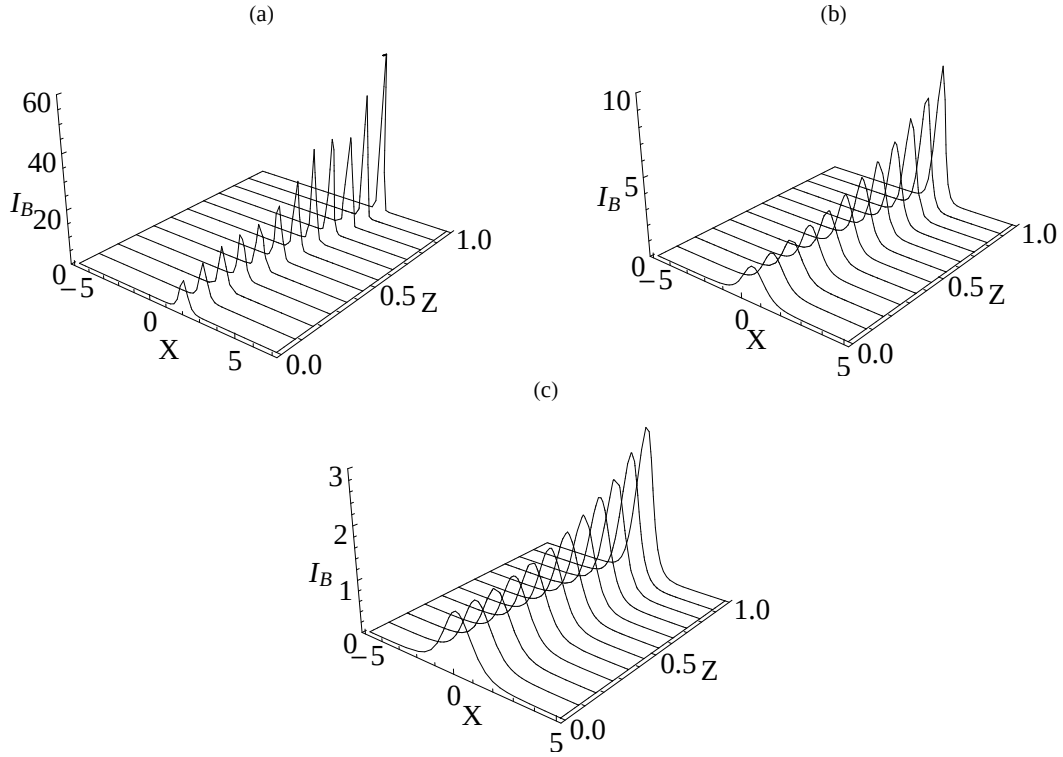

Figure 2.8: Evolution of bright similariton for generalized tapering for $c = 0.1,\ 1$ and 10, respectively. The parameters used in the plots are $C_{02} = 0.3, X_0 = 0, \zeta_0 = 0, v = 0.3$ and $a = 1$.

Now using Eq. (2.63), the intensity of optical bright and dark similaritons for $\widehat{F}(Z)$ can be found from Eqs. (2.56) and (2.57). Here, the evolution of bright similariton is shown in Fig. 2.8 for $\widehat{W}(Z)$ given by Eq. (2.63) for $c = 0.1,\ 1$ and 10, respectively. It is clear from the plots that the intensity is more for smaller values of c and as value of c increases it decreases and goes back to the profile without the Riccati generalization, as shown in Fig. 2.6(a). Similar effect has also been observed

in the case of dark similaritons (see Fig. 2.9).

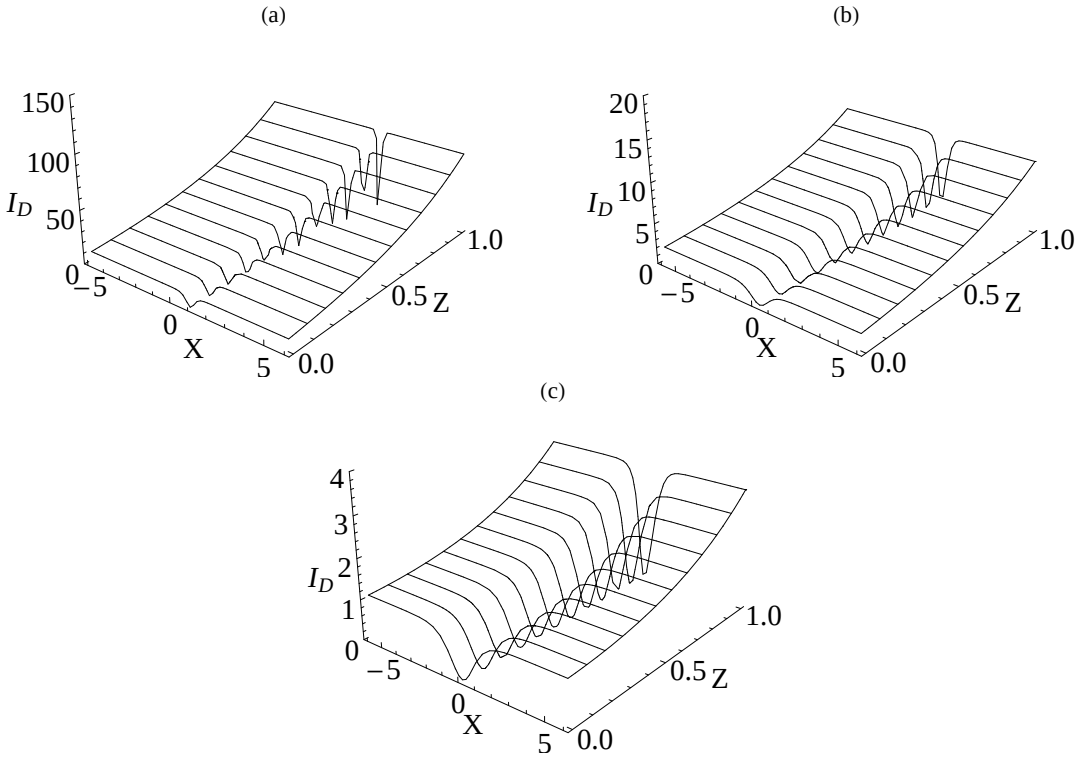

Figure 2.9: Evolution of dark similariton for generalized tapering for $c = 0.1,\ 1$ and 10, respectively. The parameters used in the plots are $C_{02} = 0.3, X_0 = 0, \zeta_0 = 0, u_0 = 1$ and $\phi = 0$.

Case (ii) : For $n = 2$, Eqs. (2.59)-(2.61) reads

$$F(Z) = 4 - 6\ \mathrm{sech}^2 Z, \quad W(Z) = \mathrm{sech}^2 Z, \text{ and } \quad G(Z) = 2\tanh Z. \tag{2.64}$$

In Fig. 2.10, the profiles for tapering, width and gain is shown for the expressions given by Eq. (2.64). For this choice of tapering, the evolution of bright and dark similaritons is shown in Fig. 2.11. Substituting $W(Z) = \mathrm{sech}^2 Z$ into Eq. (2.53), a class of $\widehat{W}(Z)$ can be obtained as

$$\widehat{W}(Z) = \frac{\sqrt{c(c+1)}\ \mathrm{sech}^2 Z}{c + \frac{1}{3}\left(2 + \left(2 + \mathrm{sech}^2 Z\right)\tanh Z\right)}. \tag{2.65}$$

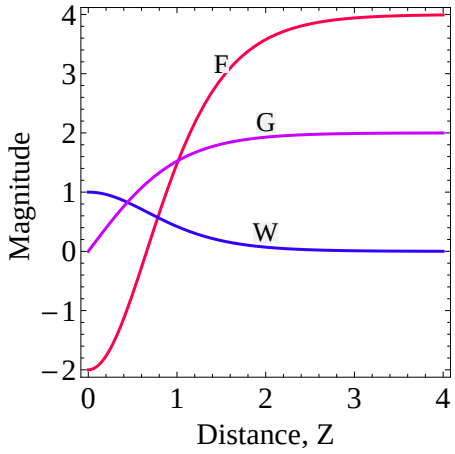

Figure 2.10: Profiles of tapering, width and gain, respectively, for $n = 2$.

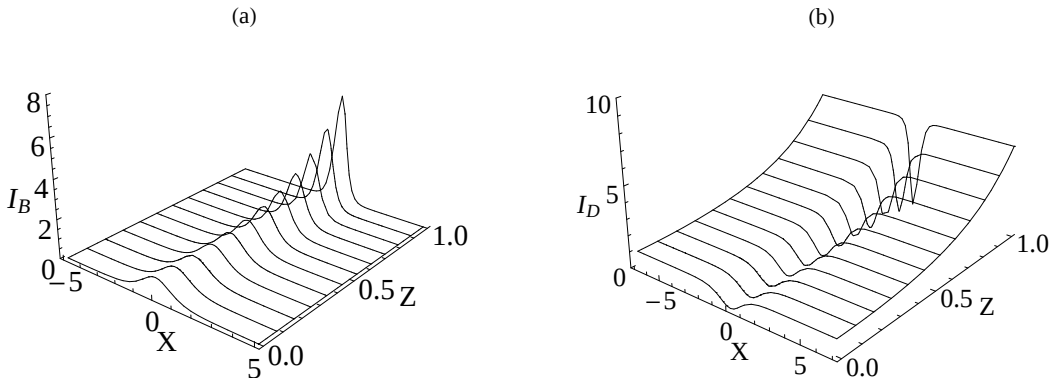

Figure 2.11: Evolution of bright and dark similaritons for tapering profile given by Eq. (2.64). The parameters used in the plots are $C_{02} = 0.3, X_0 = 0, \zeta_0 = 0, v = 0.3, a = 1, u_0 = 1$ and $\phi = 0$.

In a similar way, $\widehat{F}(Z)$ and $\widehat{G}(Z)$ can also be found from Eqs. (2.54) and (2.55). In order to see the effect of c, we have plotted $\widehat{F}(Z)$, $\widehat{W}(Z)$ and $\widehat{G}(Z)$ for different values of c (see Fig. 2.12). It can be seen from the figure that for large value of Riccati parameter the generalized profiles, of all the three functions, approach to the profiles given by Eq. (2.64). In this case, $\widehat{F}(Z)$ is always positive i.e. the linear inhomogeneity of the waveguide is of the defocusing type for $c \leq 0.333$.

Now using Eq. (2.65), the intensity of optical bright and dark similaritons for $\widehat{F}(Z)$ can be found from Eqs. (2.56) and (2.57). Here we have shown the evolution of bright and dark similaritons (see Fig. 2.13 and 2.14) for $\widehat{W}(Z)$ given by Eq. (2.65)

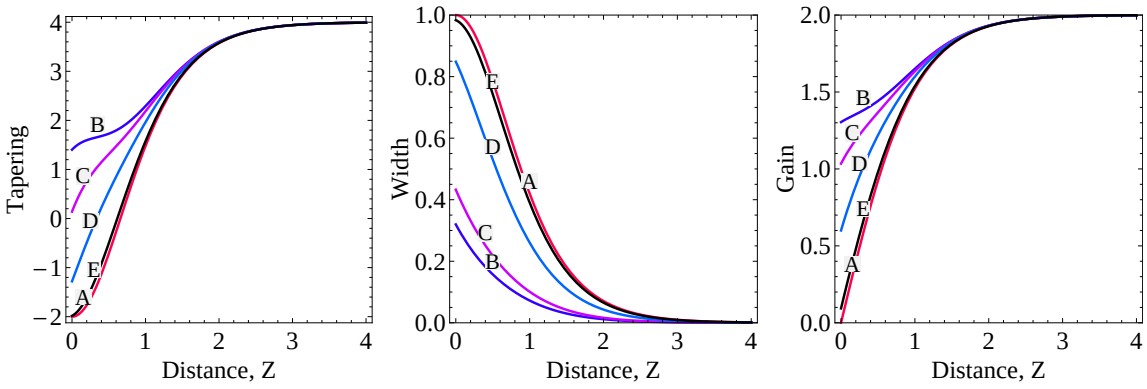

Figure 2.12: Profiles of tapering, width and gain, respectively, for $n = 2$. Curve A corresponds to profile given by Eq. (2.64) and curves B, C, D, E correspond to generalized class for different values of c; $c = 0.1$, $c = 0.3$, $c = 1$, $c = 10$ respectively.

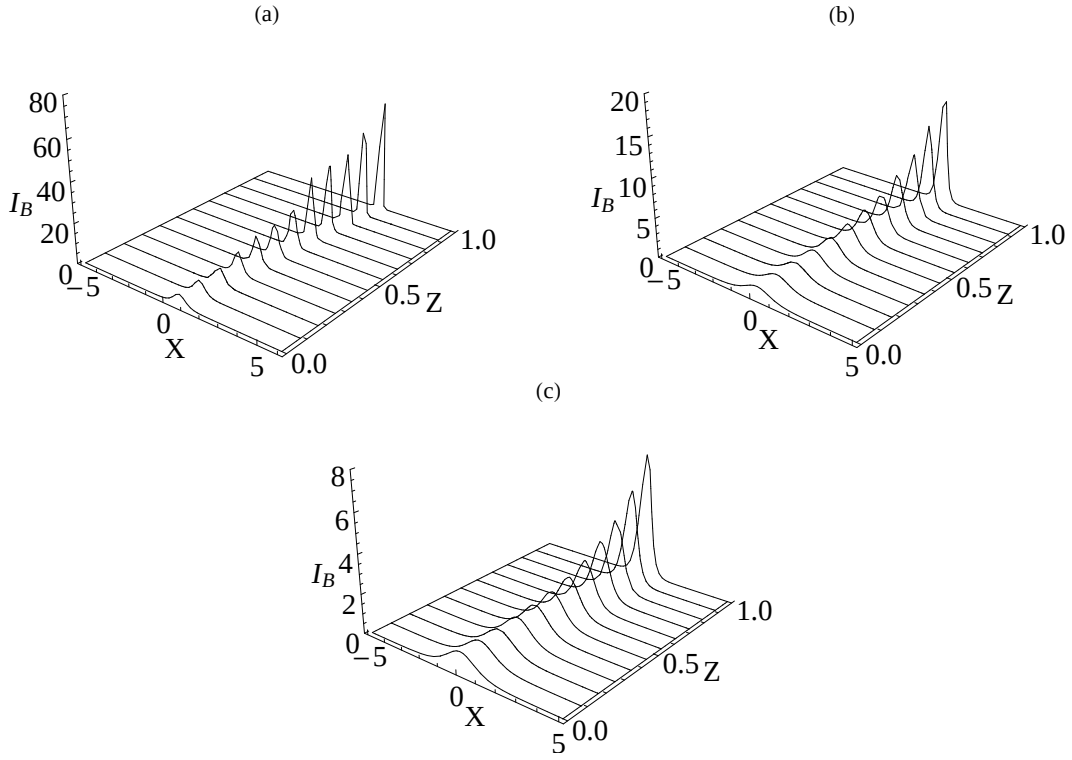

Figure 2.13: Evolution of bright similariton for generalized tapering for $c = 0.1,\ 1$ and 10, respectively. The parameters used in the plots are $C_{02} = 0.3, X_0 = 0, \zeta_0 = 0, v = 0.3$ and $a = 1$.

for $c = 0.1,\ 1$ and 10, respectively. For small values of c, Fig. 2.13 and 2.14 depict the self-compression of bright and dark similaritons. As the value of c is reduced

more, the similaritons undergoes rapid self-compression.

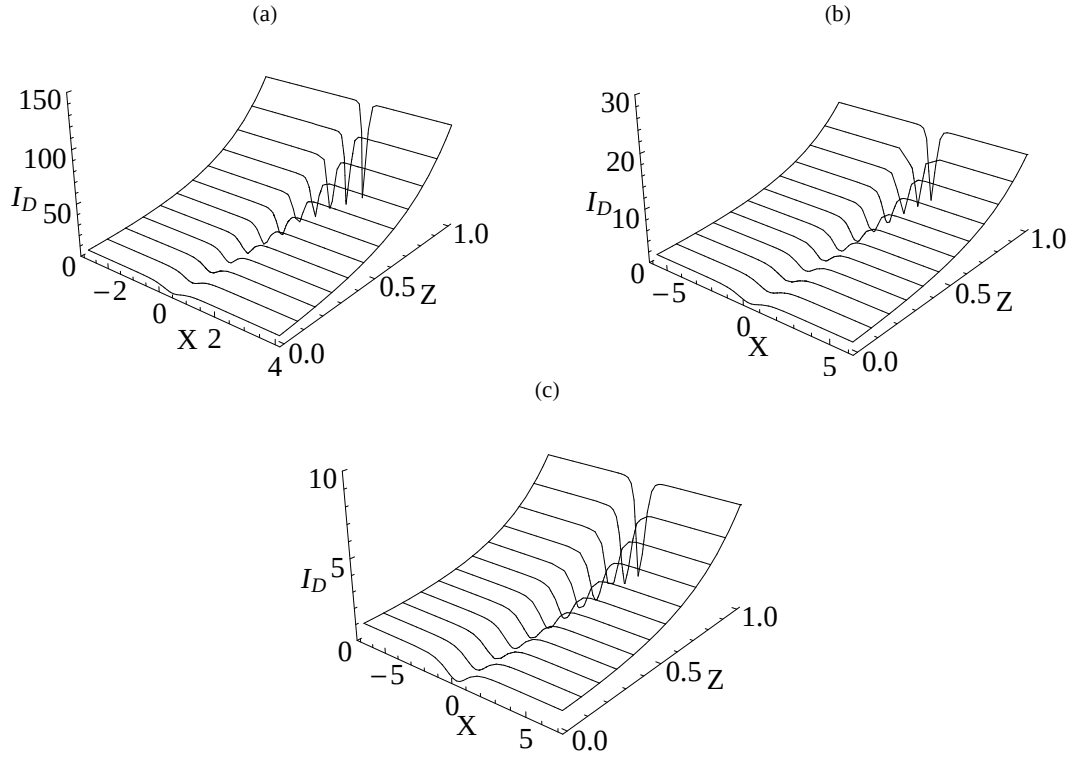

Figure 2.14: Evolution of dark similariton for generalized tapering for $c = 0.1,\ 1$ and 10, respectively. The parameters used in the plots are $C_{02} = 0.3, X_0 = 0, \zeta_0 = 0, u_0 = 1$ and $\phi = 0$.

2.4.3 Self-similar Akhmediev breathers

For +ve sign of Kerr nonlinearity, Eq. (2.49) can also be solved for Akhmediev breathers (ABs) using Eq. (2.22). Hence, the intensity expression of the self-similar AB for GNLSE (with +ve Kerr nonlinearity in Eq. (2.46)), taking $a = 1/2$ in Eq. (2.22), is given by

$$I_{AB} = \frac{1}{W^2}\left[\frac{\cos^2(\sqrt{2}\chi) + 2\ \sinh^2\zeta}{\left(\cos(\sqrt{2}\chi) - \sqrt{2}\cosh\zeta\right)^2}\right]. \tag{2.66}$$

The intensity plot for self-similar AB for sech^2-type tapering profile with $n = 1$,

given by Eq. (2.62), is shown in Fig. 2.15.

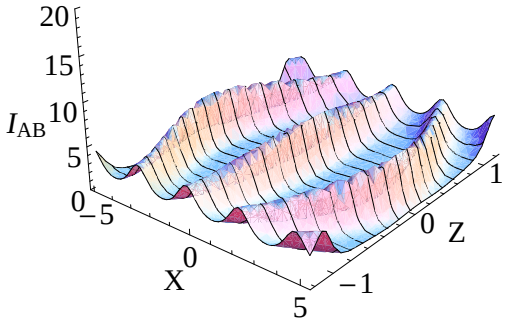

Figure 2.15: Intensity profile of self-similar AB for tapering profile given by Eq. (2.62). The parameters used in the plots are $C_{02} = 0.3, X_0 = 0, \zeta_0 = 0,\ u_0 = 0.3$ and $\phi = 0$.

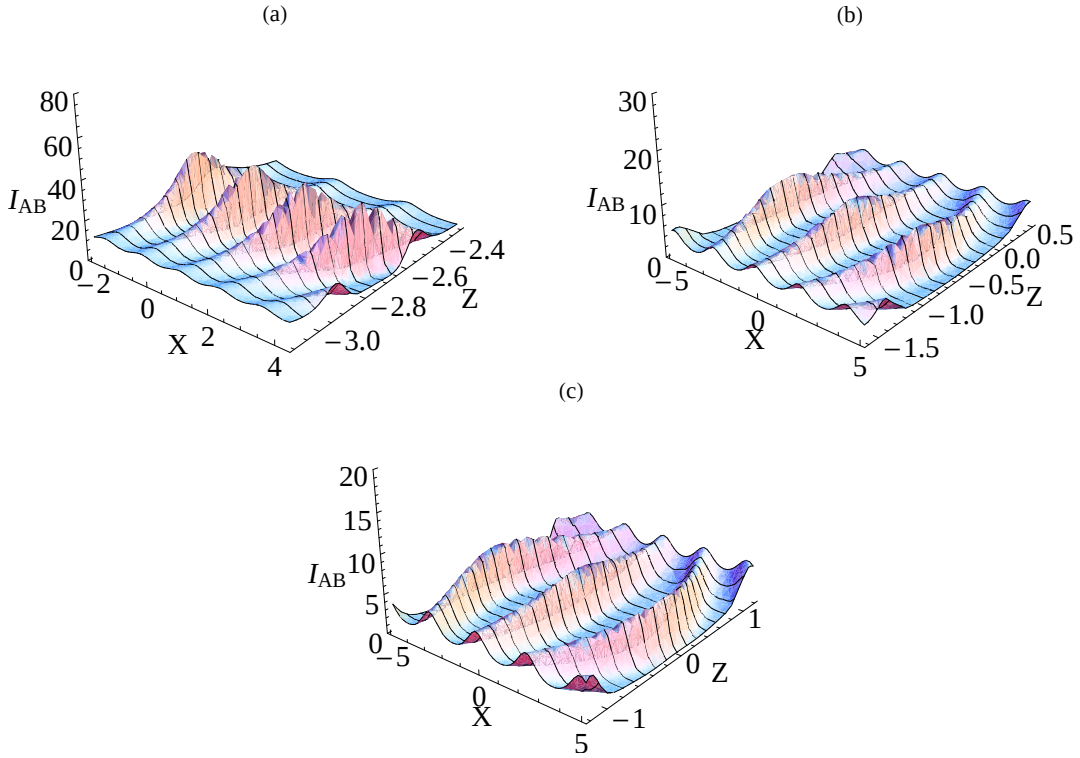

Figure 2.16: Intensity profiles of self-similar AB for generalized tapering for $n = 1$, $c = 0.1,\ 1$ and 10, respectively. The parameters used in the plots are $C_{02} = 0.3, X_0 = 0$ and $\zeta_0 = 0$.

Now using Eq. (2.63), the intensity of optical self-similar AB, for generalized

class of tapering i.e. $\widehat{F}(Z)$, can be found from Eq. (2.66). Here, we have shown (see Fig. 2.16) the intensity plots for self-similar ABs for different values of c; $c = 0.1,\ 1$ and 10, respectively.

2.4.4 Self-similar rogue waves

For +ve sign of Kerr nonlinearity, Eq. (2.49) also have rogue wave solutions given by general solution Eq. (2.23). The intensity expression of the self-similar first-order rogue wave for GNLSE, using Eq. (2.25), can be written as

$$I_{R_1} = \frac{1}{W^2}\left[1 + 8\frac{1 + 4\zeta^2 - 4\chi^2}{(1 + 4\zeta^2 + 4\chi^2)^2}\right]. \tag{2.67}$$

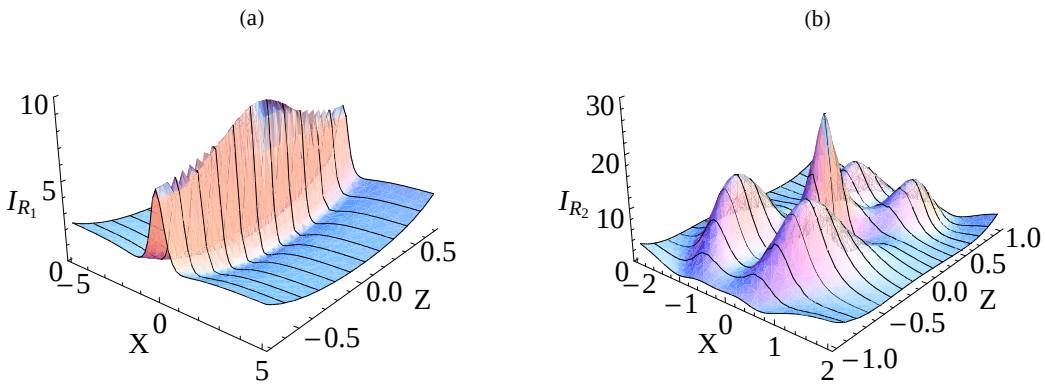

Figure 2.17: Intensity profiles of self-similar first- and second-order rogue waves for tapering profile given by Eq. (2.64). The parameters used in the plots are $C_{02} = 0.3, X_0 = 0, \zeta_0 = 0,\ u_0 = 0.3$ and $\phi = 0$.

Similarly, the intensity expression of the self-similar second-order rogue wave for GNLSE can also be found from Eq. (2.27) as

$$I_{R_2} = \frac{1}{W^2}\left[\left(\frac{D - K}{D}\right)^2 + \left(\frac{H}{D}\right)^2\right], \tag{2.68}$$

with K, H and D given by

$$K = \left(\chi^2 + \zeta^2 + \frac{3}{4}\right)\left(\chi^2 + 5\zeta^2 + \frac{3}{4}\right) - \frac{3}{4},$$
$$H = \zeta\left(\zeta^2 - 3\chi^2 + 2(\chi^2 + \zeta^2)^2 - \frac{15}{8}\right),$$
$$D = \frac{1}{3}\left(\chi^2 + \zeta^2\right)^3 + \frac{1}{4}\left(\chi^2 - 3\zeta^2\right)^2 + \frac{3}{64}\left(12\chi^2 + 44\zeta^2 + 1\right), \tag{2.69}$$

The intensity plots for self-similar first- and second-order rogue waves for sech^2-type tapering profile with $n = 2$, given by Eq. (2.64), are shown in Fig. 2.17. Using Eq. (2.65), the intensity of optical self-similar first- and second-order rogue waves, for generalized class of tapering i.e. $\widehat{F}(Z)$ for $n = 2$, can be found from Eqs. (2.67) and (2.68). Here, we have shown (see Figs. 2.18 and 2.19) the intensity plots for different values of c; $c = 0.1,\ 1$ and 10, respectively.

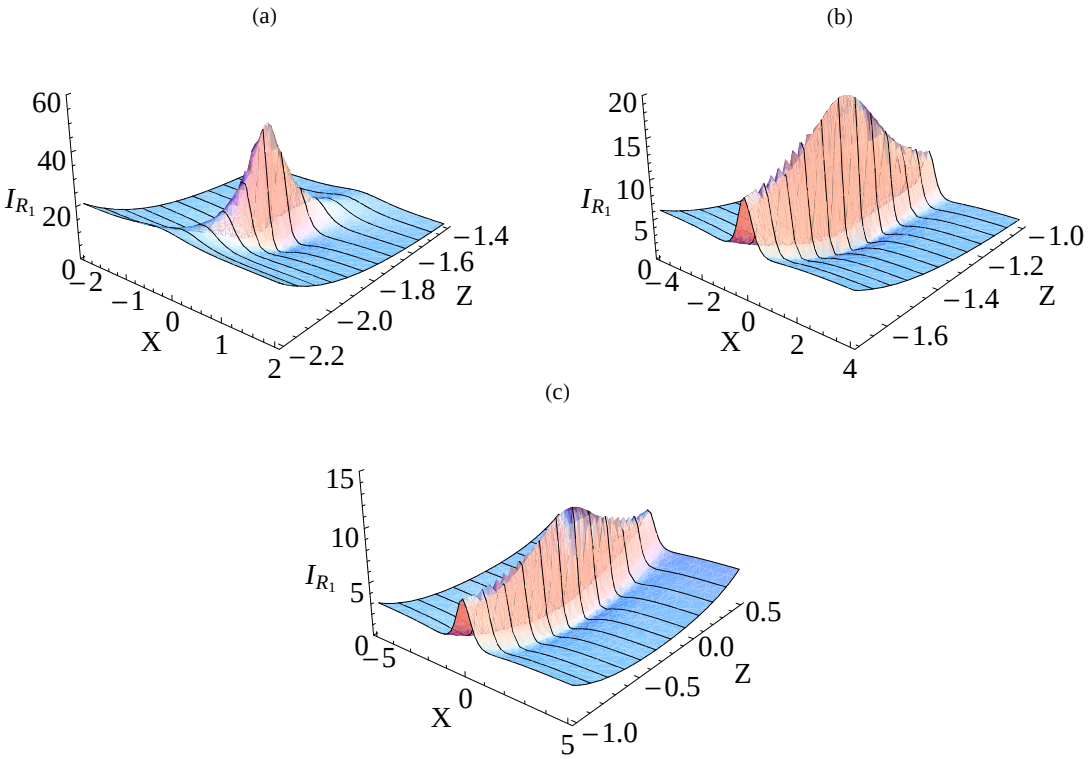

Figure 2.18: Intensity profiles of self-similar first-order rogue waves for generalized tapering for $n = 2$, and $c = 0.1,\ 1$ and 10, respectively. The parameters used in the plots are $C_{02} = 0.3, X_0 = 0$ and $\zeta_0 = 0$.

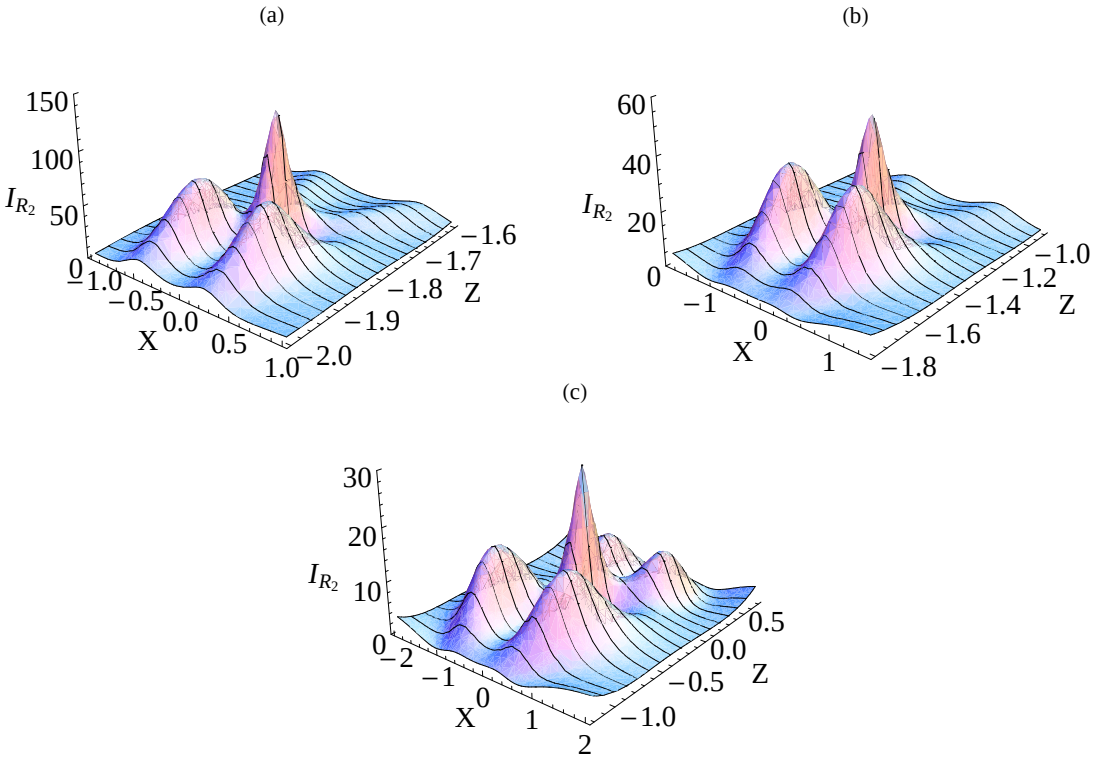

Figure 2.19: Intensity profiles of self-similar second-order rogue waves for generalized tapering for $n = 2$, and $c = 0.1,\ 1$ and 10, respectively. The parameters used in the plots are $C_{02} = 0.3, X_0 = 0$ and $\zeta_0 = 0$.

2.5 Riccati parameterized self-similar waves in sech^2-type tapered waveguide with cubic-quintic nonlinearity

Generally, as we discussed earlier, the wave propagation in graded-index nonlinear waveguide can be modelled by generalized nonlinear Schrödinger equation with cubic nonlinearity [32, 28]. However, when the intensity of the optical beam exceeds a certain value, in order to produce ultrashort pulses, a higher-order nonlinearity term arises due to nonlinear correction to the refractive index of medium. In this case, the refractive index distribution inside the waveguide will be

$$n(z,x) = n_0 + n_1 F(z)x^2 + n_2\alpha(z)|u|^2 + n_4\beta(z)|u|^4, \tag{2.70}$$

where the first two terms correspond to the linear part of refractive index and the last two terms correspond to cubic and quintic nonlinearities. The function $F(z)$ describe the geometry of tapered waveguide along the waveguide axis. The propagation of beam through tapered graded-index nonlinear waveguide amplifier with cubic-quintic nonlinearities is governed by inhomogeneous cubic-quintic nonlinear Schrödinger equation (CQNLSE)

$$i\frac{\partial U}{\partial Z}+\frac{1}{2}\frac{\partial^2 U}{\partial X^2}+F(Z)\frac{X^2}{2}U+\alpha(Z)|U|^2U+\beta(Z)|U|^4U-\frac{i}{2}G(Z)U=0. \quad (2.71)$$

Apart from nonlinear optics, Eq. (2.71) also arises in the context of Bose-Einstein condensates where quintic nonlinearity corresponds to an effective three-body interaction [51]. Recently, Dai *et al.* [52] and He *et al.* [53] investigated the self-similar bright and dark similaritons for inhomogeneous CQNLSE using similarity transformations. Motivated by their work, we have explored interesting double-kink solutions (also known as wide localized solitons [54]) for this equation. It has been found that the width of double-kink dark similaritons can be controlled by varying a wave parameter. Further we reported the existence of algebraic bright similaritons which are necessarily of the Lorentzian-type.

Employing similarity transformation, i.e. substituting Eq. (2.47) into Eq. (2.71), one obtains the standard CQNLSE as

$$i\frac{\partial \Psi}{\partial \zeta}+\frac{1}{2}\frac{\partial^2 \Psi}{\partial \chi^2}+a_1|\Psi|^2\Psi+a_2|\Psi|^4\Psi=0, \quad (2.72)$$

where the effective propagation distance, similarity variable, amplitude, guiding-center position and phase are given respectively as

$$\zeta(Z)=\zeta_0+\int_0^Z\frac{dS}{W^2(S)},\quad \chi(X,Z)=\frac{X-X_c(Z)}{W(Z)},$$

$$A(Z)=\frac{1}{W^2(Z)},\quad X_c(Z)=W(Z)\left(X_0+C_{02}\int_0^Z\frac{dS}{W^2(S)}\right),$$

$$\Phi(X,Z)=\frac{X^2}{2W}\frac{dW}{dZ}+\frac{C_{02}X}{W}-\frac{C_{02}^2}{2}\int_0^Z\frac{dS}{W^2(S)}, \quad (2.73)$$

with $C_2(0) = C_{02},\ X_c(0) = X_0$ and $W(0) = 1$. Further, the tapering function, gain and cubic-quintic nonlinearity coefficients are related to similariton width as

$$d^2W/dZ^2 - F(Z)W = 0, \quad G(Z) = -d[\ln W(Z)]/dZ, \tag{2.74}$$

$$\alpha(Z) = a_1\ W^2(Z), \quad \beta(Z) = a_2\ W^6(Z). \tag{2.75}$$

Now, in order to find exact soliton-like solutions of Eq. (2.72), we have chosen the following ansatz

$$\Psi(\zeta, \chi) = \rho(\xi)\ e^{i[\theta(\xi) - k\zeta]}, \tag{2.76}$$

where $\xi = (\chi - u\zeta)$ is the travelling coordinate. Substituting Eq. (2.76) into Eq. (2.72) and separating out the real and imaginary parts of the equation, one obtain the coupled equations in ρ and θ. One of these equations can be completely solved to obtain $\theta'(\xi) = u$. Using this, the other equation can be reduced to

$$\rho'' + (2k + u^2)\rho + 2a_1\rho^3 + 2a_2\rho^5 = 0. \tag{2.77}$$

This elliptic equation is known to admit a variety of solutions such as periodic, kink and solitary wave-type-solutions. In general, all travelling wave solutions of Eq. (2.77) can be expressed in a generic form by means of the Weierstrass $\wp$-function [55]. In the most general case, this equation can be mapped to ϕ^6 field equation to obtain double kink-type [56] as well as bright and dark soliton solutions [57]. It is interesting to note that if coefficient of linear term in ρ is zero i.e. $2k + u^2 = 0$, then Eq. (2.77) admits Lorentzian-type solutions [58].

2.5.1 Double-kink similaritons

In the most general case, when all the coefficients have nonzero values, one can obtain double-kink type soliton solutions for Eq. (2.77) of the form [56]

$$\rho(\xi) = \frac{p \sinh(q\xi)}{\sqrt{\epsilon + \sinh^2(q\xi)}}, \tag{2.78}$$

where $a_1 = \frac{q^2}{p^2}\left(\frac{2\epsilon-3}{\epsilon}\right)$, $a_2 = -\frac{3q^2}{2p^4}\left(\frac{\epsilon-1}{\epsilon}\right)$, and $2k + u^2 = -q^2\left(\frac{\epsilon-3}{\epsilon}\right)$. These relations can be solved to fix the wave parameters p, q and k. Here ϵ is a free parameter which control the width of soliton solution. The amplitude profile for soliton solution given by Eq. (2.78) is shown in Fig. 2.20 for different values of ϵ. From figure, it is clear that the interesting 'double-kink' feature of the solution exists only for sufficiently large values of ϵ. One can also point out that as value of ϵ changes, it only effects the width of wave but amplitude of wave remains same.

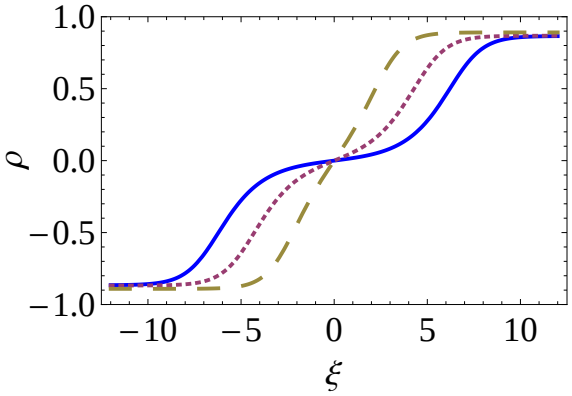

Figure 2.20: Amplitude profiles for double-kink soliton given by Eq. (2.78) for different values of ϵ. The parameters used in the plots are $a_1 = 1$, $a_2 = -1$ and $u = 1.2$. Solid line corresponds to $\epsilon = 1000$, $p = 0.866$ and $q = 0.612$. Dotted line corresponds to $\epsilon = 100$, $p = 0.868$ and $q = 0.618$. Dashed line corresponds to $\epsilon = 10$, $p = 0.891$ and $q = 0.680$.

The general expression of the intensity of double-kink similariton for Eq. (2.71) is given as

$$\begin{aligned} I_{DK} &= |U(X,Z)|^2 = A^2(Z)|\Psi(\zeta,\chi)|^2 \\ &= \frac{1}{W^4(Z)}\left(\frac{p^2\sinh^2(q(\chi-u\zeta))}{\epsilon+\sinh^2(q(\chi-u\zeta))}\right). \end{aligned} \tag{2.79}$$

In order to gain further insight into the dynamical behavior of double-kink similariton, one needs a functional form of tapering and width functions. Considering sech^2-type tapering for $n = 1$ given by Eq. (2.62), one can find the intensity of double-kink similariton from Eq. (2.79). In Fig. 2.21, the intensity profiles for double-kink dark similaritons are shown for different values of ϵ.

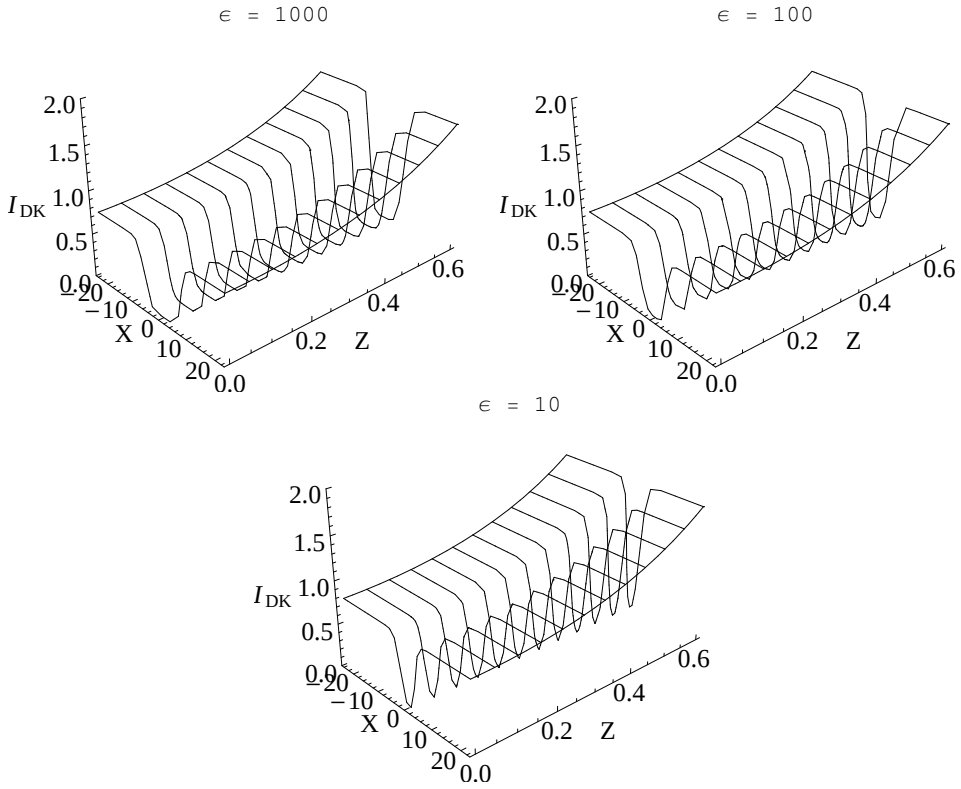

Figure 2.21: Evolution of double-kink dark similaritons of Eq. (2.71) for different values of ϵ, $\epsilon = 1000$, $\epsilon = 100$ and $\epsilon = 10$ respectively. The parameters used in the plots are $C_{02} = 0.3, X_0 = 0$ and $\zeta_0 = 0$. The values of other parameters are same as mentioned in the caption of Fig. 2.20.

Now using Eq. (2.63), the intensity of double-kink similaritons, for generalized class of tapering i.e. $\widehat{F}(Z)$, can be found from Eq. (2.79). Here, the evolution of double-kink similaritons is shown (see Fig. 2.22) for different values of c; $c = 0.4$, $c = 1$, $c = 10$ respectively.

2.5.2 Lorentzian-type similaritons

For the parametric condition $k = \frac{-u^2}{2}$, Eq. (2.77) can be solved to obtain very interesting algebraic soliton solutions. In particular, for $a_1 < 0$ and $a_2 > 0$, the solution of Eq. (2.77) is of the following form

$$\rho(\xi) = \frac{1}{\sqrt{M + N\xi^2}}, \tag{2.80}$$

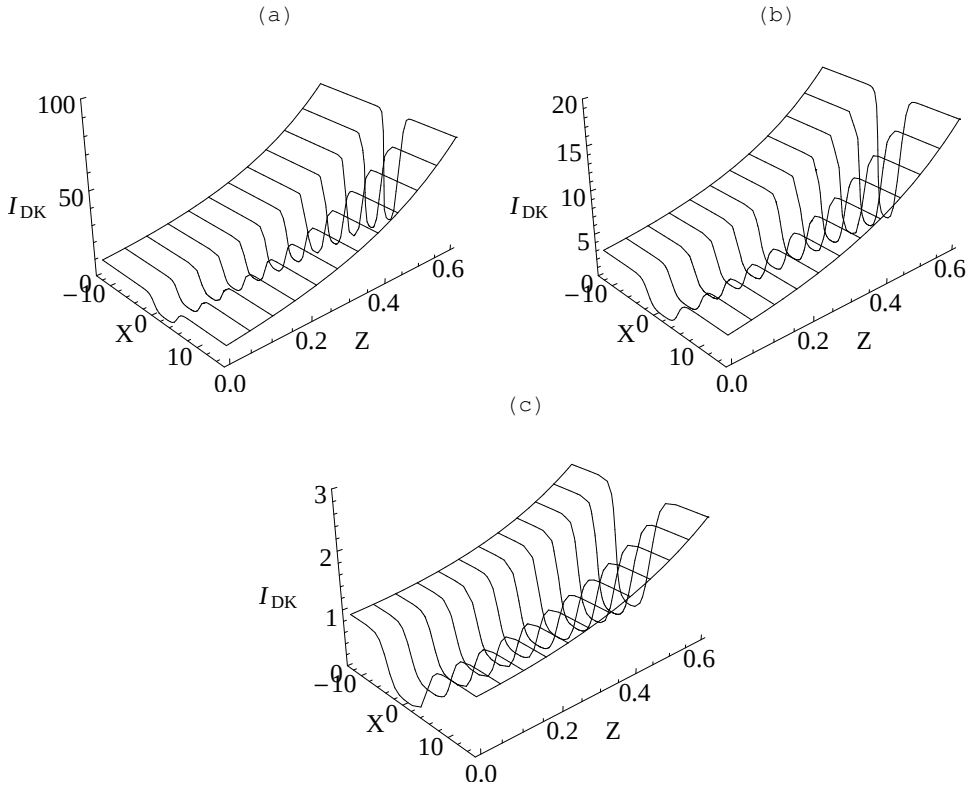

Figure 2.22: Evolution of double-kink dark similaritons of Eq. (2.71) for generalized tapering for $n = 1$, and $c = 0.4,\ 1$ and 10, respectively. The parameters used in the plots are $\epsilon = 100, C_{02} = 0.3, X_0 = 0$ and $\zeta_0 = 0$. The values of other parameters are same as mentioned in the caption of Fig. 2.20.

where $M = \frac{-2a_2}{3a_1}$ and $N = -a_1$. The amplitude profile for soliton solution given by Eq. (2.80) is shown in Fig. 2.23. The expression of the intensity of these

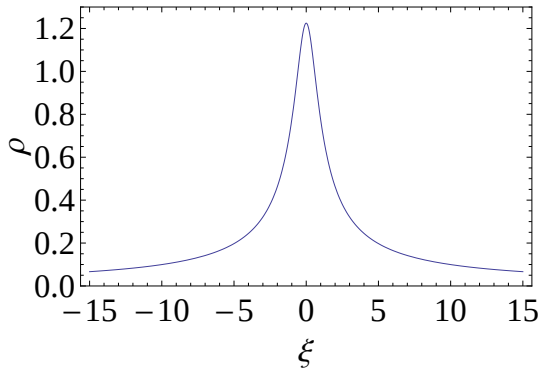

Figure 2.23: Amplitude profile for Lorentzian-type soliton given by Eq. (2.80) for $a_1 = -1,\ a_2 = 1$ and $u = 1.2$.

Lorentzian-type similaritons for Eq. (2.71) will be of the following form

$$I_2 = \frac{1}{W^4(Z)} \left(\frac{-3a_1}{2a_2 + 3a_1^2(\chi - u\zeta)^2} \right). \tag{2.81}$$

Now using sech^2-type tapering for $n = 1$ given by Eq. (2.62), the intensity of Lorentzian-type similaritons can be found from Eq. (2.81) which is shown in Fig. 2.24.

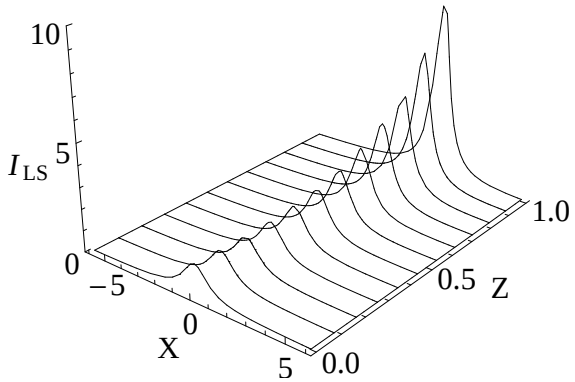

Figure 2.24: Evolution of Lorentzian-type bright similariton of Eq. (2.71) for $a_1 = -1,\ a_2 = 1$ and $u = 1.2$. The other parameters used in the plot are $C_{02} = 0.3, X_0 = 0$ and $\zeta_0 = 0$.

Again using Eq. (2.63), the intensity of Lorentzian-type similaritons, for generalized class of tapering i.e. $\widehat{F}(Z)$, can be found from Eq. (2.81). The evolution of Lorentzian-type similaritons is shown (see Fig. 2.25) for different values of c; $c = 0.4,\ c = 1,\ c = 10$ respectively.

2.6 Self-similar waves in parabolic tapered waveguide

Other type of possible tapering is the parabolic tapering, which finds applications in a number of passive and active optical devices for the propagation of guided wave through them. For instance, parabolic tapering has been proved advantageous

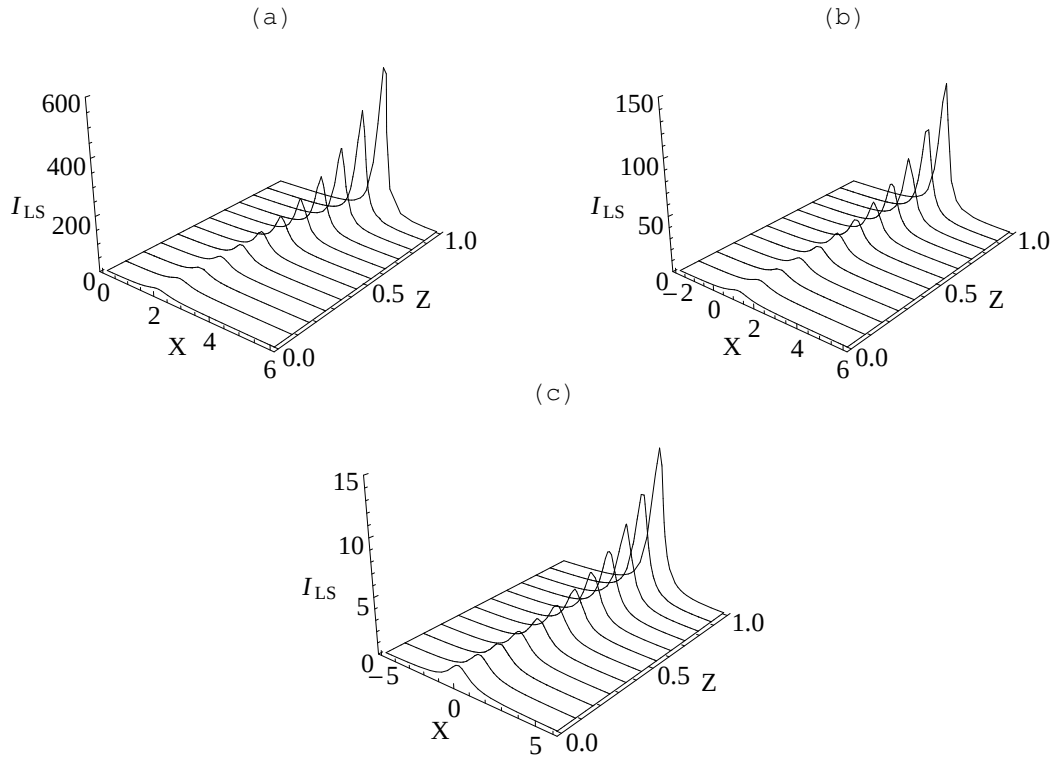

Figure 2.25: Evolution of Lorentzian-type bright similaritons of Eq. (2.71) for generalized tapering for $n = 1$, and $c = 0.4,\ 1$ and 10, respectively. The parameters used in the plots are $a_1 = -1, a_2 = 1, u = 1.2, C_{02} = 0.3, X_0 = 0$ and $\zeta_0 = 0$.

for mode coupling as it reduces the length of multi-mode interference device [59, 60, 61]. Apart from this, it also finds applications in fiber-based sensors [62, 63]. Here, we study the propagation of similaritons through perimetrically controlled parabolically tapered wave guide and also looking to the effects of these parameters on the intensity of similaritons. For parabolic tapered fiber the functional form of $F(Z)$ is given as

$$F(Z) = -2\alpha(1 - 2\alpha z^2), \tag{2.82}$$

where, α is a positive real number. For choice of α the tapered profile changes its width as shown in Fig. 2.26. The width and gain profiles from Eqs. (2.51) and (2.52) can be written as

$$W(Z) = \exp(-\alpha Z^2), \tag{2.83}$$

and

$$G(Z) = 2\alpha Z. \tag{2.84}$$

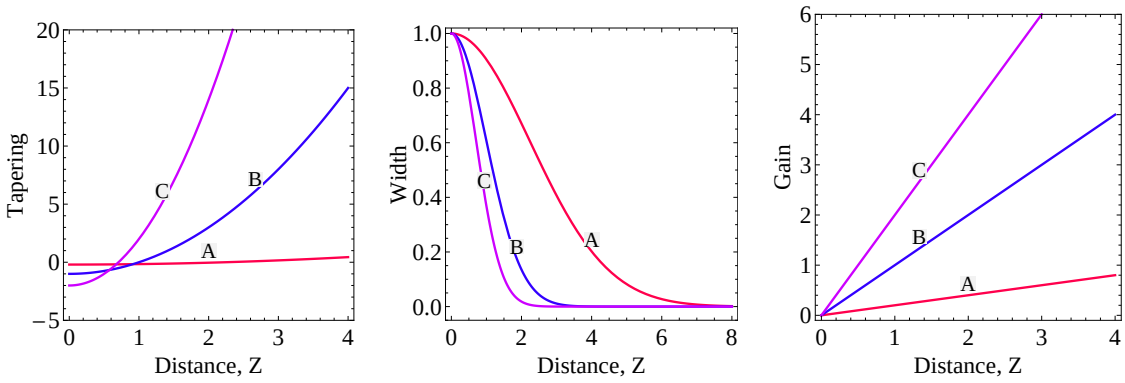

Figure 2.26: Profiles of tapering, width and gain, respectively, for different values of taper parameter α. Curves A, B, C corresponds to profile for $\alpha = 0.1, 0.5$ and 1, respectively.

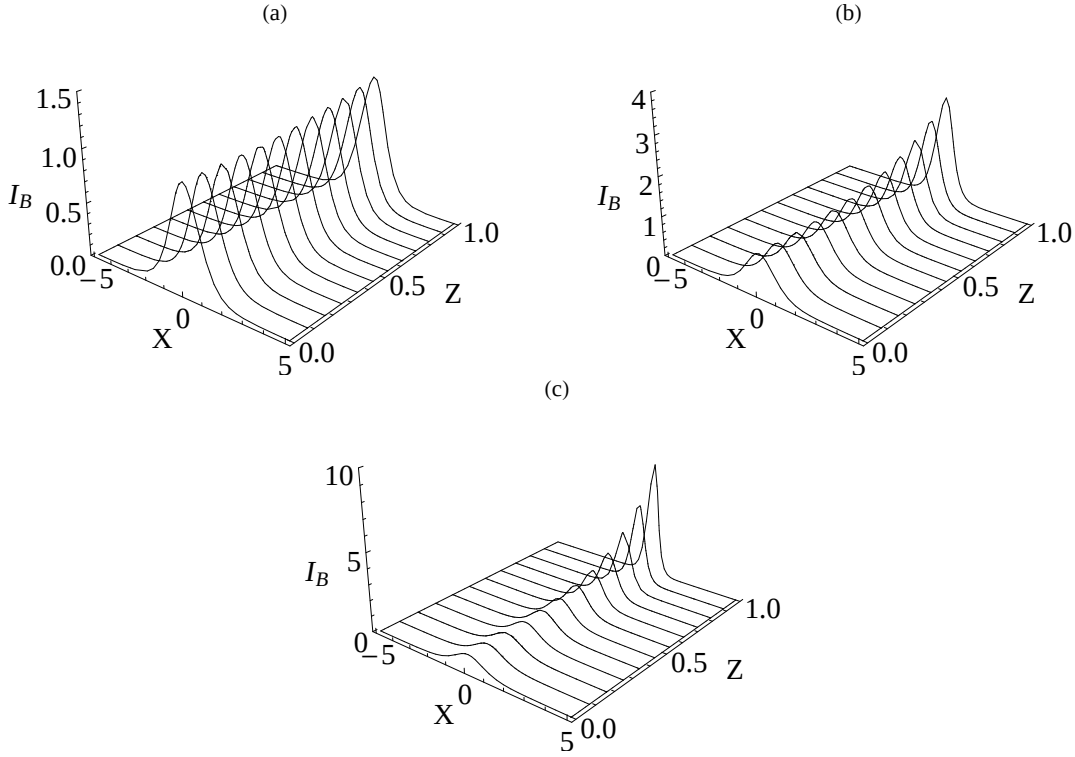

Figure 2.27: Evolution of bright similariton for parabolic tapering for different values of taper parameter α: (a) $\alpha = 0.1$, (b) $\alpha = 0.5$, and (c) $\alpha = 1$. The parameters used in the plots are $C_{02} = 0.3, X_0 = 0, \zeta_0 = 0, v = 0.3$ and $a = 1$.

In Fig. 2.26, we depict the behavior of tapering profile, width, and gain functions along the propagation distance for different values of α. Variation of gain coefficient depends on various factors, such as temperature, wavelength fluctuation, pump power etc.. Under ideal conditions if these conditions are controlled properly then parabolic tapering results into linear increase in the gain, which in turn act as an amplifier, can help the propagation of the light beam even in the anti-guiding situation.

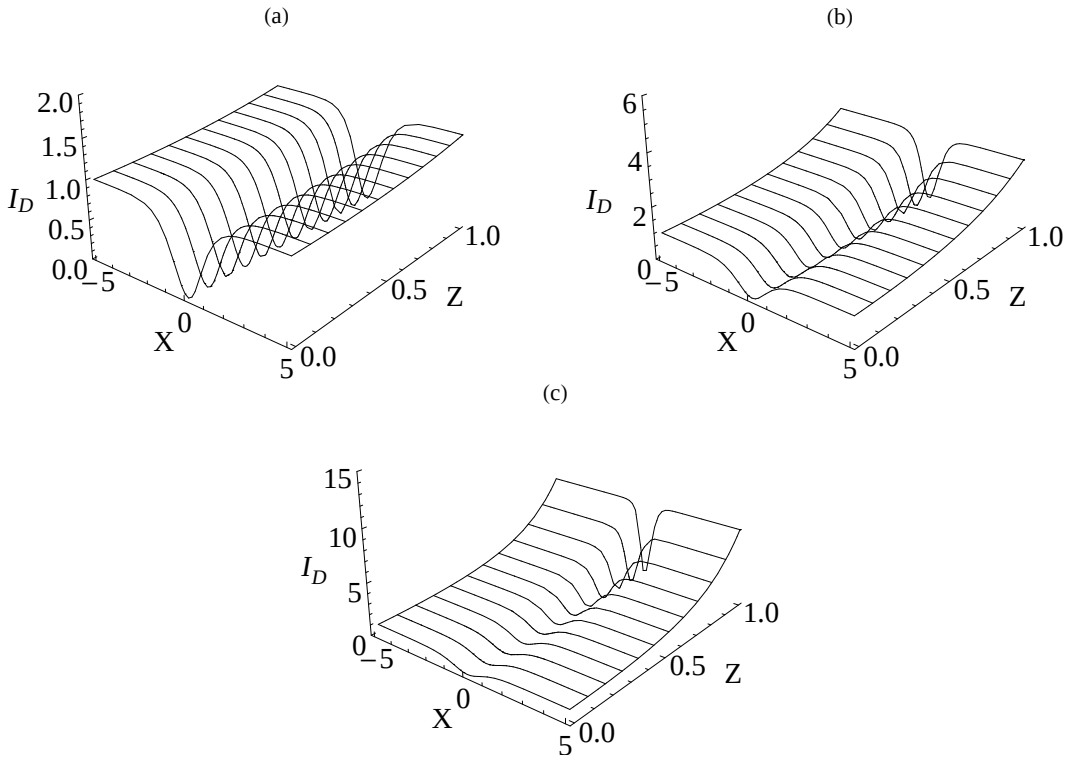

Figure 2.28: Evolution of dark similariton for parabolic tapering for different values of taper parameter α: (a) $\alpha = 0.1$, (b) $\alpha = 0.5$, and (c) $\alpha = 1$. The parameters used in the plots are $C_{02} = 0.3, X_0 = 0, \zeta_0 = 0, u_0 = 1$ and $\phi = 0$.

Now using Eq. (2.83), the intensity of optical bright and dark similaritons for parabolic tapering can be found from Eqs. (2.56) and (2.57). Here we have depicted the evolution of bright and dark similariton (see Figs. 2.27 and 2.28) for $\alpha = 0.1, 0.5$ and 1, respectively. It is clear from the plots that the intensity of similaritons undergoes self-compression as the taper expansion coefficient α increases.

Lastly, one can extend the isospectral deformation technique to tailor the parabolic tapering profile also, but due to the complex mathematical structure, it becomes too difficult to handle it analytically.

2.7 Conclusion

2.7.1 Summary and discussion

In this chapter, a systematic analytical approach is presented to control the dynamical behavior of self-similar waves for generalized nonlinear Schrödinger equation (GNLSE), given by (2.46), governing the wave propagation through tapered graded-index waveguide amplifier. This has been accomplished by first reducing the GNLSE into a standard NLSE using similarity transformation and then invoking the isospectral Hamiltonian approach to obtain a family of self-similar solutions containing bright and dark similaritons, self-similar Akhmediev breathers (ABs) and self-similar rogue waves [44].

First, we have studied the wave propagation assuming sech^2-type tapering profile, $F(Z) = n^2 - n(n+1)\,\mathrm{sech}^2 Z$ for $n = 1$ and $n = 2$, in a cubic nonlinear medium. From the Figs. 2.5 and 2.10, one can see that for $n = 2$ the variation in the magnitude of tapering profile is more as compared to $n = 1$ profile, which also effects the corresponding width and gain functions. For $n = 2$, the width profile approaches its asymptotic value more rapidly and hence the intensity of bright and dark similaritons is more Fig. 2.11 for same range of Z as used for $n = 1$ Fig. 2.6. Further, for both cases, a class of allowed tapering, width and gain profiles has been identified for different values of Riccati parameter c, using Eqs. (2.53) to (2.55), as shown in Figs. 2.7 and 2.12 for $n = 1$ and $n = 2$, respectively. Here for each case, it is clear that all tapering profiles, corresponding to different values of c, have same asymptotic value but have different magnitude variation for small range of Z. It means this generalization gives us freedom to generate a class of tapering profiles in a same asymptotic range. This imposes a significant effect on the width profile that

it approaches the asymptotic value more recently as value of c decreases. Due to this, the intensity of bright and dark similaritons experience rapid self-compression as value of c decreases, shown in Figs. 2.8 and 2.9 for $n = 1$, and Figs. 2.13 and 2.14 for $n = 2$. The same analysis has also been carried out for the self-similar ABs Eq. (2.66), and first- and second-order rogue waves Eqs. (2.67) and (2.68), respectively. The generalized intensity profiles have been shown for self-similar ABs Fig. 2.16 and for self-similar rogue waves Figs. 2.18 and 2.19. Hence, the intensity of these rational solutions can be made sufficiently large for small values of c, paving the way for practical applications of energetic rogue waves in nonlinear optics.

Further, the study has been done for wave propagation in a tapered graded-index waveguide with cubic-quintic nonlinearity and report the existence of double-kink dark similaritons Eq. (2.79) and Lorentzian-type bright similaritons Eq. (2.81). The width of double-kink similaritons can be controlled by varying a wave parameter as shown in Fig. 2.21. The generalized intensity profiles for these similaritons is shown in Figs. 2.22 and 2.25 and it is found that they undergoes more rapid self-compression with small values of c as compared to the similaritons in a cubic nonlinear medium. It is because here the amplitude of similariton varies as inversely proportional to the square of the width function unlike it varies inversely proportional to the width function linearly in a cubic nonlinear medium.

We have also explored the existence of self-similar waves in a parametrically controlled parabolic tapered waveguide, given by $F(Z) = -2\alpha(1 - 2\alpha z^2)$ where α is a taper parameter. It is found that α has a remarkable effect on the intensity of bright similaritons Fig. 2.27 and also on dark similaritons Fig. 2.28, as both undergoes self-compression with increasing value of taper parameter α.

Most part of the work, presented here, is appeared in the Refs. [44, 50].

2.7.2 Concluding remark

In conclusion, employing the isospectral Hamiltonian approach one can obtain a class of tapering profile which leads to rapid self-compression of self-similar waves.

Interestingly, the intensity of self-similar waves can be made very large, thus paving the way for experimental realization of highly energetic waves. These results are quite general and can be obtained for any tapering profile. The choice of sech^2-type tapered waveguide was made for illustrative purposes. Owing to the exact nature of these results, we hope that procedure described here can help in modeling the tapered profiles that find practical applications in optical telecommunication systems. Apart from it, this approach can also be used to control the dynamics of self-similar waves in Bose-Einstein condensate through the modulation of time dependent trapping potential. We construct a family of self-similar waves, related through a Riccati parameter, in quasi one-dimension Gross-Pitaevskii equation with time-varying parameters [15].

Bibliography

[1] YS Kivshar and GP Agrawal. *Optical solitons: from fibers to photonic crystals*. Academic Press, London, 2003.

[2] RY Chiao, E Garmire, and CH Townes. Self-trapping of optical beams. *Physical Review Letters*, 13(15):479, 1964.

[3] A Barthelemy, S Maneuf, and C Froehly. Propagation soliton et auto-confinement de faisceaux laser par non linearité optique de kerr. *Optics Communications*, 55(3):201–206, 1985.

[4] SL McCall and EL Hahn. Self-induced transparency by pulsed coherent light. *Physical Review Letters*, 18(21):908, 1967.

[5] A Hasegawa and F Tappert. Transmission of stationary nonlinear optical pulses in dispersive dielectric fibers. i. Anomalous dispersion. *Applied Physics Letters*, 23:142, 1973.

[6] LF Mollenauer, RH Stolen, and JP Gordon. Experimental observation of picosecond pulse narrowing and solitons in optical fibers. *Physical Review Letters*, 45:1095–1098, 1980.

[7] AB Shabat and VE Zakharov. Exact theory of two-dimensional self-focusing and one-dimensional self-modulation of waves in nonlinear media. *Soviet Physics JETP*, 34:62–69, 1972.

[8] VE Zakharov and AB Shabat. Interaction between solitons in a stable medium. *Soviet Physics JETP*, 37(5):823–828, 1973.

[9] YS Kivshar and BL Davies. Dark optical solitons: physics and applications. *Physics Reports*, 298(2):81–197, 1998.

[10] N Akhmediev, A Ankiewicz, and M Taki. Waves that appear from nowhere and disappear without a trace. *Physics Letters A*, 373(6):675–678, 2009.

[11] DR Solli, C Ropers, P Koonath, and B Jalali. Optical rogue waves. *Nature*, 450(7172):1054–1057, 2007.

[12] B Kibler, J Fatome, C Finot, G Millot, F Dias, G Genty, N Akhmediev, and JM Dudley. The Peregrine soliton in nonlinear fibre optics. *Nature Physics*, 6(10):790–795, 2010.

[13] CN Kumar, R Gupta, A Goyal, S Loomba, TS Raju, and PK Panigrahi. Controlled giant rogue waves in nonlinear fiber optics. *Physical Review A*, 86(2):025802, 2012.

[14] YV Bludov, VV Konotop, and N Akhmediev. Matter rogue waves. *Physical Review A*, 80(3):033610, 2009.

[15] PK Panigrahi, R Gupta, A Goyal, and CN Kumar. Riccati generalization of self-similar solutions of nonautonomous Gross-Pitaevskii equation. *The European Physical Journal Special Topics*, 222(3-4):655–663, 2013.

[16] JM Dudley, G Genty, F Dias, B Kibler, and N Akhmediev. Modulation instability, Akhmediev breathers and continuous wave supercontinuum generation. *Optics Express*, 17(24):21497, 2009.

[17] K Hammani, B Kibler, C Finot, and A Picozzi. Emergence of rogue waves from optical turbulence. *Physics Letters A*, 374(34):3585–3589, 2010.

[18] N Akhmediev and VI Korneev. Modulation instability and periodic solutions of the nonlinear Schrödinger equation. *Theoretical and Mathematical Physics*, 69(2):1089–1093, 1986.

[19] DH Peregrine. Water waves, nonlinear Schrödinger equations and their solutions. *The Journal of the Australian Mathematical Society*, 25(01):16–43, 1983.

[20] N Akhmediev, A Ankiewicz, and JM Soto-Crespo. Rogue waves and rational solutions of the nonlinear Schrödinger equation. *Physical Review E*, 80(2):026601, 2009.

[21] SA Ponomarenko and GP Agrawal. Optical similaritons in nonlinear waveguides. *Optics Letters*, 32(12):1659–1661, 2007.

[22] VR Almeida, RR Panepucci, and M Lipson. Nanotaper for compact mode conversion. *Optics Letters*, 28(15):1302–1304, 2003.

[23] M Krause, H Renner, and E Brinkmeyer. Efficient Raman lasing in tapered silicon waveguides. *Spectroscopy*, 21(1):26, 2006.

[24] TA Birks, WJ Wadsworth, and PStJ Russell. Supercontinuum generation in tapered fibers. *Optics Letters*, 25(19):1415–1417, 2000.

[25] WK Burns, M Abebe, and CA Villarruel. Parabolic model for shape of fiber taper. *Applied Optics*, 24(17):2753–2755, 1985.

[26] J Bures, S Lacroix, and J Lapierre. Analysis of a directional coupler based on fused single-mode optical fibers. *Applied Optics*, 22:1918–1922, 1983.

[27] JC Campbell. Tapered waveguides for guided wave optics. *Applied Optics*, 18(6):900–902, 1979.

[28] TS Raju and PK Panigrahi. Optical similaritons in a tapered graded-index nonlinear-fiber amplifier with an external source. *Physical Review A*, 84(3):033807, 2011.

[29] GL Lamb. *Elements of soliton theory*. John Wiley&Sons, New York, 1980.

[30] AC Peacock. *Applications of light propagation in novel photonic devices*. PhD thesis, University of Southampton, 2004.

[31] VI Kruglov, AC Peacock, and JD Harvey. Exact self-similar solutions of the generalized nonlinear Schrödinger equation with distributed coefficients. *Physical Review Letters*, 90(11):113902, 2003.

[32] SA Ponomarenko and GP Agrawal. Do solitonlike self-similar waves exist in nonlinear optical media? *Physical Review Letters*, 97(1):013901, 2006.

[33] JM Dudley, C Finot, DJ Richardson, and G Millot. Self-similarity in ultrafast nonlinear optics. *Nature Physics*, 3(9):597–603, 2007.

[34] ME Fermann, VI Kruglov, BC Thomsen, JM Dudley, and JD Harvey. Self-similar propagation and amplification of parabolic pulses in optical fibers. *Physical Review Letters*, 84(26):6010, 2000.

[35] VI Kruglov, AC Peacock, JM Dudley, and JD Harvey. Self-similar propagation of high-power parabolic pulses in optical fiber amplifiers. *Optics Letters*, 25(24):1753–1755, 2000.

[36] PJ Olver. *Applications of Lie groups to differential equations*, volume 107. Springer, 2000.

[37] F Cooper, A Khare, and UP Sukhatme. *Supersymmetry in quantum mechanics*. World Scientific Publishing Company, 2001.

[38] L Infeld and TE Hull. The factorization method. *Reviews of Modern Physics*, 23(1):21, 1951.

[39] B Mielnik. Factorization method and new potentials with the oscillator spectrum. *Journal of Mathematical Physics*, 25:3387, 1984.

[40] CN Kumar. Isospectral Hamiltonians: generation of the soliton profile. *Journal of Physics A: Mathematical and General*, 20(15):5397, 1987.

[41] A Khare and CN Kumar. Landau level spectrum for charged particle in a class of non-uniform magnetic fields. *Modern Physics Letters A*, 8(06):523–529, 1993.

[42] ED Filho and JR Ruggiero. H-bond simulation in DNA using a harmonic oscillator isospectral potential. *Physical Review E*, 56(4):4486, 1997.

[43] W Alka, A Goyal, and CN Kumar. Nonlinear dynamics of DNA–Riccati generalized solitary wave solutions. *Physics Letters A*, 375(3):480–483, 2011.

[44] A Goyal, R Gupta, S Loomba, and CN Kumar. Riccati parameterized self-similar waves in tapered graded-index waveguides. *Physics Letters A*, 376(45):3454–3457, 2012.

[45] VN Serkin, A Hasegawa, and TL Belyaeva. Nonautonomous solitons in external potentials. *Physical Review Letters*, 98(7):074102, 2007.

[46] VN Serkin, A Hasegawa, and TL Belyaeva. Solitary waves in nonautonomous nonlinear and dispersive systems: nonautonomous solitons. *Journal of Modern Optics*, 57(14-15):1456–1472, 2010.

[47] R Atre, PK Panigrahi, and GS Agarwal. Class of solitary wave solutions of the one-dimensional Gross–Pitaevskii equation. *Physical Review E*, 73(5):056611, 2006.

[48] CQ Dai, YY Wang, Q Tian, and JF Zhang. The management and containment of self-similar rogue waves in the inhomogeneous nonlinear Schrödinger equation. *Annals of Physics*, 327(2):512–521, 2012.

[49] Q Tian, Q Yang, CQ Dai, and JF Zhang. Controllable optical rogue waves: Recurrence, annihilation and sustainment. *Optics Communications*, 284(8):2222–2225, 2011.

[50] A Goyal, R Gupta, CN Kumar, TS Raju, and PK Panigrahi. Controlling optical similaritons in a graded-index nonlinear waveguide by tailoring of the tapering profile. *Optics Communications*, 300:236–243, 2013.

[51] P Das, M Vyas, and PK Panigrahi. Loss of superfluidity in the Bose-Einstein condensate in an optical lattice with cubic and quintic nonlinearity. *Journal of Physics B: Atomic, Molecular and Optical Physics*, 42(24):245304, 2009.

[52] CQ Dai, YY Wang, and XG Wang. Ultrashort self-similar solutions of the cubic-quintic nonlinear Schrödinger equation with distributed coefficients in the inhomogeneous fiber. *Journal of Physics A: Mathematical and Theoretical*, 44(15):155203, 2011.

[53] JD He and JF Zhang. Self-similar optical pulses tunneling in cubic-quintic nonlinear media with distributed coefficients. *Journal of Physics A: Mathematical and Theoretical*, 44(20):205203, 2011.

[54] LEA Meza, ADS Dutra, and MB Hott. Wide localized solitons in systems with time-and space-modulated nonlinearities. *Physical Review E*, 86(2):026605, 2012.

[55] E Magyari. Kinks and periodons at a t = 0 first-order phase transition point in one-dimensional anharmonic lattices. *Zeitschrift für Physik B: Condensed Matter*, 43(4):345–351, 1981.

[56] NH Christ and TD Lee. Quantum expansion of soliton solutions. *Physical Review D*, 12(6):1606, 1975.

[57] SN Behera and A Khare. Classical φ6-field theory in (1+ 1) dimensions. A model for structural phase transitions. *Pramana-Journal of Physics*, 15(3):245–269, 1980.

[58] Alka, A Goyal, R Gupta, CN Kumar, and TS Raju. Chirped femtosecond solitons and double-kink solitons in the cubic-quintic nonlinear Schrödinger equation with self-steepening and self-frequency shift. *Physical Review A*, 84(6):63830, 2011.

[59] WK Burns and M Abebe. Coupling model for fused fiber couplers with parabolic taper shape. *Applied Optics*, 26(19):4190–4192, 1987.

[60] DS Levy, R Scarmozzino, and RM Osgood Jr. Length reduction of tapered n x n mmi devices. *IEEE Photonics Technology Letters*, 10(6):830–832, 1998.

[61] A Hosseini, J Covey, DN Kwong, and RT Chen. Tapered multi-mode interference couplers for high order mode power extraction. *Journal of Optics A: Pure and Applied Optics*, 12(7):075502, 2010.

[62] M Ahmad and LL Hench. Effect of taper geometries and launch angle on evanescent wave penetration depth in optical fibers. *Biosensors and Bioelectronics*, 20(7):1312–1319, 2005.

[63] RK Verma, AK Sharma, and BD Gupta. Surface plasmon resonance based tapered fiber optic sensor with different taper profiles. *Optics Communications*, 281(6):1486–1491, 2008.

Chapter 3

Chirped solitons in an optical gain medium with two-photon absorption

3.1 Introduction

Optical solitons are a subject of intense research owing to their potential applications in high speed communications [1] and all-optical processing [2, 3]. In many optical applications, it is desirable to reduce the pulse power required to form a soliton, particularly for switching applications. The switching devices are very useful in connecting input and output ports. In order to reduce the required power and the switching threshold, one can use materials with high nonlinear index coefficients than that of silica. However, in many cases the increased nonlinear index coefficient is accompanied by an enhanced nonlinear absorption coefficient of the material, which corresponds to two-photon absorption (TPA). It is therefore important to study the optical wave propagation in the presence of TPA. In this work, we have considered the effect of TPA in nonlinear optical medium and obtained chirped bright and dark solitons supported by localized gain. The chirped solitons attracted a lot of attention because of their practical applications in optical communication systems

in the terms of pulse compression. It is observed that inhomogeneous gain exactly balance the losses due to TPA, which results into soliton solution for arbitrary value of TPA coefficient [4]. The existence of double-kink and fractional-transform solitons have been reported for this model. Interestingly, the width of double-kink solitons and their corresponding chirp can be controlled by modulating the gain profile. The chapter begins with the introduction of chirped optical solitons and the process of two-photon absorption. Then a short overview of the work done on this problem is presented. Finally, considering modified form of nonlinear Schrödinger equation, a class of soliton solutions will be presented in different parameter regimes with corresponding chirp and gain profiles.

3.2 Chirped solitons

Nonlinear pulse propagation in optical medium is governed by nonlinear Schrödinger equation (NLSE) which is completely integrable and allows for either bright or dark solitons depending on the signs of dispersion or nonlinearity. These conventional solitons are chirp free pulses because the chirp produced by group velocity dispersion is balanced by the chirp produced by the Kerr nonlinearity [5]. However, if, in addition, one includes the gain/loss, higher order or variable coefficient terms in NLSE then chirped solitons are possible in the optical medium [6, 7, 8]. The chirp of an optical pulse is usually understood as the time dependence of its instantaneous frequency and can be found as the rate of change of phase of pulse. It means that if a pulse has a phase $\phi(z,t)$ then its chirp frequency is given by

$$\delta\omega(t) = -\frac{\partial\phi}{\partial t}. \tag{3.1}$$

The chirp play an important role in the subsequent pulse evolution. The chirped solitons are formed due to the growth of initially present chirp in the pulse, in contrast to the zero chirp in the case of the conventional solitons. Desaix *et al.* [9] studied the effect of the linear and nonlinear chirp on the subsequent development

of pulses. They have found that the properties of chirped solitons depend not only on the amplitude, but also on the form, of the initial chirp. The case of linear chirp frequency was first investigated by Hmurcik *et al.* [10] for a sech-shaped pulse with quadratic variation of phase in time. G.P. Agrawal [11] studied the pulse propagation in doped fiber amplifier and obtained soliton solutions with nonlinear chirping. Afterwards a lot of work has been done on the existence of chirped solitons in nonlinear optical systems [6, 7, 8, 12]. The chirped solitons have been utilized to achieve efficient chirp and pedestal free pulse compression or amplification [12, 13]. Hence, chirped pulses are useful in the design of optical devices such as optical fiber amplifiers, optical pulse compressors and solitary wave based communication links [6, 14]. Apart from this, chirped solitons also find applications in the generation of ultrahigh peak power pulses [15], ultrafast nonlinear spectroscopy [16] and coherent control of high-order harmonics [17].

3.3 An overview of the process of two-photon absorption

Two-photon absorption (TPA) is the process by which a molecule or material simultaneously absorbs either a pair of photons from a single beam of light or two single photons form two beams. First of all this process was described by Maria Göppert-Mayer in 1931 [18]. As a result of this process, two photons are absorbed from the light field and molecule is excited to a high energy state. The transition probability for the TPA process depends on the square of the intensity of the light used for excitation. In Fig. 3.1, a schematic energy level diagram is shown for the excitation of a molecule from the ground state g to an excited state f, by the absorption of two photons. The photons are either from same beam of light having same energy E_1 (degenerate case, $E_f = 2E_1$), or from different beams having the different energies E_1 and E_2 (non-degenerate case, $E_f = E_1 + E_2$).

As TPA is proportional to the square of the intensity of light, it reduces the

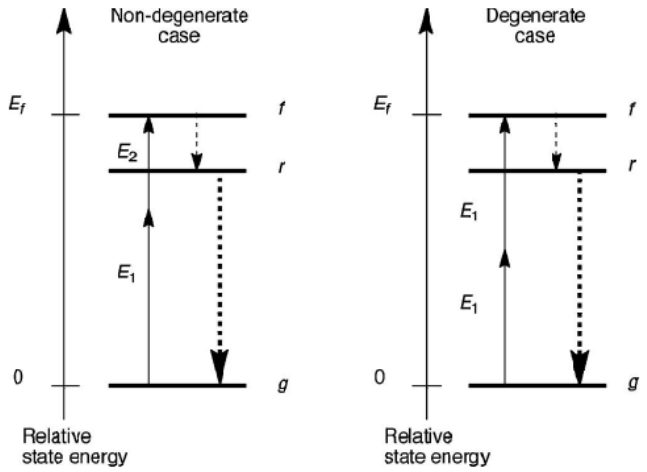

Figure 3.1: Energy level diagram for the process of two-photon absorption.

power required to form a soliton. Due to this, TPA find applications in all-optical switching [19, 20, 21] and optical data processing [22, 23, 24, 25]. TPA effects are more prominent in the materials which have more refractive index than that of silica. Hence, TPA are likely to become important in semiconductor-doped and lead silicate fibers [26]. The probability that a material will experience TPA when exposed to a light depends on the intrinsic properties of the material. Hence, TPA is useful in spectroscopy to probe the molecular properties [27, 28]. Apart from it, this process also helps in studying the light-matter interactions and to generate novel classical effects. As a result, TPA is also useful in various nonlinear and quantum optical phenomena such as in ultrafast photodetection [29], fiber lasers [30], nonlinear mirrors [31], optical parametric oscillators [32], generation of single photons [33], and quantum nonlinear effects [34].

3.4 Background of the problem

The effect of TPA on optical (temporal and spatial) solitons was first studied numerically by Silberberg in 1990 [35]. He considered the NLSE in the presence of TPA, given as

$$iu_z + \frac{1}{2}u_{ss} + (1 + iK)|u|^2 u = 0, \tag{3.2}$$

where u is the normalized amplitude, z and s are the normalized propagation distance and transverse coordinate (time or space), respectively, and K is the normalized TPA coefficient, defined as $K = \frac{\beta}{2kn_2}$. Here, k is the free space wave vector, β and n_2 are the intensity dependent absorption and refractive index coefficients, respectively. As, it is clear that wave propagation is highly perturbed in the range of $K \approx 1$, hence Silberberg studied the effect of weak TPA coefficient on soliton propagation. It was found that the amplitude of fundamental soliton decreases adiabatically with the broadening of soliton under the action of weak TPA. However, depending upon the soliton power and strength of TPA, the higher-order solitons split up into two or more fundamental solitons with equal amplitudes but with different propagation angles. Later, these results are verified experimentally, see Ref. [36]. The splitting of higher-order solitons into fundamental solitons was described as due to the sequence of the amplitude jumps which eventually leads to a structural bifurcation [37]. Motivated by the fact that loss and gain can be cancel each other to form a stable solution, the authors have found approximate slow solitary wave solutions, until the soliton behavior become significantly deformed, in the presence of linear gain [38]. In 1993, Agrawal [39] considered the effects of TPA on the pulse propagation in a fiber amplifier and concluded that an amplified chirped pulse splits into several chirped solitons whose number and peak power depends on the amplifier parameters. Later, this effect was studied in the presence of linear gain by adopting Rayleigh's dissipation function approach in the framework of variational formalism and found that pulse shape is distorted with the distance for increasing TPA coefficient [40]. During the last few years, the study on the emergence of optical pattern supported by localized gain has grown steadily. There have been reported the stable solitons for cubic complex Ginzburg-Landau equation [41] and periodic lattices [42]. Recently, Kartashov *et al.* [43, 44] have shown the existence of asymptotic soliton solutions supported by localized gain in the presence of TPA in a cubic nonlinear medium. Motivated by this work, we have obtained analytically exact chirped soliton solutions supported by localized gain in the presence of TPA [4]. We reported the existence of some new soliton solutions, like double-kink and

fractional-transform solitons, for this model.

3.5 Modified nonlinear Schrödinger equation and soliton solutions

Incorporating the effects of two-photon absorption and inhomogeneous gain, the nonlinear Schrödinger equation can be modified to [4]

$$iu_z = -\frac{1}{2}u_{tt} - \sigma|u|^2u - iK|u|^2u + ig(t)u, \tag{3.3}$$

where u is the normalized amplitude, z and t are the normalized propagation distance and time (or space, for spatial solitons) coordinate, respectively. For temporal solitons $\sigma = 1$ always, and for spatial solitons $\sigma = 1$ ($\sigma = -1$) represents the focusing (defocusing) media, respectively. Here, K is normalized TPA coefficient and $g(t)$ is normalized gain.

The value of TPA coefficient depends on the properties of material. For silica based fibers TPA coefficient has the value $K << 1$, but for semiconductor doped glasses or other high index materials $K \approx 1$. As an example, K has the value 0.01 for lead silicate fibers [26] and 0.1 for As_2S_3 glasses (for Ref. see [39]). From earlier works, it is clear that soliton propagation is highly perturbed in the range of $K \approx 1$, but for better operation of all-optical processes it is necessary to limit the value of K up to the order of unity [19]. In this work, the localized gain profiles have been shown, in order to exactly balance the losses due to TPA, for different ranges of TPA coefficient, i.e. for $K = 0.01$ and $K = 0.5$.

To start with, we have chosen the following form for complex field

$$u(z,t) = \rho(t)\ e^{i(\phi(t)+\gamma z)}, \tag{3.4}$$

where ρ and ϕ are the real functions of t and γ is the propagation constant. The corresponding chirp is given by $\delta\omega(t) = -\frac{\partial}{\partial t}[\phi(t) + \gamma z] = -\phi_t(t)$. Substituting Eq.

(3.4) in Eq. (3.3) and separating out the real and imaginary parts of the equation, we arrive at the following coupled equations in ρ and ϕ,

$$\rho_{tt} - 2\gamma\rho - \phi_t^2\rho + 2\sigma\rho^3 = 0 \tag{3.5}$$

and

$$2\phi_t\rho_t + \phi_{tt}\rho + 2K\rho^3 - 2g(t)\rho = 0. \tag{3.6}$$

To solve these coupled equations, one can choose the ansatz

$$\phi_t = c_1 + c_2\rho^2. \tag{3.7}$$

Hence, chirping is given as $\delta\omega(t) = -(c_1 + c_2\rho^2)$, where c_1 and c_2 denote the constant and nonlinear chirp parameters, respectively. It means chirping of wave is directly proportional to the intensity of wave. Using ansatz Eq. (3.7), Eqs. (3.5) and (3.6) reduces to

$$\rho_{tt} = (2\gamma + c_1^2)\rho + (2c_1c_2 - 2\sigma)\rho^3 + c_2^2\rho^5, \tag{3.8}$$

$$g(t) = c_1\frac{\rho_t}{\rho} + 2c_2\ \rho\rho_t + K\rho^2. \tag{3.9}$$

The elliptic equation given by Eq. (3.8) can be mapped to ϕ^6 field equation to obtain a variety of solutions such as periodic, kink and solitary wave type solutions [8]. In general, all travelling wave solutions of Eq. (3.8) can be expressed in a generic form by means of the Weierstrass $\wp$ function [45]. In this work, we report only those soliton-like solutions for which gain profile, given by Eq. (3.9), remains localized. For $c_2 = 0$, Eq. (3.8) reduces to well known cubic elliptic equation for which non-chirped soliton solutions can be found easily. Here, we studied Eq. (3.8) for different parameter conditions and obtained chirped soliton solutions. The reported solutions consist various soliton solutions like double-kink, fractional -transform, bell and kink-type solitons. For double-kink and bell-type solitons, we consider the case $c_1 = 0$ because for non-zero values of c_1 the corresponding gain will no longer be localized.

3.5.1 Double-kink solitons

Eq. (3.8) admits double-kink solutions of the form [46]

$$\rho(t) = \frac{m \sinh(nt)}{\sqrt{\epsilon + \sinh^2(nt)}}, \tag{3.10}$$

where $m = \sqrt{\frac{2\gamma(2\epsilon-3)}{\sigma(\epsilon-3)}}$, $n = \sqrt{\frac{2\gamma\epsilon}{\epsilon-3}}$, $c_2 = \frac{\sqrt{2(m^2\sigma-\gamma)}}{m^2}$ and $c_1 = 0$. The choice $c_1 = 0$ has been made in order to avoid the singularities in gain profile. Here, ϵ is a free parameter which controls the width of soliton solutions. The interesting double-kink feature of the solution is prominent for large values of ϵ. Now, for m, n and c_2 to be real numbers, ϵ should be always greater than 1 and never be equal to 3/2 and 3. Depending upon the model parameter, solutions are possible for some constraint conditions on ϵ and γ :

- for $\sigma = -1$, ϵ should lie between $1 < \epsilon < 3/2$ with negative values of γ.
- for $\sigma = +1$, ϵ can take any value either in the region $3/2 < \epsilon < 3$ with negative γ or $\epsilon > 3$ with positive value of γ.

For solution given in Eq. (3.10), the gain will be of the following form

$$g(t) = \frac{m^2 \left(K \sinh^2(nt) \left(\epsilon + \sinh^2(nt)\right) + c_2 n\epsilon \sinh(2nt)\right)}{\left(\epsilon + \sinh(nt)^2\right)^2}, \tag{3.11}$$

and the chirping will be

$$\delta\omega(t) = -\frac{c_2\ m^2 \sinh^2(nt)}{\epsilon + \sinh^2(nt)}. \tag{3.12}$$

The variation of gain, amplitude and chirp for different values of ϵ is shown in Fig. 3.2. The parameters used in the plots are $\sigma = 1$, $\gamma = 10$ and $K = 0.5$. One can point out that as the value of ϵ changes, there is a small change in the gain profile which in turn have significant effect on the amplitude and chirp of double-kink solution. Hence, one can observe that the double-kink feature of the wave is more prominent for a gain medium with large values of ϵ, and different gain medium

effects only the width of the double-kink wave whereas the amplitude of the wave always remains same. From the plot of chirp, it is clear that it has a maximum at the center of the wave and saturates at the some finite value with time.

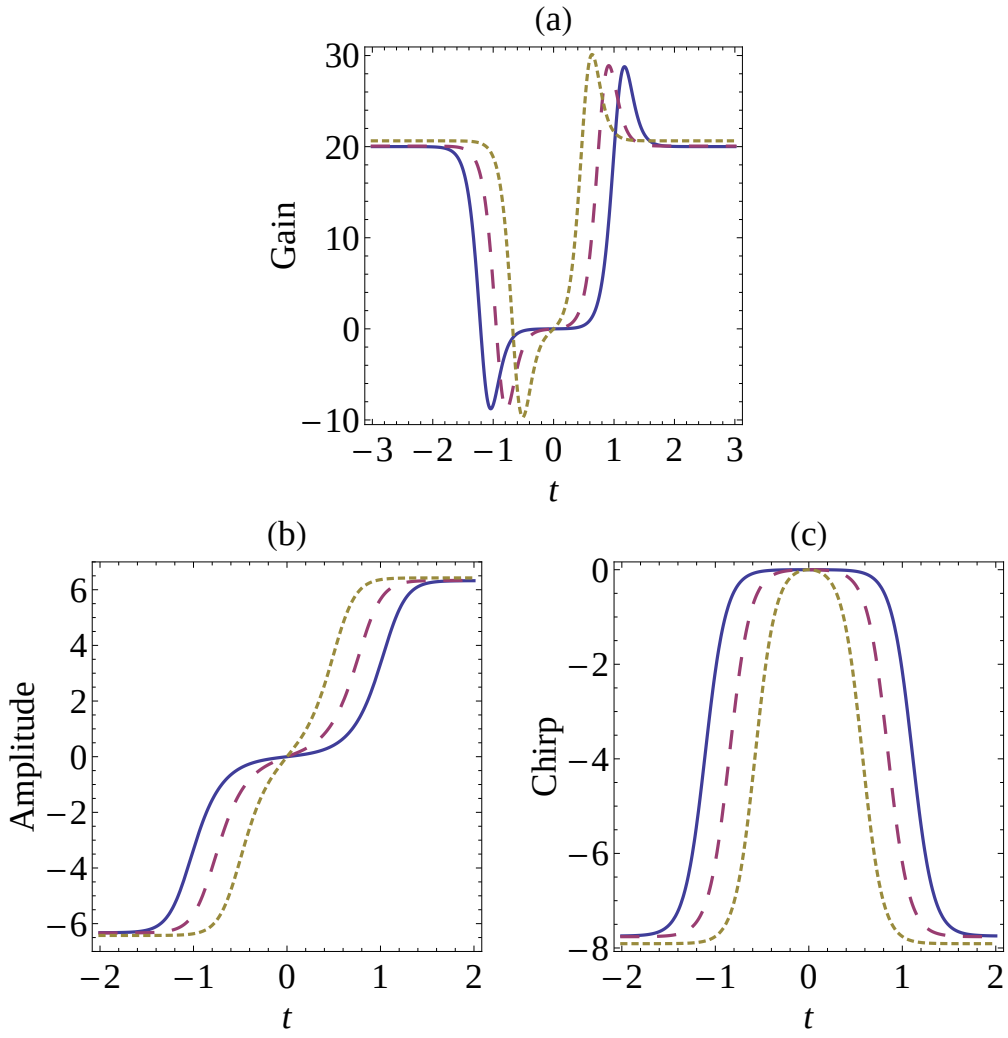

Figure 3.2: (a) Gain, (b) amplitude, and (c) chirp profiles for double-kink solitons for different values of ϵ, $\epsilon = 5000$ (thick line), $\epsilon = 500$ (dashed line) and $\epsilon = 50$ (dotted line). The other parameters used in the plots are $\sigma = 1, \gamma = 10$ and $K = 0.5$.

From the expressions of amplitude, gain and chirp Eqs. (3.10)-(3.12), it is clear that TPA coefficient K has no effect on amplitude and chirp of wave, whereas it has significant effect on the gain expression. Hence, for different values of K, only the gain profile is modified which results a localized solution. In Fig. 3.3, the gain profile is shown for different values of K, $K = 0.5$ and $K = 0.01$. The other

parameters used in the plots are $\epsilon = 500,\ \sigma = 1$ and $\gamma = 10$. From the plots, it is clear that the gain profile is transversally localized and has more amplitude for large values of K.

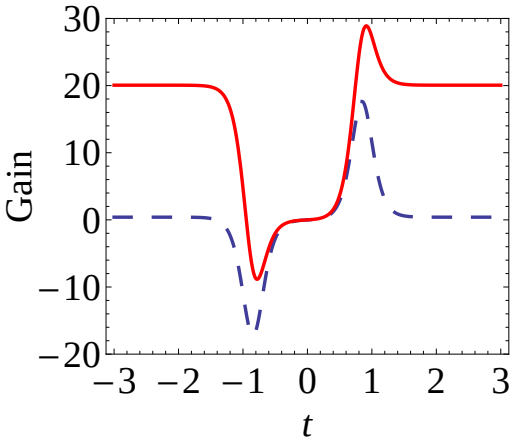

Figure 3.3: Gain profile for double-kink solitons for $K = 0.5$ (thick line) and $K = 0.01$ (dashed line). The parameters used in the plots are $\epsilon = 500,\ \sigma = 1$ and $\gamma = 10$.

3.5.2 Fractional-transform solitons

For the parametric condition $c_1 c_2 = \sigma$, Eq. (3.8) can be solved for very interesting fractional-transform solitons. To accomplish this, one can substitute $\rho^2 = y$ in Eq. (3.8) to obtain the following elliptic equation:

$$y'' + b_1 y^3 + b_2 y + c_0 = 0, \tag{3.13}$$

where $b_1 = -(8/3)c_2^2,\ b_2 = -4(2\gamma + c_1^2)$ and c_0 is integration constant. It is shown here that this elliptic equation connects to the well-known elliptic equation $f'' \pm af \pm bf^3 = 0$, where a and b are real, using a fractional transformation [47]

$$y(t) = \frac{A + Bf^2(t)}{1 + Df^2(t)}. \tag{3.14}$$

Our main aim is to study the localized solutions, we consider the case where $f = \mathrm{cn}(t, m)$ with modulus parameter $m = 1$, which reduces $\mathrm{cn}(t)$ to $\mathrm{sech}(t)$. One

can see that Eq. (3.8) connects $y(t)$ to the elliptic equation, provided $AD \neq B$, and the following conditions should be satisfied for the localized solution

$$b_2 A + b_1 A^3 + c_0 = 0, \tag{3.15}$$

$$2b_2 AD + b_2 B + 4(B - AD) + 3b_1 A^2 B + 3c_0 D = 0, \tag{3.16}$$

$$b_2 AD^2 + 2b_2 BD + 4(AD - B)D + 6(AD - B) + 3b_1 AB^2 + 3c_0 D^2 = 0, \tag{3.17}$$

$$b_2 BD^2 + 2(B - AD)D + b_1 B^3 + c_0 D^3 = 0. \tag{3.18}$$

The set of Eqs. (3.15) to (3.18) can be solved consistently for the unknown parameters A, B, D and for a particular value of c_0. The generic profile of the solution reads

$$y(t) = \frac{A + B\ \mathrm{sech}^2 t}{1 + D\ \mathrm{sech}^2 t}. \tag{3.19}$$

And, $\rho(t)$ can be written as

$$\rho(t) = \sqrt{\frac{A + B\ \mathrm{sech}^2 t}{1 + D\ \mathrm{sech}^2 t}}. \tag{3.20}$$

Since the analytical form of solution is known, a simple maxima-minima analysis can be done to distinguish parameter regimes supporting dark and bright soliton solutions [47]. In this case, when $AD < B$ one gets a bright soliton, whereas if $AD > B$ then a dark soliton exists.

For soliton solution given in Eq. (3.20), the chirping is given by

$$\delta\omega(t) = -\left(c_1 + c_2 \frac{A + B\ \mathrm{sech}^2 t}{1 + D\ \mathrm{sech}^2 t}\right), \tag{3.21}$$

The amplitude and chirp profiles for fractional-transform soliton are shown in Figs. 3.4(a) and 3.4(b) respectively for $\sigma = 1, c_1 = 1, c_2 = 1$ and $\gamma = -10$. For these values, the various unknown parameters found to be $A = 5.427,\ B = 18.351,\ D = 3.381$ and $c_0 = 13.817$. Here, solution is of the form of bright soliton and has a small amplitude over a finite background. For this case, chirping is minimum at the center of the wave and is dominant away from the center.

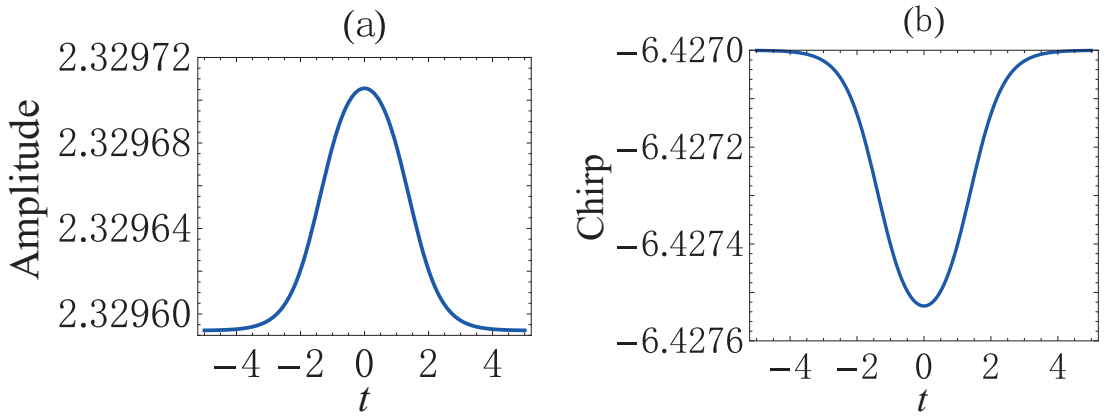

Figure 3.4: (a) Amplitude, and (b) chirp profiles for fractional-transform bright soliton for $\sigma = 1, c_1 = 1, c_2 = 1$ and $\gamma = -10$.

The corresponding gain will be of the following form

$$g(t) = \frac{(AD - B)\text{sech}^2 t \tanh t}{1 + D\ \text{sech}^2 t}\left(\frac{c_1}{A + B\ \text{sech}^2 t} + \frac{2c_2}{1 + D\ \text{sech}^2 t}\right) + K\left(\frac{A + B\ \text{sech}^2 t}{1 + D\ \text{sech}^2 t}\right). \tag{3.22}$$

The profiles of localized gain are shown in Fig. 3.5 for different values of TPA coefficient with $\sigma = 1,\ \gamma = -10,\ c_1 = 1$ and $c_2 = 1$. Here also it can be seen that the amplitude of localized gain depends on the value of TPA coefficient.

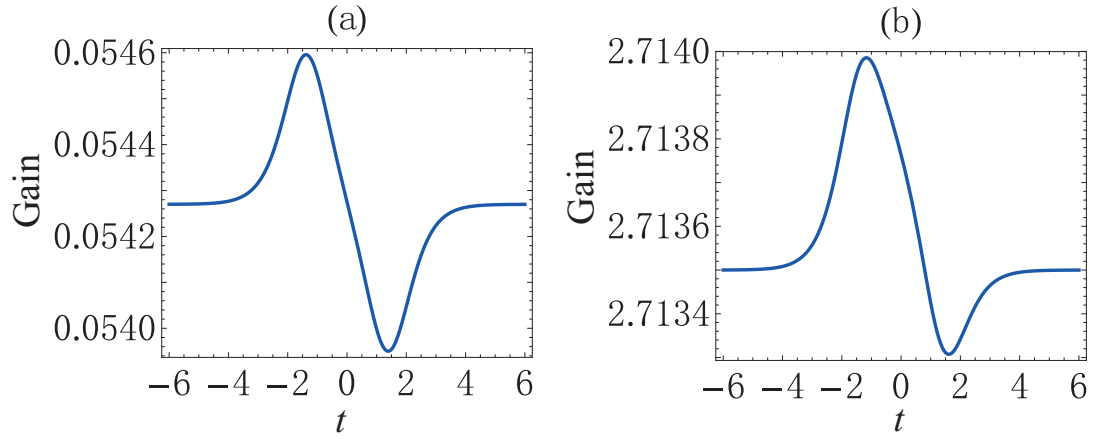

Figure 3.5: Gain profiles for fractional-transform solitons for, (a) $K = 0.01$ and (b) $K = 0.5$. The other parameters used in the plots are $\sigma = 1, c_1 = 1, c_2 = 1$ and $\gamma = -10$.

3.5.3 Bell and kink-type solitons

Bell-type solitons

For $c_1 = 0$ and $\gamma < \frac{3}{8}\left(\frac{\sigma}{c_2}\right)^2$, Eq. (3.9) have bright solitons of the bell shaped [48]

$$\rho(t) = \frac{p}{\sqrt{1 + r\cosh(qt)}}, \tag{3.23}$$

where $q = 2\sqrt{2\gamma}$, $r = \sqrt{1 - \frac{8\gamma c_2^2}{3\sigma^2}}$ and $p = 2\sqrt{\frac{\gamma}{\sigma}}$. Hence, these bell-type solitons exist only for $\sigma = 1$, and q, r and p to be real numbers. The corresponding chirping will take the form

$$\delta\omega(t) = -\frac{c_2\ p^2}{1 + r\cosh(qt)}. \tag{3.24}$$

The amplitude and chirp profiles for bell-type soliton are shown in Figs. 3.6(a) and 3.6(b), respectively. The parameters used in the plots are $\sigma = 1$ and $c_2 = 2$. For these values, γ should be less than 3/32. It is clear from the figure that chirping for the bright soliton has a minimum at the center of the wave.

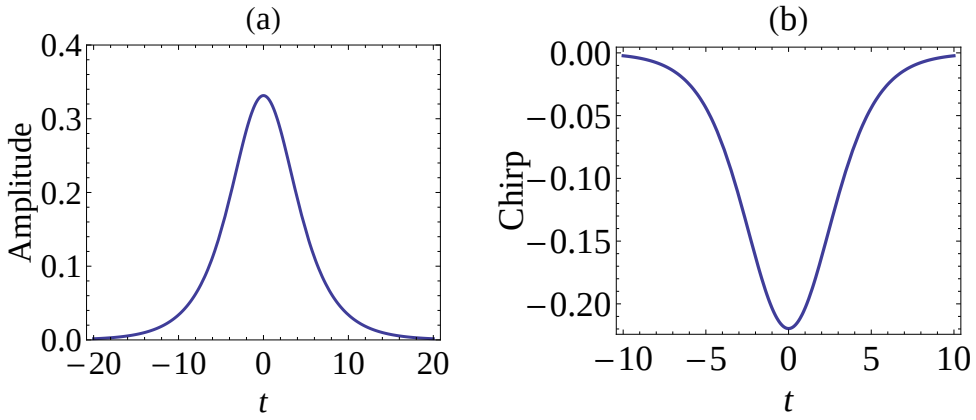

Figure 3.6: (a) Amplitude, and (b) chirp profiles for bell-type bright soliton for $\sigma = 1,\ \gamma = 3/64$ and $c_2 = 2$.

The gain profile for this case is given by

$$g(t) = \frac{2Kp^2(1 + r\cosh(qt)) - 2\ c_2\ p^2 qr\sinh(qt)}{2(1 + r\cosh(qt))^2}. \tag{3.25}$$

The plot for inhomogeneous gain is shown in Fig. 3.7 for different values of TPA coefficient with $\sigma = 1$ and $c_2 = 2$. Here also gain is transversally localized and saturates at some finite value as the time approaches its asymptotic value.

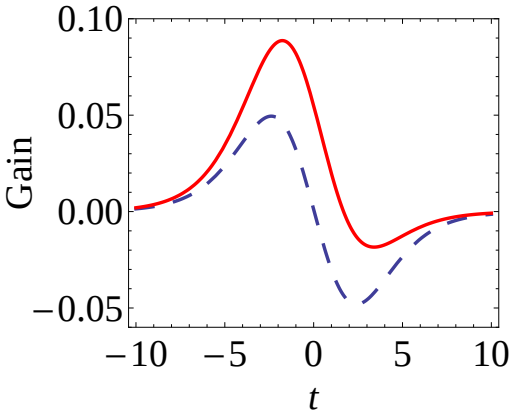

Figure 3.7: Gain profiles for bell-type solitons for $K = 0.5$ (thick line) and $K = 0.01$ (dashed line). The other parameters used in the plots are $\sigma = 1$, $\gamma = 3/64$ and $c_2 = 2$.

Kink-type solitons

If $c_2 = \frac{\sigma}{c_1 - \sqrt{\frac{4}{3}\left(2\gamma + c_1^2\right)}}$, then Eq. (3.9) admits kink and anti-kink type solitons as [48]

$$\rho_{\pm}(t) = p\sqrt{1 \pm \tanh(qt)}, \tag{3.26}$$

where $q = \sqrt{2\gamma + c_1^2}$, $p = \sqrt{\frac{2\gamma + c_1^2}{(\sigma - c_1 c_2)}}$. On the basis of these conditions, solutions are possible for some constraint conditions on c_1 and γ :

- for $\sigma = +1$, either $c_1^2 > -8\gamma$ with negative values of γ or $c_1^2 > -2\gamma$ with positive values of γ.
- for $\sigma = -1$, c_1^2 should lie between $-2\gamma < c_1^2 < -8\gamma$ with negative values of γ.

The corresponding chirping for $\rho_+(t)$ solution is given by

$$\delta\omega_+(t) = -\left(c_1 + c_2 p^2 (1 + \tanh(qt))\right), \tag{3.27}$$

The amplitude and chirp profiles for kink-type soliton are shown in Figs. 3.8(a) and 3.8(b) respectively for $\sigma = 1, c_1 = 1$ and $\gamma = 10$. For these parameters, c_2 comes out to be -0.23. Here chirp associated with the wave also have kink-like behavior. Hence, the gain for $\rho_+(t)$ solution will be of the form

$$g_+(t) = -\frac{1}{2}qc_1(-1 + \tanh(qt)) + p^2\left(K + qc_2\mathrm{sech}^2(qt) + K\tanh(qt)\right). \tag{3.28}$$

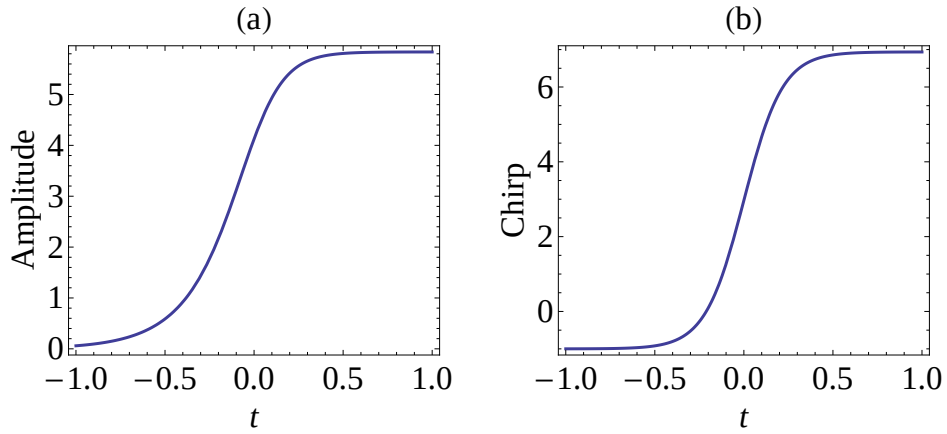

Figure 3.8: (a) Amplitude, and (b) chirp profiles for kink-type soliton. The parameters used in the plots are $\sigma = 1, c_1 = 1$ and $\gamma = 10$.

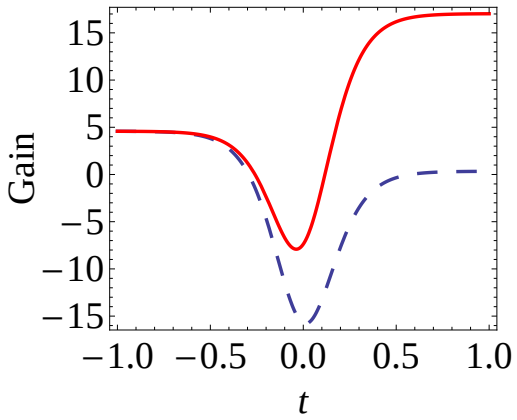

Figure 3.9: Gain profiles for kink-type solitons for $K = 0.5$ (thick line) and $K = 0.01$ (dashed line). The parameters used in the plots are $\sigma = 1, c_1 = 1$ and $\gamma = 10$.

The plot for localized gain is shown in Fig. 3.9 for different values of TPA coefficient with $\sigma = 1, c_1 = 1$ and $\gamma = 10$. From the plot, it is clear that amplitude

of gain depends on the value of TPA coefficient.

3.6 Conclusion

In this work, it is demonstrated that nonlinear losses due to TPA are exactly balanced by localized gain and induces the optical solitons in nonlinear medium, and reported the existence of chirped double-kink, fractional-transform, bell and kink-type soliton solutions. The parameter domain is delineated in which these optical solitons exist. The width of double-kink solitons can be controlled by modulating the gain profile. Interestingly, fractional-transform solutions supports both bright or dark solitons depending on model parameters. Further, bell and kink-type solitons are found to exist in this system for different choice of parameters. The chirp related to solitons has also been identified and found that it is directly proportional to the intensity of wave. The amplitude of localized gain is directly proportional to the value of TPA coefficient and saturates at some finite value as the retarded time approaches its asymptotic value. We hope that these chirped optical solitons supported by localized gain may find useful for pulse compression or amplification in various nonlinear optical processes accompanied by TPA.

Bibliography

[1] A Hasegawa. Soliton-based ultra-high speed optical communications. *Pramana-Journal of Physics*, 57(5-6):1097–1127, 2001.

[2] EM Wright. All-optical switching using solitons. *Optical and Quantum Electronics*, 24(11):3, 1992.

[3] SV Serak, NV Tabiryan, M Peccianti, and G Assanto. Spatial soliton all-optical logic gates. *IEEE Photonics Technology Letters*, 18(12):1287–1289, 2006.

[4] A Goyal, V Sharma, and CN Kumar. Optical solitons supported by localized gain in the presence of two-photon absorption. In *International Conference on Fibre Optics and Photonics*. OSA Technical Digest (online), Optical Society of America, 2012.

[5] YS Kivshar and GP Agrawal. *Optical solitons: from fibers to photonic crystals*. Academic Press, London, 2003.

[6] VI Kruglov, AC Peacock, and JD Harvey. Exact self-similar solutions of the generalized nonlinear Schrödinger equation with distributed coefficients. *Physical Review Letters*, 90(11):113902, 2003.

[7] J Wang, L Li, and S Jia. Exact chirped gray soliton solutions of the nonlinear Schrödinger equation with variable coefficients. *Optics Communications*, 274(1):223–230, 2007.

[8] Alka, A Goyal, R Gupta, CN Kumar, and TS Raju. Chirped femtosecond solitons and double-kink solitons in the cubic-quintic nonlinear Schrödinger

equation with self-steepening and self-frequency shift. *Physical Review A*, 84(6):63830, 2011.

[9] M Desaix, L Helczynski, D Anderson, and M Lisak. Propagation properties of chirped soliton pulses in optical nonlinear kerr media. *Physical Review E*, 65(5):56602, 2002.

[10] LV Hmurcik and DJ Kaup. Solitons created by chirped initial profiles in coherent pulse propagation. *Journal of the Optical Society of America*, 69(4):597–604, 1979.

[11] GP Agrawal. Optical pulse propagation in doped fiber amplifiers. *Physical Review A*, 44(11):7493, 1991.

[12] K Senthilnathan, K Nakkeeran, Q Li, and PKA Wai. Pedestal free pulse compression of chirped optical solitons. *Optics Communications*, 285(6):1449–1455, 2012.

[13] YH Chuang, DD Meyerhofer, S Augst, H Chen, J Peatross, and S Uchida. Suppression of the pedestal in a chirped-pulse-amplification laser. *Journal of the Optical Society of America B*, 8(6):1226–1235, 1991.

[14] JD Moores. Nonlinear compression of chirped solitary waves with and without phase modulation. *Optics Letters*, 21(8):555–557, 1996.

[15] P Maine, D Strickland, P Bado, M Pessot, and G Mourou. Generation of ultrahigh peak power pulses by chirped pulse amplification. *IEEE Journal of Quantum Electronics*, 24(2):398–403, 1988.

[16] ETJ Nibbering, DA Wiersma, and K Duppen. Ultrafast nonlinear spectroscopy with chirped optical pulses. *Physical Review Letters*, 68(4):514, 1992.

[17] DG Lee, JH Kim, KH Hong, and CH Nam. Coherent control of high-order harmonics with chirped femtosecond laser pulses. *Physical Review Letters*, 87(24):243902, 2001.

[18] M Göppert-Mayer. Elementary processes with two quantum transitions. *Annalen der Physik*, 18(7-8):466–479, 2009.

[19] V Mizrahi, KW DeLong, GI Stegeman, MA Saifi, and MJ Andrejco. Two-photon absorption as a limitation to all-optical switching. *Optics Letters*, 14(20):1140–1142, 1989.

[20] DD Yavuz. All-optical femtosecond switch using two-photon absorption. *Physical Review A*, 74(5):053804, 2006.

[21] SM Hendrickson, CN Weiler, RM Camacho, PT Rakich, AI Young, MJ Shaw, TB Pittman, JD Franson, and BC Jacobs. All-optical-switching demonstration using two-photon absorption and the zeno effect. *Physical Review A*, 87(2):023808, 2013.

[22] JH Strickler and WW Webb. Three-dimensional optical data storage in refractive media by two-photon point excitation. *Optics Letters*, 16(22):1780–1782, 1991.

[23] S Ma, Z Chen, and NK Dutta. All-optical logic gates based on two-photon absorption in semiconductor optical amplifiers. *Optics Communications*, 282(23):4508–4512, 2009.

[24] A Kotb, S Ma, Z Chen, NK Dutta, and G Said. All optical logic NAND gate based on two-photon absorption in semiconductor optical amplifiers. *Optics Communications*, 283(23):4707–4712, 2010.

[25] W Li, S Ma, H Hu, and NK Dutta. All-optical latches based on two-photon absorption in semiconductor optical amplifiers. *Journal of the Optical Society of America B*, 29(9):2603–2609, 2012.

[26] MA Newhouse, DL Weidman, and DW Hall. Enhanced-nonlinearity single-mode lead silicate optical fiber. *Optics Letters*, 15(21):1185–1187, 1990.

[27] T Plakhotnik, D Walser, M Pirotta, A Renn, and UP Wild. Nonlinear spectroscopy on a single quantum system: two-photon absorption of a single molecule. *Science*, 271(5256):1703–1705, 1996.

[28] JI Jang, S Park, DJ Clark, FO Saouma, D Lombardo, CM Harrison, and B Shim. Impact of two-photon absorption on second-harmonic generation in CdTe as probed by wavelength-dependent Z-scan nonlinear spectroscopy. *Journal of the Optical Society of America B*, 30(8):2292–2295, 2013.

[29] J Bravo-Abad, EP Ippen, and M Soljacic. Ultrafast photodetection in an all-silicon chip enabled by two-photon absorption. *Applied Physics Letters*, 94(24):241103–241103, 2009.

[30] ER Thoen, ME Grein, EM Koontz, EP Ippen, HA Haus, and LA Kolodziejski. Stabilization of an active harmonically mode-locked fiber laser using two-photon absorption. *Optics Letters*, 25(13):948–950, 2000.

[31] RW Schirmer and AL Gaeta. Nonlinear mirror based on two-photon absorption. *Journal of the Optical Society of America B*, 14(11):2865–2868, 1997.

[32] IB Zotova and YJ Ding. Optical parametric oscillators in the presence of strong two-photon absorption for extended applications of nonlinear optical materials. *Optics Communications*, 198(4):453–458, 2001.

[33] BC Jacobs, TB Pittman, and JD Franson. Single photon source using laser pulses and two-photon absorption. *Physical Review A*, 74(1):010303, 2006.

[34] K Saha, V Venkataraman, P Londero, and AL Gaeta. Enhanced two-photon absorption in a hollow-core photonic-band-gap fiber. *Physical Review A*, 83(3):033833, 2011.

[35] Y Silberberg. Solitons and two-photon absorption. *Optics Letters*, 15(18):1005–1007, 1990.

[36] JS Aitchison, Y Silberberg, AM Weiner, DE Leaird, MK Oliver, JL Jackel, EM Vogel, and PWE Smith. Spatial optical solitons in planar glass waveguides. *Journal of the Optical Society of America B*, 8(6):1290–1297, 1991.

[37] VV Afanasjev, JS Aitchison, and YS Kivshar. Splitting of high-order spatial solitons under the action of two-photon absorption. *Optics Communications*, 116(4):331–338, 1995.

[38] MJ Steel and CM de Sterke. Gap solitary waves with gain and two-photon absorption. *Physical Review A*, 48(2):1625, 1993.

[39] GP Agrawal. Effect of two-photon absorption on the amplification of ultrashort optical pulses. *Physical Review E*, 48(3):2316, 1993.

[40] S Roy and S Bhadra. Effect of two photon absorption on nonlinear pulse propagation in gain medium. *Communications in Nonlinear Science and Numerical Simulation*, 13(10):2157–2166, 2008.

[41] CK Lam, BA Malomed, KW Chow, and PKA Wai. Spatial solitons supported by localized gain in nonlinear optical waveguides. *The European Physical Journal Special Topics*, 173(1):233–243, 2009.

[42] YV Kartashov, VV Konotop, VA Vysloukh, and L Torner. Dissipative defect modes in periodic structures. *Optics Letters*, 35(10):1638–1640, 2010.

[43] YV Kartashov, VV Konotop, and VA Vysloukh. Symmetry breaking and multipeaked solitons in inhomogeneous gain landscapes. *Physical Review A*, 83(4):041806, 2011.

[44] YV Kartashov, VV Konotop, and VA Vysloukh. Two-dimensional dissipative solitons supported by localized gain. *Optics Letters*, 36(1):82–84, 2011.

[45] E Magyari. Kinks and periodons at a t = 0 first-order phase transition point in one-dimensional anharmonic lattices. *Zeitschrift für Physik B: Condensed Matter*, 43(4):345–351, 1981.

[46] NH Christ and TD Lee. Quantum expansion of soliton solutions. *Physical Review D*, 12(6):1606, 1975.

[47] VM Vyas, TS Raju, CN Kumar, and PK Panigrahi. Soliton solutions of driven nonlinear Schrödinger equation. *Journal of Physics A: Mathematical and General*, 39(29):9151, 2006.

[48] SN Behera and A Khare. Classical φ6-field theory in (1+ 1) dimensions. A model for structural phase transitions. *Pramana-Journal of Physics*, 15(3):245–269, 1980.

Chapter 4

Study of inhomogeneous nonlinear systems for solitary wave solutions

4.1 Introduction

In this chapter, we have considered two nonlinear systems in the presence of inhomogeneous conditions and obtained solitary wave solutions for them. First, a prototype inhomogeneous model is studied which describes the interaction between reaction mechanism, convection effect and diffusion process. The reaction-diffusion equations arises in many areas, such as flow in porous media, heat conduction in plasma, combustion problems, liquid evaporation, population genetics etc. The most of nonlinear physical phenomena are described by nonlinear reaction-diffusion (NLRD) equations with variable coefficients because external factors make the density and/or temperature change in time. The exact solitary wave solutions have been obtained for NLRD equations with time-dependent coefficients of convection and reaction terms using auxiliary equation method. The effect of variable coefficients is studied on physical parameters (amplitude and velocity) of solitary wave solutions.

Second, the complex Ginzburg-Landau equation (CGLE) has been investigated in the presence of ac-source. It is a well-known nonlinear equation in the field of

nonlinear science, which describes various nonlinear physical and chemical phenomena. Although, CGLE is a well studied dynamical system, the exact solutions of ac-driven CGLE are rarely appeared in the literature. We have explored fractional transform solutions of ac-driven complex Ginzburg-Landau equation, in which there is a phase difference between the external driver and the solutions. The reported solutions are necessarily of the Lorentzian-type solitons and also kink-type solitons.

4.2 Nonlinear reaction diffusion equations with variable coefficients

Reaction diffusion (RD) equations appear in many branches of science and engineering. These equations have attracted considerable attention, as it can be used to model the evolution systems in real world. So far, a lot of studies like travelling eaves, chaotic dynamics, pattern formation etc., has been done on RD systems both theoretically and experimentally. Exact travelling wave solutions, specially solitary wave-type solutions, to nonlinear reaction diffusion (NLRD) equations plays an important role in the qualitative description of many phenomena such as flow in porous media [1], heat conduction in plasma [2], chemical reactions [3], population genetics [4], image processing [5] and liquid evaporation [6]. The solitary wave solutions to NLRD equations are particularly interesting because experimental findings suggest that reaction diffusion systems may carry spatially well localized solitary patterns that behave like particles and retain their identity while interacting [7, 8].

4.2.1 NLRD equation: Derivation and variants

RD equation describe the evolution of a system under the influence of diffusion and reaction. In the assembly of particles, for example cells, bacteria, chemicals, animals and so on, each particle moves in random way. This microscopic irregular movement results in some macroscopic regular motion of the group of particles which is called diffusion process. The gross movement is not a simple diffusion, but one have to

consider the interaction between the particles and environment, which results the production of new particles. This constitutes the reaction process. Time evolution of a system under these two effects can be written as

$$q_t = Dq_{xx} + R(x), \tag{4.1}$$

where $q(x,t)$ represents the concentration of the substance, D is diffusion coefficient, $R(x)$ represents the reaction term. The study of these equations becomes even more interesting for nonlinear reaction term, because the balance between diffusion and nonlinear reaction term may results to the existence of solitary wave solutions.

Derivation of RD equation

It is very hard to get a macroscopic behavior from the knowledge of individual microscopic behavior, so we drive a continuum model equation for the global behavior in terms of the particle density, concentration or population. Assuming $c(x,t)$ as number of particles at time t per unit spatial dimension (area, volume, length according to the dimension which we are using), the total concentration at the spatial position x of the system is given by

$$\int_x c(x,t)dx.$$

Here the functional form $c(x,t)$ is well behaved i.e. evolution of system is continuous and differentiable. This assumption seems to be quite reasonable for the system with large concentration. The diffusion equation can be obtained easily from this when combined with the phenomenological **Fick's first law**. This law states that the magnitude of flux flow from the regions of the high concentration to the regions of the low concentration is proportional to the concentration gradient, that is

$$J(x,t) = -D(x)\frac{\partial c}{\partial x}, \tag{4.2}$$

where $J(x,t)$ is the diffusion flux which gives the amount of the substance that will flow through a small area during a small time interval. D is the diffusion coefficient and c represents the concentration.

Now, if the rate of change of the number of particles due to physical or chemical reasons is given by $f(x,t,c)$, then according to the Balance law

$$\frac{\partial}{\partial t}\int_x c(x,t)dx = \int_s J.ds + \int_x f(x,t,c(x,t))dx, \tag{4.3}$$

where the term on left hand side represents the rate of change of total concentration, the first term on right hand side gives the total flux and the second term represents the net growth of concentration inside the region x.

Applying the Divergence theorem to the surface integral in Eq. (4.3), one obtains

$$\int_s J.ds = \int_x \nabla.J(x,t)dx. \tag{4.4}$$

Now using Eqs. (4.2) and (4.4) in Eq. (4.3), it reads

$$\int_x \frac{\partial}{\partial t}c(x,t)dx = \int_x D(x)\frac{\partial^2}{\partial x^2}c(x,t) + \int_x f(x,t,c(x,t))dx. \tag{4.5}$$

Since the choice of region is arbitrary, it can be written as

$$\frac{\partial}{\partial t}c(x,t) = D(x)\frac{\partial^2}{\partial x^2}c(x,t) + f(x,t,c(x,t)). \tag{4.6}$$

This equation is known as the RD equation. Here first term on right side is the diffusion term which describes the movement of the particles and $f(x,t,c(x,t))$ is the reaction term which describes the various reactions occurring in the system. The diffusion coefficient $D(x)$ is not constant in general but considering approximately homogeneous system, one can assume $D(x) = D$, and rewriting $c(x,t)$ as $u(x,t)$ Eq. (4.6) reads

$$\frac{\partial u}{\partial t} = D\frac{\partial^2 u}{\partial x^2} + f(u). \tag{4.7}$$

Now, the reaction term would be either linear or nonlinear depending upon the system. If it is a linear term then it can be solved easily using variable separable method. But, if reaction term is nonlinear then these nonlinear reaction diffusion (NLRD) equations can not be solved using direct methods. The two well known

examples of the nonlinear reaction terms are the quadratic and cubic nonlinearity.

1. Reaction terms with quadratic nonlinearity as

$$f(u) = k_1 u(1-u). \tag{4.8}$$

Hence Eq. (4.7) reads

$$u_t = Du_{xx} + k_1 u(1-u). \tag{4.9}$$

This equation models the propagation of a mutant gene with $u(x,t)$ denoting the density of advantageous. It is also appeared in chemical kinetics, population dynamics, flame propagation, autocatalytic chemical reactions and brownian motion process. In the past century, this equation has become a basis for a variety of equations of spatial spread. For example, the reaction term in an ecological context may represent the birth-death process, with u as the population density, with logistic population growth

$$f = ru(1-\frac{u}{k}), \tag{4.10}$$

where r is the linear reproduction rate and k is the carrying capacity of the environment. The resulting NLRD equation will be

$$\frac{\partial u}{\partial t} = D\frac{\partial^2 u}{\partial x^2} + ru(1-\frac{u}{k}). \tag{4.11}$$

This equation is known as the Fisher equation [9] after Fisher (1937) who proposed the one dimensional model for the spread of a advantageous gene in a population.

2. Reaction terms with cubic nonlinearity:

$$f(u) = k_2 u(1-u^2). \tag{4.12}$$

The corresponding NLRD equation is known as Fisher-Kolmogorov (FK) equation [10], which arises in the study of pattern formation in bistable systems [11].

NLRD equations with convection term

In a reaction diffusion system, generally, it is assumed that field is fixed i.e. spatial transport is only through diffusion. But, in a real world phenomena, the field itself usually moves. Hence, in many processes, in addition to diffusion, motion can also be due to advection or convection with some kind of back reaction, such as the spread of a favored gene, ecological competition, and so on [12]. Nonlinear convection terms arise naturally, for example, in the motion of chemotactic cells [13]. From a physical point of view convection, diffusion and reaction processes are quite fundamental to describe a wide variety of problems in physical, chemical, biological sciences [14]. A general form of such NLRD equation with convection term is

$$u_t + v\ u^m u_x = Du_{xx} + f(u), \tag{4.13}$$

where v is convection coefficient and m is a real number. The few examples of the nonlinear equations involving the convection term are given below.

- **Burgers equation**

  It is one of the simplest nonlinear equation representing the theory of turbulence described by the interaction of convection and diffusion [15]

  $$u_t + v\ uu_x = Du_{xx}. \tag{4.14}$$

  It appears in various areas of applied mathematics such as modeling of fluid dynamics, turbulence, boundary layer behavior, shock wave formation and traffic flow.

- **Burgers-Fisher equation**

  Combining Burgers and Fisher equation, the resulting equation is known as Burger-Fisher equation [16], which describes the interaction of reaction mech-

anisms, convection effects and diffusion processes. The equation is

$$u_t + v\ uu_x = Du_{xx} + k_3u(1-u). \tag{4.15}$$

The Burger-Fisher equation has a wide range of applications in plasma physics, fluid physics, capillary-gravity waves, nonlinear optics and chemical physics.

- **Newell-Whitehead-Segel equation**

$$u_t + v\ u_x = Du_{xx} + k_4u(1-u^2). \tag{4.16}$$

This equation describes the slow spatial modulation of the stripe patterns in usual pattern forming systems [17] and optical systems [18].

4.2.2 Motivation and model equation

The literature discussing the NLRD equations is massive, but these results assume that the environment is temporally and spatially homogenous. However, this may be a rough approximation to many systems, because most of physical and biological systems are inhomogeneous due to fluctuations in environmental conditions and non-uniform media. Hence, most of real nonlinear physical equations possess variable coefficients, both in space and over time [19, 20, 21]. The effect of spatial inhomogeneities on NLRD systems [12, 22, 23] has been discussed by many authors, but the effect of temporal inhomogeneities has not been much explored. We shall work on this problem here. There are many NLRD systems where the relevant parameters are time dependent [24, 25] because external factors make the density and/or temperature change in time. For example, in biological applications, such as population range expansion, for which reproductive (reactive) and mobility (diffusive) parameters change in time driven by climatic changes.

The dimensionless form of the variable coefficient NLRD equation, studied

here, is

$$u_t + v(t)\ u^m u_x = D u_{xx} + \alpha(t)\ u - \beta(t)\ u^n, \tag{4.17}$$

where $u = u(x,t)$, is the concentration or density variable depending on the phenomena under study; D is diffusion coefficient; v is convection term coefficient; α, β are reaction term coefficients and $m,\ n$ are real numbers.

In this work, we have considered Eq. (4.17) for different values of m and n, and obtained propagating kink-type solitary wave solutions by using the auxiliary equation method [26]. For $m = 0$ and $n = 3$, Eq. (4.17) represents the Newell-Whitehead-Segel equation with variable coefficients. This model has been solved for bell-type solitary wave solutions with constant reaction coefficients [27, 28]. For the same model, we have obtained kink-type solitary wave solutions and extend the formalism to obtain solitary wave solutions with inhomogeneous reaction terms. Further, we extend the analysis for inhomogeneous nonlinear convection term, i.e. for $m = 1$. For $m = 1$ and $n = 3$, Eq. (4.17) with constant coefficients describes the various biological and physical phenomena [see Ref. [13], and references therein]. In last, we have considered the case $m = 1$ and $n = 2$, for which Eq. (4.17) represents the Burger-Fisher equation with variable coefficients, and explored kink-type solutions. We have found that variable coefficients have significant effect on the amplitude and velocity of propagating kink solutions [29]. First, we shall explain auxiliary equation method and then use it to solve variable coefficient NLRD equation for different cases.

4.2.3 Auxiliary equation method

Sirendaoreji and Jiong [26] proposed auxiliary equation method to solve nonlinear partial differential equations (PDE's) with constant coefficients. Suppose, for a given nonlinear evolution equation with independent variables x and t, and dependent variable u:

$$F(u, u_x, u_t, u_{xx}, u_{tt}, u_{xt}, ...) = 0. \tag{4.18}$$

By using Galilean transformation, we can write Eq. (4.18) in travelling wave frame as

$$G(u, u_\xi, u_{\xi\xi}, u_{\xi\xi\xi}, ...) = 0, \tag{4.19}$$

where $\xi = kx - \omega t$, k and ω are constants. Let us assume that the solution of Eq. (4.19) is of the following form

$$u(\xi) = \sum_{i=0}^{n} a_i z^i(\xi), \tag{4.20}$$

where a_i $(i = 0, 1, 2, ...)$ are real constants to be determined, n is a positive integer and $z(\xi)$ represents the solutions of the following auxiliary ordinary differential equation, viz.

$$z_\xi = az(\xi) + z^2(\xi), \tag{4.21}$$

where a, b, c are constants. To determine u explicitly, take the following four steps.

Step 1 Substitute Eq. (4.20) along with Eq. (4.21) into Eq. (4.19) and balancing the highest order derivative terms with the highest power nonlinear terms in Eq. (4.19), to find the value of n.

Step 2 Again substitute Eq. (4.20), with the value of n found in Step 1, along with Eq. (4.21)into Eq. (4.19), collecting coefficients of $z^i z_\xi{}^j (j = 0, 1;\ i = 0, 1, 2, ...)$ and then setting each coefficient to zero, to get a set of over-determined partial differential equations for $a_i (i = 0, 1, 2...)$, k and ω.

Step 3 By solving the equations obtained in Step 2, get the explicit expressions for $a_i (i = 0, 1, 2...)$, k and ω.

Step 4 By using the results obtained in previous steps, obtain the exact travelling wave solution of Eq. (4.18) from Eq. (4.20) depending on the solution $z(\xi)$ of Eq. (4.21).

This method can also be used to solve nonlinear PDE's with variable coefficients by converting these equations into ODE's in accelerated travelling wave frame with the help of extended Galilean transformation [30]. Yomba [31] follow this procedure to solve KdV equation with variable coefficients using auxiliary equation method and Bekir *et al.* [32] used it to solve Zakharov-Kuznetsov equation with

variable coefficients using exp. function method.

4.2.4 Solitary wave solutions

(1) Exact solutions of Eq. (4.17) for $m = 0$ and $n = 3$

Case (a): *Only v is time dependent*

For this case, Eq. (4.17) reads

$$u_t + v(t)\ u_x = Du_{xx} + \alpha u - \beta u^3. \tag{4.22}$$

To begin with, one can assume the solution of Eq. (4.22) in extended Galilean frame of reference [30], $\xi = kx + \eta(t)$, k is constant, as

$$u(\xi) = a(t) + b(t)\ \phi(\xi), \tag{4.23}$$

where $\phi(\xi)$ satisfies an ordinary differential equation, viz.

$$\phi_\xi = p\phi + \phi^2, \tag{4.24}$$

where p is constant. Substituting Eqs. (4.23) and (4.24) in Eq. (4.22), and equating the coefficients of ϕ^i's $(i = 0, 1, 2, 3)$ to zero, a set of equations can be found as

$$\begin{aligned}
&\phi^3 :\ -2bDk^2 + \beta b^3 = 0,\\
&\phi^2 :\ b\eta_t + bkv - 3pbDk^2 + 3ab^2\beta = 0,\\
&\phi^1 :\ b_t - p^2bDk^2 + 3a^2b\beta - \alpha b + pb\eta_t + pbkv = 0,\\
&\phi^0 :\ a_t + \beta a^3 - \alpha a = 0.
\end{aligned} \tag{4.25}$$

Solving these equations consistently, the various unknown parameters, a, b, k and $\eta(t)$, found to be

$$\begin{aligned}
a = \frac{p}{2}b = \sqrt{\frac{\alpha}{\beta}},\\
k^2 = \frac{2\alpha}{p^2D},\ \eta(t) = -k\int v(t)\ dt.
\end{aligned} \tag{4.26}$$

It indicates that a and b are constants. Integrating Eq. (4.24), the solution for $\phi(\xi)$ is found as

$$\phi(\xi) = -\frac{p}{2}\left[1 + \tanh\left(\frac{p}{2}\xi\right)\right]. \tag{4.27}$$

Using Eqs. (4.23), (4.26) and (4.27), the solution for Eq. (4.22) reads

$$u(\xi) = -\sqrt{\frac{\alpha}{\beta}}\tanh\left(\frac{p}{2}\xi\right), \tag{4.28}$$

where $\xi = k\left(x - \int v(t)\,dt\right)$. This implies that non-trivial time dependence of ξ can be expressed only in terms of function of $v(t)$. Here, $v(t)$ can be assumed as an arbitrary function of time which effects the velocity of wave. Typical amplitude profile of Eq. (4.28) is shown in Fig. 4.1, for $\alpha = 1,\ \beta = 1,\ D = 2,\ p = -1,\ k = 1$ and $v(t) = \cos(2t)$. It is a kink-type solitary wave solution. It is interesting to note that for small magnitude of x the function $u(x,t)$ has periodic structure in time but as magnitude of x increases, $u(x,t)$ approaches a constant value, i.e. amplitude of wave becomes constant.

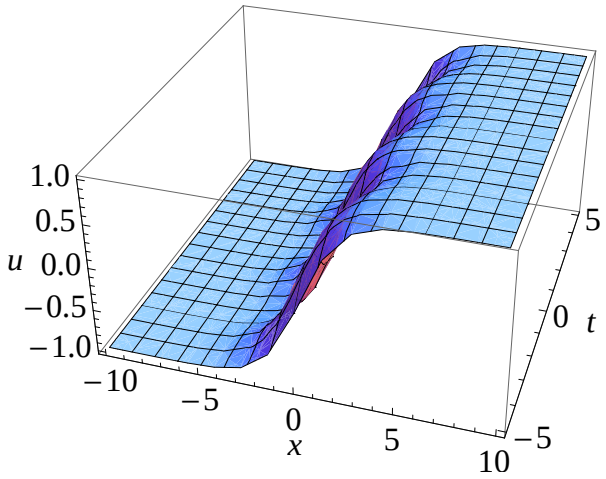

Figure 4.1: Amplitude profile of $u(x,t)$, Eq. (4.28) for values mentioned in the text.

If it is assumed that $v(t)$ is also a constant, then the solution for Eq. (4.22) reads

$$u(\xi) = -\sqrt{\frac{\alpha}{\beta}}\tanh\left(\sqrt{\frac{\alpha}{2D}}(x - vt)\right), \tag{4.29}$$

which is same as obtained by Kumar *et al.* [33].

Case (b): v, α *and* β, *all are time dependent*

In order to solve Eq. (4.22) for the case when v, α and β all are time dependent, following the same procedure as in last section, one will get the same set of equations as Eq. (4.25) with $v(t)$, $\alpha(t)$ and $\beta(t)$. Solving these equations consistently, the following relations can be found,

$$\begin{aligned} b(t) &= \mathrm{e}^{\left(\int \alpha(t)\ dt - 2p^2Dk^2t\right)}, \\ a(t) &= p\ b(t)\ , \quad \beta(t) = \frac{2Dk^2}{b^2(t)}, \\ \eta(t) &= \left(-3pDk^2t - k\int v(t)\ dt\right). \end{aligned} \tag{4.30}$$

The complete solution for $u(\xi)$, Eq. (4.17) for $m = 0$ and $n = 3$, comes out to be

$$u(\xi) = \frac{p}{2}\ \mathrm{e}^{\left(\int \alpha(t)\ dt - 2p^2Dk^2t\right)}\left[1 - \tanh\left(\frac{p}{2}\xi\right)\right]. \tag{4.31}$$

Here, $\beta(t)$ is fixed, but $v(t)$ and $\alpha(t)$ can be chosen arbitrary functions of time. From solution, it is clear that convection coefficient effects the velocity of wave and reaction coefficient effects the amplitude of wave exponentially. Amplitude profile of Eq. (4.31) is shown in Fig. 4.2, for $D = 1,\ p = 2,\ k = 1,\ \alpha(t) = \cos(t)$ and $v(t) = \tanh(t)$. Here, the amplitude of profile is varying exponentially due to inhomogeneous reaction coefficient.

(2) Exact solutions of Eq. (4.17) for $m = 1$ and $n = 3$

Case (a): *Only* v *is time dependent*

For this case, Eq. (4.17) reads

$$u_t + v(t)\ uu_x = Du_{xx} + \alpha u - \beta u^3. \tag{4.32}$$

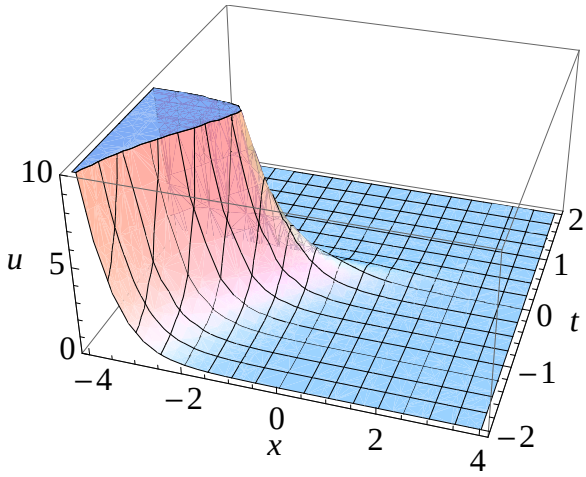

Figure 4.2: Amplitude profile of $u(x,t)$, Eq. (4.31) for values mentioned in the text.

Again, substituting Eqs. (4.23) and (4.24) in Eq. (4.32), and equating the coefficients of ϕ^i's $(i = 0, 1, 2, 3)$ to zero, the following set of equations can be found

$$\begin{aligned}
\phi^3 &: \; 2bDk^2 - \beta b^3 - b^2 kv = 0, \\
\phi^2 &: \; 3pbDk^2 - 3\beta ab^2 - pb^2 kv - abkv - b\eta_t = 0, \\
\phi^1 &: \; p^2 bDk^2 + \alpha b - 3\beta a^2 b - b_t - pb\eta_t - pabkv = 0, \\
\phi^0 &: \; a_t - \alpha a + \beta a^3 = 0.
\end{aligned} \tag{4.33}$$

These equations can be solved only for $\alpha \;\&\; \beta < 0$. Assume $\alpha = -\alpha_1$ and $\beta = -\beta_1$, such that $\alpha_1 \;\&\; \beta_1 > 0$, and solve these equations consistently, to obtain the following relations

$$\begin{aligned}
a(t) = p \;\; b(t) &= p\sqrt{\frac{\alpha_1}{p^2\beta_1 + \mathrm{e}^{2\alpha_1 t}}}, \\
v(t) &= \frac{2Dk}{b(t)} + \frac{\beta_1 b(t)}{k}, \\
\eta(t) &= -Dpk^2 t - \frac{1}{2p}\ln\left[p^2\beta_1 \mathrm{e}^{-2\alpha_1 t} + 1\right].
\end{aligned} \tag{4.34}$$

The solution for Eq. (4.32) using Eq. (4.23) and (4.27) becomes

$$u(\xi) = \frac{p}{2}\sqrt{\frac{\alpha_1}{p^2\beta_1 + \mathrm{e}^{2\alpha_1 t}}}\left[1 - \tanh\left(\frac{p}{2}\xi\right)\right]. \tag{4.35}$$

Typical profile of Eq. (4.35) is shown in Fig. 4.3, for $\alpha_1 = 1$, $\beta_1 = 1$, $D = 1$, $p = 1$ and $k = 1$. It is also a kink-type solitary wave solution, whose amplitude and velocity are changing with time due to time-dependent coefficient of convection term.

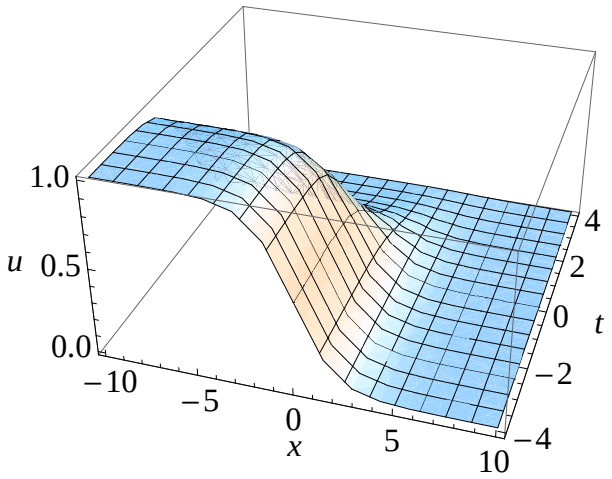

Figure 4.3: Amplitude profile of $u(x,t)$, Eq. (4.35) for values mentioned in the text.

Case (b): v, α *and* β, *all are time dependent*

In order to solve Eq. (4.32) for the case when v, α and β all are time dependent, we considered the same set of equations as Eq. (4.33) with $v(t)$, $\alpha(t)$ and $\beta(t)$. Solving these equations consistently one can obtain the following relations,

$$\begin{aligned} a(t) = p\ b(t) &= \frac{p}{\sqrt{p^2 + \mathrm{e}^{-2\int \alpha(t)\ dt}}}, \\ v(t) &= \frac{2Dk}{b(t)} - \frac{\beta(t)b(t)}{k}\ , \quad \beta(t) = \alpha(t), \\ \eta(t) &= -Dpk^2t - \frac{1}{2p}\ln\left[p^2\mathrm{e}^{2\int \alpha(t)\ dt} + 1\right]. \end{aligned} \tag{4.36}$$

The complete solution for $u(\xi)$, Eq. (4.17) for $m = 1$ and $n = 3$, reads

$$u(\xi) = \frac{p}{2\sqrt{p^2 + \mathrm{e}^{-2\int \alpha(t)\ dt}}} \left[1 - \tanh\left(\frac{p}{2}\xi\right)\right]. \tag{4.37}$$

Here, $v(t)$ is fixed but $\alpha(t)$ can be chosen arbitrarily which effects the both parameters, amplitude and velocity, of wave. Amplitude profile of Eq. (4.37) is shown in Figure 4.4, for $D = 1,\ p = 2,\ k = 1$ and $\alpha(t) = \mathrm{sech}(t)$.

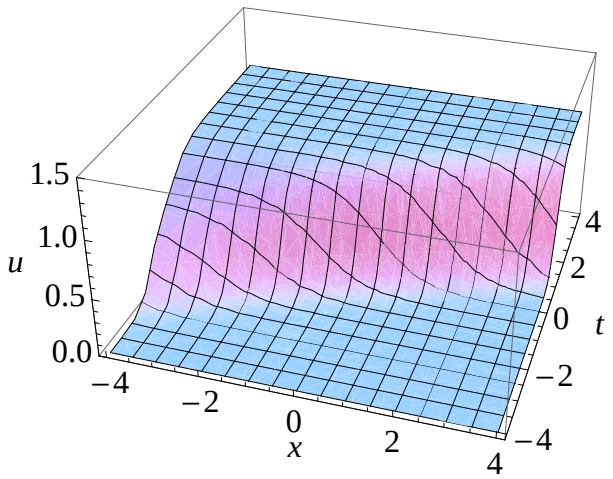

Figure 4.4: Amplitude profile of $u(x,t)$, Eq. (4.37) for values mentioned in the text.

(3) Exact solutions of Eq. (4.17) for $m = 1$ and $n = 2$

Case (a): *Only v is time dependent*

For this case, Eq. (4.17) reads

$$u_t + v(t)\ uu_x = Du_{xx} + \alpha u - \beta u^2. \tag{4.38}$$

Substituting Eqs. (4.23) and (4.24) in Eq. (4.38), and equating the coefficients of ϕ^i's $(i = 0, 1, 2, 3)$ to zero, a set of equations can be found as

$$\begin{aligned}
\phi^3 &: \quad b^2kv - 2bDk^2 = 0.\\
\phi^2 &: \quad \beta b^2 + abkv + pb^2kv - 3pbDk^2 + b\eta_t = 0,\\
\phi^1 &: \quad -\alpha b + 2\beta ab + pabkv - p^2bDk^2 + b_t + pb\eta_t = 0,\\
\phi^0 &: \quad -\alpha a + \beta a^2 + a_t = 0.
\end{aligned} \tag{4.39}$$

Solving these equations consistently, the various unknown parameters can be obtained as

$$\begin{aligned}
\beta = \alpha, \quad a(t) &= p\ b(t),\\
b(t) = \frac{1}{2p}\left[1 - \tanh\left(\frac{-\alpha t}{2}\right)\right] &= \frac{1}{p(1+e^{-\alpha t})},\\
v(t) = \frac{2Dk}{b(t)} &= 2pDk(1+e^{-\alpha t}),\\
\eta(t) = \int -(pDk^2 + \alpha\ b(t))\ dt &\\
= -\left(pDk^2 + \frac{\alpha}{2p}\right)\ t - \frac{1}{p}\ln\cosh\left(\frac{-\alpha t}{2}\right). &
\end{aligned} \tag{4.40}$$

Using Eqs. (4.23), (4.27) and (4.40), the solution for Eq. (4.38) will take the form as

$$u(\xi) = \frac{1}{4}\left(1 - \tanh\left(\frac{-\alpha t}{2}\right)\right)\left[1 - \tanh\left(\frac{p}{2}\xi\right)\right]. \tag{4.41}$$

Typical amplitude profile of Eq. (4.41) is shown in Figure 4.5, for $\alpha = 1,\ D = 1,\ p = 1$ and $k = 1$. It is a kink-type solitary wave solution, whose amplitude and velocity are changing with time due to time-dependent coefficient of convection term.

Case (b): v, α *and* β, *all are time dependent*

In order to solve Eq. (4.38) for the case when v, α and β all are time dependent, following the same procedure, the same set of equations can be found as Eq. (4.39) with time dependent coefficients. Solving these equations the unknown parameters

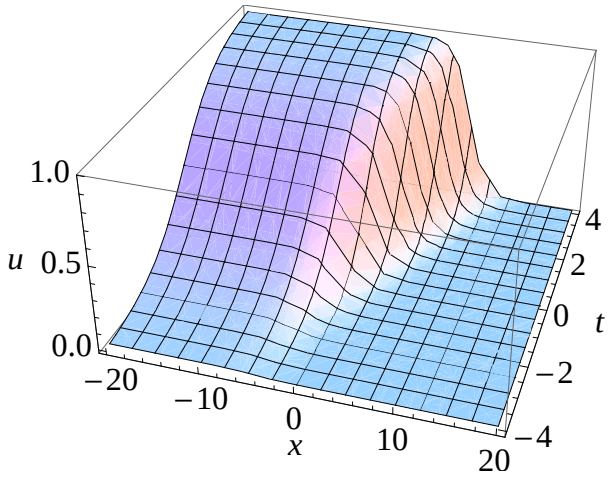

Figure 4.5: Amplitude profile of $u(x,t)$, Eq. (4.41) for values mentioned in the text.

are

$$\beta(t) = \alpha(t), \qquad a(t) = p\ b(t),$$
$$b(t) = \frac{1}{2p}\left[1 - \tanh\left(\frac{-\int \alpha(t)\ dt}{2}\right)\right] = \frac{1}{p(1+e^{-\int \alpha(t)\ dt})},$$
$$v(t) = \frac{2Dk}{b(t)} = 2pDk(1+e^{-\int \alpha(t)\ dt}),$$
$$\eta(t) = \int -(pDk^2 + \alpha(t)\ b(t))\ dt$$
$$= -pDk^2t - \frac{1}{2p}\int \alpha(t)\ dt - \frac{1}{p}\ln\cosh\left(-\frac{1}{2}\int \alpha(t)\ dt\right).$$

The complete solution for $u(\xi)$, Eq. (4.17) for $m = 1$ and $n = 2$, comes out to be

$$u(\xi) = \frac{1}{4}\left(1 - \tanh\left(\frac{-\int \alpha(t)\ dt}{2}\right)\right)\left[1 - \tanh\left(\frac{p}{2}\xi\right)\right]. \tag{4.42}$$

Here, $v(t)$ is fixed but $\alpha(t)$ can be chosen arbitrarily which effects the both parameters, amplitude and velocity, of wave. Typical amplitude profile of Eq. (4.42) is shown in Figure 4.6, for $p = 1,\ D = 1,\ k = 1,$ and $\alpha(t) = \cos(t)$.

Special case

If we assume Eq. (4.38) for the case when v, α and β all are constant, then by

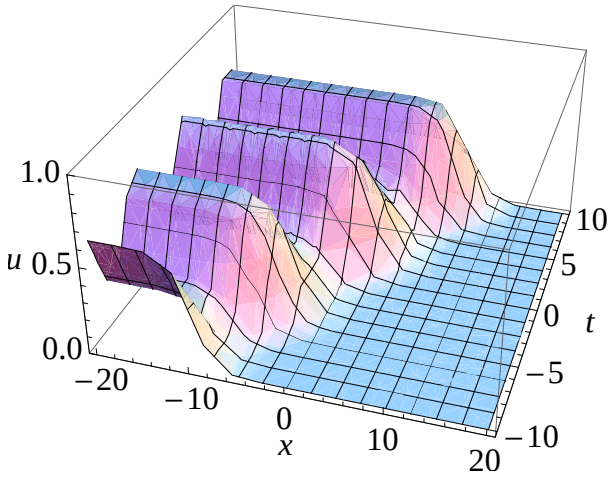

Figure 4.6: Amplitude profile of $u(x,t)$, Eq. (4.42) for values mentioned in the text.

following the same procedure, one can obtain the various parameters as

$$a = 1, \quad b = \frac{1}{p}, \quad v = 2pDk,$$
$$\eta(t) = -\left(pDk^2 + \frac{\alpha}{p}\right) t. \tag{4.43}$$

Hence, the solution for constant coefficient equation becomes

$$u(\xi) = \frac{1}{2}\left[1 - \tanh\left(\frac{p}{2}\xi\right)\right], \tag{4.44}$$

which is of same form as obtained by Chen *et al.* [16].

4.2.5 Conclusion

We have studied a prototype model for the reaction, diffusion and convection processes with inhomogeneous coefficients. Employing auxiliary equation method, the kink-type solitary wave solutions have been found for variable coefficient Burgers-Fisher and Newell-Whitehead-Segel (NWS) equation. It is observed that time dependent reaction and convection coefficients will effect the wave parameters, like amplitude and velocity. It is found that for linear convection term and cubic non-

linear reaction term, that is NWS equation for $m = 0$ and $n = 3$, the convection coefficient $v(t)$ and one of the reaction coefficient $\alpha(t)$ can be chosen arbitrary functions of time whereas other reaction coefficient $\beta(t)$ is fixed. Here, the convection coefficient effects the velocity of wave whereas reaction coefficient effects the amplitude of wave exponentially. For $m = 1$ and $n = 3$ case, only reaction term coefficient can be chosen arbitrarily which effects the both parameters of wave. For Burgers-Fisher equation, that is $m = 1$ and $n = 2$ case, again reaction term coefficient can be chosen arbitrarily. For constant coefficients, the results are same as the previous results. Hence, the variable coefficients help us to control the properties of solitary wave solutions in RD system. The variation of amplitude of waves has been shown for different functional form of the variable coefficients. The results obtained here may be useful for the one who is working on specific phenomena based on RD type equations. The approach applied in this work is general and can be employed in further works to obtain exact solutions for other types of nonlinear equations with variable coefficients.

4.3 Complex Ginzburg-Landau equation with ac-source

4.3.1 Introduction to CGLE

The complex Ginzburg-Landau equation (CGLE) is a well-known nonlinear equation in the field of nonlinear science. It can be used to describe various nonlinear physical and chemical phenomena, such as surface waves in viscous liquids [34], chemical waves [35], binary-fluid convection [36], dynamic phase transitions [37], optical fiber lasers [38, 39] and pattern forming systems [40]. The CGLE, in many versions, has been studied by various authors. The stationary Ginzburg-Landau equation was first given by Landau and Ginzburg in a work on superconductivity. The Ginzburg-Landau equation with real coefficients was derived by Newell and Whitehead in 1969 [17] for the study of Rayleigh-Bénard convection. The full CGLE was derived by

Stewartson and Stuart [41] in the context of plane Poiseuille flow and by DiPrima *et al.* [42] in the context of the destabilization of plane shear flow. Earlier this equation was known as 'amplitude equation' or 'modulation equation', but later it is recognized by the Ginzburg-Landau equation although they did not derive it in their paper.

As mentioned in previous chapters that the nonlinear Schrödinger equation (NLSE) describes the various phenomena in nonlinear optics and fluid dynamics. However, it is worth noting that NLSE does not include the nonlinear gain and spectral filtering (or diffusion). But, there are many physical phenomena where energy attenuation/dissipation is involved. These types of processes are described by the CGLE which is an extension of NLSE model, given as [43]

$$\frac{\partial H}{\partial t} = H + (1 + ic_1)\,\frac{\partial^2 H}{\partial x^2} - (1 + ic_3)\,|H|^2\,H, \tag{4.45}$$

where H is a complex function. The CGLE originates in physics in particular as a modulation (or amplitude) equation. This equation possesses a larger variety of solutions, including localized structures such as fronts, pulses, sources and sinks, periodic solutions and transition to chaos (for Refs. see [44]). An extensive mathematical studies on CGLE was presented in Refs. [40, 43].

4.3.2 Motivation and model equation

The cubic CGLE, given by Eq. (4.45), has been studied extensively for pulse solutions [45, 46]. But, a close inspection reveals that they are singular at some values of the parameters or unstable in general [see Ref. [44]]. But, these soliton-like solutions can be stabilized by adding quintic term to CGLE [44, 47]. Apart from it, these solutions can also be stabilized using driven CGLE either parametrically [48, 49] or by ac source [50]. The external feedback also helps in controlling the diffusion induced amplitude and phase turbulence (or spatiotemporal) in CGLE systems [51, 52, 53]. Recently, spiral waves in the CGLE with a time-dependent periodic external force has been studied [54]. Despite its simplicity, the forced CGLE, depending on several

factors, such as the spatial dimension, the mode of the frequency locking and the behavior of the corresponding unforced system, describes a large variety of phenomena [55, 56, 57, 58, 59, 60, 61]. Also, existence of steadily moving solitary pulses in CGLE which includes cubic-quintic nonlinearity and a conservative linear driving term has been studied [62]. Although, CGLE is a well studied dynamical system, the exact solutions of ac-driven CGLE are rarely appeared in the literature [52]. We are interested here in the modified CGLE [40, 51] with an ac driver, in the form of a travelling wave.

In this work, we have considered the CGLE driven by external force as [63]

$$\frac{\partial H}{\partial t} = (1 + ic_1)\,\frac{\partial^2 H}{\partial x^2} - (c_2 + ic_3)\,|H|^2\,H + \epsilon H + f(x,t), \tag{4.46}$$

where H is a complex function, c_1 is the dispersion coefficient, the coefficients c_2 and c_3 represent nonlinear effects in the system, ϵ is the linear gain coefficient and $f(x,t)$ represents external driver. We have solved the driven CGLE for the case when external force $f(x,t)$ is out of phase with the complex function H. It is interesting to note that the phase difference between them found to be depends on dispersion coefficient, as $\tan^{-1}(c_1)$.

4.3.3 Soliton-like solutions

The exact soliton solutions can be found for Eq. (4.46) by choosing the following ansatz, in which there is a phase difference between the solution and the external driver, as

$$H(x,t) = \rho(\xi)e^{i(\chi(\xi)-\omega t)} \tag{4.47}$$

and

$$f(x,t) = Fe^{i\phi}e^{i(\chi(\xi)-\omega t)}, \tag{4.48}$$

where $\xi = (x - vt)$, ϕ and F are real parameters. Here, ϕ represents the phase difference and F gives the amplitude of driven source.

Substituting Eqs. (4.47) and (4.48) in Eq. (4.46) and separating out the real

and imaginary parts of the equation, one arrives at the following coupled equations in ρ and χ,

$$-v\rho' = \rho'' - \rho\chi'^2 - c_1\rho\chi'' - 2c_1\rho'\chi' - c_2\rho^3 + \epsilon\rho + F_r \tag{4.49}$$

and

$$-v\rho\chi' - \omega\rho = \rho\chi'' + 2\rho'\chi' - c_1\rho\chi'^2 + c_1\rho'' - c_3\rho^3 + F_i, \tag{4.50}$$

where $F_r = F\cos\phi$, $F_i = F\sin\phi$ and prime refers to the differentiation w.r.t to ξ variable. These coupled equations can be solved consistently by assuming the ansatz $\chi'(\xi) = K$ (a constant). Using this ansatz, Eqs. (4.49) and (4.50) reduced to

$$\rho'' + (v - 2c_1K)\rho' + (\epsilon - K^2)\rho - c_2\rho^3 + F_r = 0 \tag{4.51}$$

and

$$\rho'' + \frac{2K}{c_1}\rho' + \frac{vK + \omega - c_1K^2}{c_1}\rho - \frac{c_3}{c_1}\rho^3 + \frac{F_i}{c_1} = 0. \tag{4.52}$$

Eqs. (4.51) and (4.52) can be mapped into a single equation

$$\rho'' + M\rho' + N\rho - P\rho^3 + Q = 0, \tag{4.53}$$

with the identification of

$$M \equiv \left(\frac{2K}{c_1} = v - 2c_1K\right) \tag{4.54}$$

$$N \equiv \left(\frac{vK + \omega - c_1K^2}{c_1} = \epsilon - K^2\right) \tag{4.55}$$

$$P \equiv \left(\frac{c_3}{c_1} = c_2\right) \tag{4.56}$$

$$Q \equiv \left(\frac{F_i}{c_1} = F_r\right). \tag{4.57}$$

Solving Eqs. (4.54) to (4.57), one can obtain the following constraint conditions as

$$v = \frac{2K}{c_1}(1 + {c_1}^2),\ \omega = c_1\epsilon - vK,\ c_3 = c_1c_2 \ \text{ and } \ F_i = c_1F_r. \tag{4.58}$$

For a particular choice of external phase and amplitude, given as $\phi = \tan^{-1}(c_1)$ and $F = F_r\sqrt{1 + {c_1}^2}$, one can solve Eq. (4.53) for two different cases as discussed below.

***Case I*: $K = 0$, Fractional transform solitons**

Under this parametric condition the velocity v becomes zero and Eq. (4.53) reduces to

$$\rho_{xx} + N\rho - P\rho^3 + Q = 0. \tag{4.59}$$

This equation can be solved for standing wave solutions by using a fractional transformation [64]

$$\rho(x) = \frac{A + By^2(x)}{1 + Dy^2(x)}, \tag{4.60}$$

which maps the solutions of Eq.(4.59) to the elliptic equation $y'' \pm ay \pm by^3 = 0$, provided $AD \neq B$. For explicitness, we consider the case where $y = \mathrm{cn}(x, m)$ with m as modulus parameter. Then upon substitution of Eq. (4.60) into Eq. (4.57) and equating the coefficients of equal powers of $\mathrm{cn}(x, m)$ will yield the following consistency conditions:

$$NA - 2(AD - B)(1 - m) - PA^3 + Q = 0, \tag{4.61}$$

$$2NAD + NB + 6(AD - B)D(1 - m) - 4(AD - B)(2m - 1) - 3PA^2B + 3QD = 0, \tag{4.62}$$

$$NAD^2 + 2NBD + 4(AD - B)D(2m - 1) + 6(AD - B)m - 3PAB^2 + 3QD^2 = 0, \tag{4.63}$$

$$NBD^2 - 2(AD - B)Dm - PB^3 + QD^3 = 0. \tag{4.64}$$

For different values of m, one can obtain different types of standing wave solutions.

(i) Trigonometric solution : For $m = 0$ and $A = 0$, Eq. (4.59) admits the

non-singular periodic solution of the following type

$$\rho(x) = \frac{2Q}{N}\left(\frac{\cos^2 x}{1-\frac{2}{3}\cos^2 x}\right), \tag{4.65}$$

where $N = -4$ and $Q^2 = (-128/27P)$. Rewriting N, P and Q in terms of original parameters of Eq. (4.46), one can find that the solution is consistent only for $c_2 < 0$, which corresponds to two cases: either (a) $c_1 > 0$ and $c_3 < 0$, or (b) $c_1 < 0$ and $c_3 > 0$. The complete solution for CGLE driven by external source with the phase difference of $\phi = \tan^{-1}(c_1)$, reads

$$H(x,t) = \frac{2F_r}{\epsilon}\left(\frac{\cos^2 x}{1-\frac{2}{3}\cos^2 x}\right) e^{-i\omega t}, \tag{4.66}$$

for $\epsilon = -4$ and ${F_r}^2 = -128/(27c_2)$. The amplitude and intensity profiles is shown in Fig. 4.7 for $c_1 = 2,\ c_2 = -1,\ c_3 = -2$ and $\epsilon = -4$. For these values of model parameters, the external driven source has amplitude and phase as $F = (640/27)^{1/2}$ and $\phi = \tan^{-1} 2$, respectively.

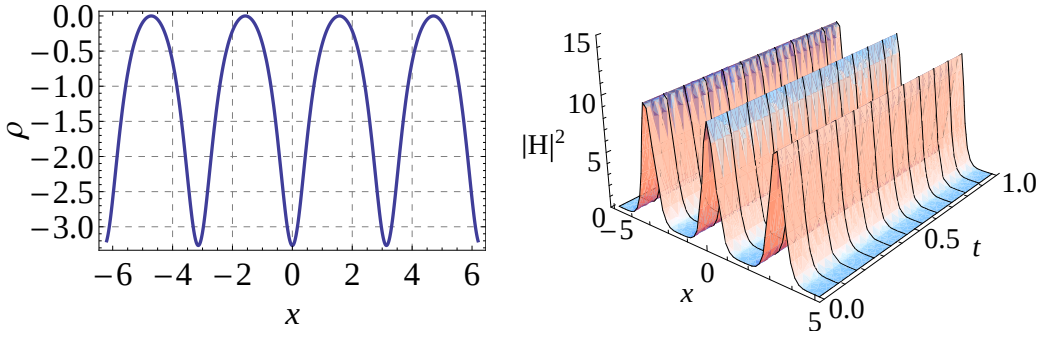

Figure 4.7: Amplitude and intensity profiles of periodic solution for $c_1 = 2,\ c_2 = -1,\ c_3 = -2$ and $\epsilon = -4$.

(ii) Hyperbolic solution : The general localized solution can be found for the case when the Jacobian elliptic modulus $m = 1$. The set of Eqs. (4.61) to (4.64) can be solved consistently for the unknown parameters A, B, D and for a particular

value of Q. The generic profile of the solution reads

$$\rho(x) = \frac{A + B\ \mathrm{sech}^2 x}{1 + D\ \mathrm{sech}^2 x}. \tag{4.67}$$

For this case, the complete solution of ac-driven CGLE can be written as

$$H(x,t) = \left(\frac{A + B\ \mathrm{sech}^2 x}{1 + D\ \mathrm{sech}^2 x}\right)\ e^{-i\omega t}. \tag{4.68}$$

We have worked out a physically interesting case, shown in Fig. 4.8, for the following parameters $c_1 = 1,\ c_2 = 2,\ c_3 = 2$ and $\epsilon = 1$. For these values of model parameters, the various unknown parameters are found out to be $A = 1.0476,\ B = 1.7707,\ D = 1.6901$ and $F_r = 1.2521$. The amplitude and phase of external driven source is given by, $F = 1.7707$ and $\phi = \tan^{-1} 1 = \pi/4$.

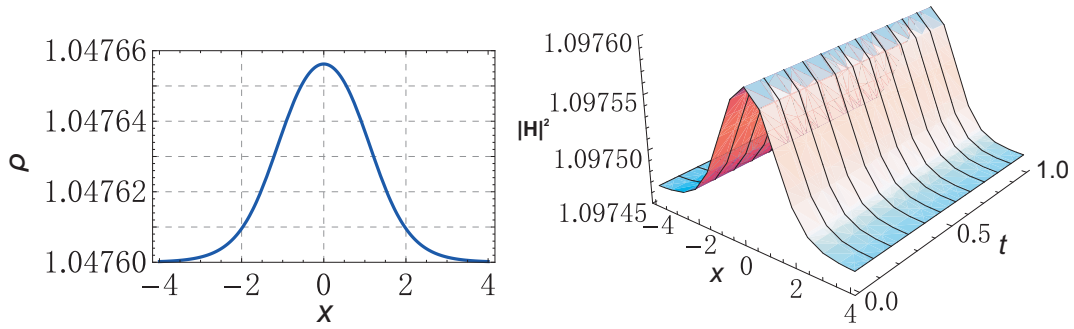

Figure 4.8: Amplitude and intensity profiles of bright soliton for $c_1 = 1,\ c_2 = 2,\ c_3 = 2$ and $\epsilon = 1$.

(iii) Pure cnoidal solutions : For $0 < m < 1$, Eq. (4.59) have different types of cnoidal solutions. We list these solutions here for some special cases. For $m = 5/8,\ A = 0$ and $D = 1$, the solution reads

$$\rho(x) = \frac{-14Q}{3N}\left(\frac{\mathrm{cn}^2(x,m)}{1 + \mathrm{cn}^2(x,m)}\right), \tag{4.69}$$

where $N = 7/2$ and $Q^2 = 9/(4P)$. Using this, the exact solution for Eq. (4.46) can be found as

$$H(x,t) = \frac{-14F_r}{3\epsilon}\left(\frac{\mathrm{cn}^2(x,m)}{1 + \mathrm{cn}^2(x,m)}\right)\ e^{-i\omega t}, \tag{4.70}$$

for $\epsilon = 7/2$ and ${F_r}^2 = 9/(4c_2)$.The amplitude and intensity profiles for this solution is shown in Fig. 4.9 for $c_1 = 2,\ c_2 = 1,\ c_3 = 2$ and $\epsilon = \frac{7}{2}$.

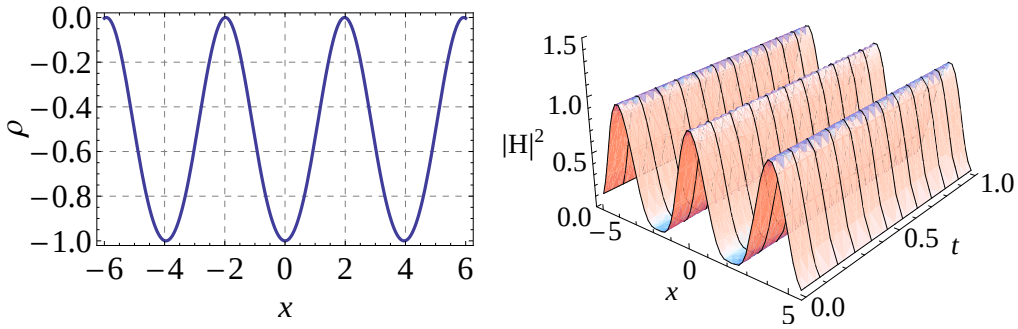

Figure 4.9: Amplitude and intensity profiles of cnoidal solution for $c_1 = 2,\ c_2 = 1,\ c_3 = 2$ and $\epsilon = \frac{7}{2}$.

For $m = 1/2$ and $A = 0$, we found that $N = 2\sqrt{3}$ and $Q^2 = 8/(3\sqrt{3}P)$, for which the solution of Eq. (4.59) reads

$$\rho(x) = \frac{-2\sqrt{3}Q}{N}\left(\frac{\mathrm{cn}^2(x,m)}{1+\frac{1}{\sqrt{3}}\,\mathrm{cn}^2(x,m)}\right). \tag{4.71}$$

Thus, the complete solution of Eq. (4.46) can be written as

$$H(x,t) = \frac{-2\sqrt{3}F_r}{\epsilon}\left(\frac{\mathrm{cn}^2(x,m)}{1+\frac{1}{\sqrt{3}}\,\mathrm{cn}^2(x,m)}\right)\ e^{-i\omega t}, \tag{4.72}$$

for $\epsilon = 2\sqrt{3}$ and ${F_r}^2 = 8/(3\sqrt{3}c_2)$.

***Case II*: $K \neq 0$, Kink-type solitons**

For this case ($v \neq 0$), an interesting kink-type solution can be obtained of Eq. (4.53), which is given by

$$\rho(\xi) = a - \sqrt{\frac{d}{b}}\tanh(\sqrt{bd}\xi), \tag{4.73}$$

where $a = -M/(3\sqrt{2}\sqrt{P})$, $b = \sqrt{P/2}$, $d = (6N - M^2)/6$ and $Q = a^3P - aN - dM$. Rewriting M, N, P and Q in terms of original parameters, the complete solution

reads

$$H(x,t) = -\left[\frac{\sqrt{2}K}{3c_1\sqrt{c_2}} + \left(\frac{2}{c_2}\right)^{1/4}\sqrt{\epsilon - K^2 - \frac{2K^2}{3{c_1}^2}}\ \tanh\left(\left(\frac{c_2}{2}\right)^{1/4}\sqrt{\epsilon - K^2 - \frac{2K^2}{3{c_1}^2}}\ \xi\right)\right] \times e^{i(K(x-vt)-\omega t)}, \tag{4.74}$$

for $F_r = \frac{4K^3}{3{c_1}^3}\left(1 - \frac{1}{9\sqrt{2c_2}}\right) - \frac{2K}{c_1}(\epsilon - K^2)\left(1 - \frac{1}{3\sqrt{2c_2}}\right)$. Fig. 4.10 depicts the amplitude and intensity profile of this kink solution, for $c_1 = 2,\ c_2 = 1,\ c_3 = 2,\ \epsilon = 1$ and $K = 1/2$. In this case, the amplitude and phase of external driven source is given by, $F = -0.597$ and $\phi = \tan^{-1} 2$.

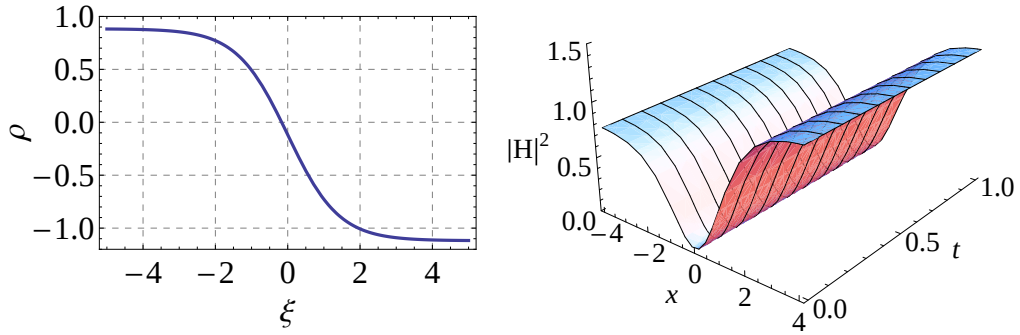

Figure 4.10: Amplitude and intensity profiles of kink-type soliton for $c_1 = 2,\ c_2 = 1,\ c_3 = 2,\ \epsilon = 1$ and $K = 1/2$.

Numerical stability of exact solutions

The stability of exact periodic and localized solutions, given by Eq. (4.66) and Eq. (4.68), has been studied numerically in the Ref. [63]. It has been done first by adding white noise and then by perturbing the solution for study of nonlinear stability. The nonlinear evolution of the trigonometric solution and soliton solution have been studied using semi-implicit Crank-Nicolson finite difference scheme, under small perturbation by directly simulating Eq. (4.46) with initial condition $H(x, t = 0) = H(x, t = 0)[1+w]e^{-i\phi t}$, where w is the perturbation . The numerical simulations indicated that these solutions are quite stable with perturbations $w = 0.2$ and $w = 0.5$.

4.3.4 Conclusion

In this work, the exact Lorentzian-type and kink-type soliton solutions has been reported of ac-driven complex Ginzburg-Landau equation. The periodic solutions has also been worked out for this model. The phase difference between the external driver and the solutions has been found to be depend on the dispersion coefficient c_1. Numerical simulations indicated that these solitons are quite stable against finite perturbations. Recently, Li *et al.* [65] studied the same model given by Eq. (4.46) using the method of dynamical systems, and analyze the dynamical behavior of the stationary solutions and their bifurcations depending on the parameters of systems. Owing to the exact nature of the solutions presented here, we hope that they serve as the seed solutions for further exploring rich structures including bifurcation and other spatiotemporal patterns prevalent in this inhomogeneous dynamical system.

Bibliography

[1] S Pamuk. Solution of the porous media equation by Adomian's decomposition method. *Physics Letters A*, 344(2):184–188, 2005.

[2] H Wilhelmsson. Simultaneous diffusion and reaction processes in plasma dynamics. *Physical Review A*, 38(3):1482, 1988.

[3] KE Yun-Quan and YU Jun. The first integral method to study a class of reaction-diffusion equations. *Communications in Theoretical Physics*, 43(4):597, 2005.

[4] JD Murray. *Mathematical biology I: an introduction*. springer, 2002.

[5] Z Krivá and K Mikula. An adaptive finite volume scheme for solving nonlinear diffusion equations in image processing. *Journal of Visual Communication and Image Representation*, 13(1):22–35, 2002.

[6] W Okrasiński, MI Parra, and F Cuadros. Modeling evaporation using a nonlinear diffusion equation. *Journal of Mathematical Chemistry*, 30(2):195–202, 2001.

[7] M Bode, AW Liehr, CP Schenk, and HG Purwins. Interaction of dissipative solitons: particle-like behaviour of localized structures in a three-component reaction-diffusion system. *Physica D: Nonlinear Phenomena*, 161(1):45–66, 2002.

[8] G Lv and M Wang. Nonlinear stability of traveling wave fronts for delayed reaction diffusion systems. *Nonlinear Analysis: Real World Applications*, 13(4):1854–1865, 2012.

[9] RA Fisher. The wave of advance of advantageous genes. *Annals of Eugenics*, 7(4):355–369, 1937.

[10] RD Benguria and MC Depassier. On the transition from pulled to pushed monotonic fronts of the extended Fisher–Kolmogorov equation. *Physica A: Statistical Mechanics and its Applications*, 356(1):61–65, 2005.

[11] LA Peletier and WC Troy. Spatial patterns described by the extended Fisher–Kolmogorov equation: periodic solutions. *SIAM Journal on Mathematical Analysis*, 28(6):1317–1353, 1997.

[12] DR Nelson and NM Shnerb. Non-Hermitian localization and population biology. *Physical Review E*, 58(2):1383, 1998.

[13] RD Benguria, MC Depassier, and V Méndez. Minimal speed of fronts of reaction-convection-diffusion equations. *Physical Review E*, 69(3):031106, 2004.

[14] L Debnath. *Nonlinear partial differential equations for scientists and engineers*. Springer, 2012.

[15] JM Burgers. A mathematical model illustrating the theory of turbulence. *Advances in Applied Mechanics*, 1:171–199, 1948.

[16] H Chen and H Zhang. New multiple soliton solutions to the general Burgers–Fisher equation and the Kuramoto–Sivashinsky equation. *Chaos Solitons and Fractals*, 19(1):71–76, 2004.

[17] AC Newell and JA Whitehead. Finite bandwidth, finite amplitude convection. *Journal of Fluid Mechanics*, 38(02):279–303, 1969.

[18] K Staliūnas and M Tlidi. Hyperbolic transverse patterns in nonlinear optical resonators. *Physical Review Letters*, 94(13):133902, 2005.

[19] C Sophocleous. Further transformation properties of generalised inhomogeneous nonlinear diffusion equations with variable coefficients. *Physica A: Statistical Mechanics and its Applications*, 345(3):457–471, 2005.

[20] S Lai, X Lv, and Y Wu. Explicit solutions of two nonlinear dispersive equations with variable coefficients. *Physics Letters A*, 372(47):7001–7006, 2008.

[21] CB Kui, MS Qiang, and WB Hong. Exact solutions of generalized Burgers–Fisher equation with variable coefficients. *Communications in Theoretical Physics*, 53(3):443, 2010.

[22] KI Nakamura, H Matano, D Hilhorst, and R Schätzle. Singular limit of a reaction-diffusion equation with a spatially inhomogeneous reaction term. *Journal of Statistical Physics*, 95(5-6):1165–1185, 1999.

[23] J Norbury and LC Yeh. Inhomogeneous fast reaction, slow diffusion and weighted curve shortening. *Nonlinearity*, 14(4):849, 2001.

[24] MG Neubert, M Kot, and MA Lewis. Invasion speeds in fluctuating environments. *Proceedings of the Royal Society of London, Series B: Biological Sciences*, 267(1453):1603–1610, 2000.

[25] J Fort and V Méndez. Wavefronts in time-delayed reaction-diffusion systems. Theory and comparison to experiment. *Reports on Progress in Physics*, 65(6):895, 2002.

[26] Sirendaoreji and J Sun. Auxiliary equation method for solving nonlinear partial differential equations. *Physics Letters A*, 309(5-6):387–396, 2003.

[27] R Kumar, RS Kaushal, and A Prasad. Soliton-like solutions of certain types of nonlinear diffusion–reaction equations with variable coefficient. *Physics Letters A*, 372(11):1862–1866, 2008.

[28] A Bekir, E Aksoy, and Ö Güner. Bright and dark soliton solutions for variable-coefficient diffusion–reaction and modified Korteweg–de Vries equations. *Physica Scripta*, 85(3):035009, 2012.

[29] A Goyal, Alka, R Gupta, and CN Kumar. Solitary wave solutions for Burgers-Fisher type equations with variable coefficients. *World Academy of Science Engineering and Technology*, 60:1742, 2011.

[30] DM Greenberger. Some remarks on the extended Galilean transformation. *American Journal of Physics*, 47:35–38, 1979.

[31] E Yomba. Construction of new soliton-like solutions for the $(2+1)$ dimensional KdV equation with variable coefficients. *Chaos Solitons and Fractals*, 21(1):75–79, 2004.

[32] A Bekir and E Aksoy. Exact solutions of nonlinear evolution equations with variable coefficients using exp-function method. *Applied Mathematics and Computation*, 217(1):430–436, 2010.

[33] R Kumar, RS Kaushal, and A Prasad. Some new solitary and travelling wave solutions of certain nonlinear diffusion–reaction equations using auxiliary equation method. *Physics Letters A*, 372(19):3395–3399, 2008.

[34] W Zhang and J Vinals. Secondary instabilities and spatiotemporal chaos in parametric surface waves. *Physical Review Letters*, 74(5):690, 1995.

[35] A Bhattacharyay. A theory for one-dimensional asynchronous chemical waves. *Journal of Physics A: Mathematical and Theoretical*, 40(13):3721, 2007.

[36] HU Voss, P Kolodner, M Abel, and J Kurths. Amplitude equations from spatiotemporal binary-fluid convection data. *Physical Review Letters*, 83(17):3422, 1999.

[37] R Graham. *Fluctuations, instabilities and phase transitions, edited by T. Riste.* Springer, Berlin, 1975.

[38] Ph Grelu, F Belhache, F Gutty, and JM Soto-Crespo. Phase-locked soliton pairs in a stretched-pulse fiber laser. *Optics Letters*, 27(11):966–968, 2002.

[39] DY Tang, B Zhao, LM Zhao, and HY Tam. Soliton interaction in a fiber ring laser. *Physical Review E*, 72(1):016616, 2005.

[40] MC Cross and PC Hohenberg. Pattern formation outside of equilibrium. *Reviews of Modern Physics*, 65(3):851, 1993.

[41] K Stewartson and JT Stuart. A non-linear instability theory for a wave system in plane Poiseuille flow. *Journal of Fluid Mechanics*, 48(03):529–545, 1971.

[42] RC DiPrima, W Eckhaus, and LA Segel. Non-linear wave-number interaction in near-critical two-dimensional flows. *Journal of Fluid Mechanics*, 49(04):705–744, 1971.

[43] IS Aranson and L Kramer. The world of the complex Ginzburg-Landau equation. *Reviews of Modern Physics*, 74(1):99, 2002.

[44] N Akhmediev and VV Afanasjev. Novel arbitrary-amplitude soliton solutions of the cubic-quintic complex Ginzburg-Landau equation. *Physical Review Letters*, 75:2320–2323, 1995.

[45] NR Pereira and Lennart Stenflo. Nonlinear Schrödinger equation including growth and damping. *Physics of Fluids*, 20:1733, 1977.

[46] R Conte and M Musette. Linearity inside nonlinearity: exact solutions to the complex Ginzburg-Landau equation. *Physica D: Nonlinear Phenomena*, 69(1):1–17, 1993.

[47] NN Akhmediev, VV Afanasjev, and JM Soto-Crespo. Singularities and special soliton solutions of the cubic-quintic complex Ginzburg-Landau equation. *Physical Review E*, 53(1):1190, 1996.

[48] IV Barashenkov, S Cross, and BA Malomed. Multistable pulselike solutions in a parametrically driven Ginzburg-Landau equation. *Physical Review E*, 68(5):056605, 2003.

[49] YB Gaididei and PL Christiansen. Ising and Bloch domain walls in a two-dimensional parametrically driven Ginzburg-Landau equation model with nonlinearity management. *Physical Review E*, 78(2):026610, 2008.

[50] H Leblond, A Niang, F Amrani, M Salhi, and F Sanchez. Motion of solitons of the complex Ginzburg-Landau equation: The effect of an external frequency-shifted source. *Physical Review A*, 88(3):033809, 2013.

[51] D Battogtokh and A Mikhailov. Controlling turbulence in the complex Ginzburg-Landau equation. *Physica D: Nonlinear Phenomena*, 90(1):84–95, 1996.

[52] TS Raju and K Porsezian. On solitary wave solutions of ac-driven complex Ginzburg–Landau equation. *Journal of Physics A: Mathematical and General*, 39(8):1853, 2006.

[53] JBG Tafo, L Nana, and TC Kofane. Time-delay autosynchronization control of defect turbulence in the cubic-quintic complex Ginzburg-Landau equation. *Physical Review E*, 88(3):32911, 2013.

[54] S Zhang, B Hu, and H Zhang. Analytical approach to the drift of the tips of spiral waves in the complex Ginzburg-Landau equation. *Physical Review E*, 67(1):016214, 2003.

[55] P Coullet, J Lega, B Houchmanzadeh, and J Lajzerowicz. Breaking chirality in nonequilibrium systems. *Physical Review Letters*, 65:1352–1355, 1990.

[56] P Coullet and K Emilsson. Strong resonances of spatially distributed oscillators: a laboratory to study patterns and defects. *Physica D: Nonlinear Phenomena*, 61(1):119–131, 1992.

[57] C Elphick, A Hagberg, and E Meron. Phase front instability in periodically forced oscillatory systems. *Physical Review Letters*, 80(22):5007, 1998.

[58] C Elphick, A Hagberg, and E Meron. Multiphase patterns in periodically forced oscillatory systems. *Physical Review E*, 59(5):5285, 1999.

[59] H Chaté, A Pikovsky, and O Rudzick. Forcing oscillatory media: phase kinks vs. synchronization. *Physica D: Nonlinear Phenomena*, 131(1):17–30, 1999.

[60] AL Lin, A Hagberg, A Ardelea, M Bertram, HL Swinney, and E Meron. Four-phase patterns in forced oscillatory systems. *Physical Review E*, 62(3):3790, 2000.

[61] HK Park. Frequency locking in spatially extended systems. *Physical Review Letters*, 86(6):1130, 2001.

[62] BB Baizakov, G Filatrella, and BA Malomed. Moving and colliding pulses in the subcritical Ginzburg-Landau model with a standing-wave drive. *Physical Review E*, 75(3):036604, 2007.

[63] A Goyal, Alka, TS Raju, and CN Kumar. Lorentzian-type soliton solutions of ac-driven complex Ginzburg-Landau equation. *Applied Mathematics and Computation*, 218(24):11931–11937, 2012.

[64] VM Vyas, TS Raju, CN Kumar, and PK Panigrahi. Soliton solutions of driven nonlinear Schrödinger equation. *Journal of Physics A: Mathematical and General*, 39(29):9151, 2006.

[65] J Li and J Shi. Bifurcations and exact solutions of ac-driven complex Ginzburg–Landau equation. *Applied Mathematics and Computation*, 221:102–110, 2013.

Chapter 5

Summary and conclusions

In this thesis, we have studied the inhomogeneous NLEEs of physical interest and obtained solitary wave or soliton-like solutions for them. The physical systems modeled by constant coefficient NLEEs tend to be very highly idealized. There are various factors, like dissipation, environmental fluctuations, spatial modulations etc., which causes deviation from the actual system. Therefore, the NLEEs with variable coefficients are supposed to be more realistic than their constant-coefficient counterparts in describing a large variety of nonlinear physical systems.

In Chapter 2, we have considered the wave propagation in tapered graded-index waveguide and presented a large family of self-similar waves by tailoring the tapering profile. It has been accomplished by first reducing the GNLSE, governing the wave propagation through the graded-index nonlinear waveguide, into integrable homogeneous NLSE, using similarity transformation, with the condition that the width function satisfies the second order differential equation. Second, a close inspection reveals that the mathematical structure of this equation being similar to linear Schrödinger equation of quantum mechanics which enables one to analytically identify a large manifold of allowed tapering profiles with compatible gain function, using isospectral Hamiltonian approach. These tapering profiles are governed by a free Riccati parameter which provides a control parameter for tuning the amplitude and width of self-similar waves. It is realized that modulation of the

tapering through the Riccati parameter imposes significant effects on the intensity of waves and thus paving the way for experimental realization of highly energetic pulses for practical applications. This analysis has been done for the sech^2-type tapering profile in the presence of only cubic nonlinearity and also for cubic-quintic nonlinearity. We have shown the existence of Riccati generalized bright and dark similaritons, self-similar Akhmediev breathers and self-similar rogue waves in cubic nonlinear medium, and double-kink dark similaritons and Lorentzian-type bright similaritons in cubic-quintic nonlinear medium. The generalized intensity profiles for the similaritons in latter case is found to undergo more rapid self-compression with small values of Riccati parameter as compared to the similaritons in a cubic nonlinear medium.

In Chapter 3, it is demonstrated that localized gain induces chirped double-kink, fractional-transform, bell and kink-type solitons in a nonlinear optical medium in the presence of two-photon absorption (TPA). The parameter domain is delineated in which these optical solitons exist. Interestingly, the width of double-kink solitons and their corresponding chirp can be controlled by modulating the gain function. For all solutions, nonlinear chirp is found to be directly proportional to the intensity of the wave. We have further investigated the variation of gain with TPA coefficient and found that the gain is transversally localized and its amplitude is directly proportional to the value of TPA coefficient. We hope that these chirped optical solitons supported by localized gain will be useful for pulse compression or amplification in various nonlinear optical processes accompanied by TPA.

Chapter 4 is divided into two parts. In first part, we have studied the nonlinear reaction diffusion (NLRD) type equations with variable coefficients and obtained propagating kink-type solitary wave solutions by using the auxiliary equation method. It is found that variable coefficients have significant effect on the amplitude and velocity of propagating kink solutions. In second part, we have investigated the dynamics of the complex Ginzburg-Landau equation (CGLE) in the presence of ac-source. It is a well-known nonlinear equation in the field of nonlinear science, which describes various nonlinear physical and chemical phenomena. The exact Lorentzian-type

and kink-type soliton solutions has been found for this model. We have solved the driven CGLE for the case when external force is out of phase with the complex field. Owing to the exact nature of the solutions presented here, it may be useful as the seed solutions for further exploring rich structures including bifurcation and other spatiotemporal patterns prevalent in this inhomogeneous dynamical system.

Apart from it, we studied the wave dynamics in other nonlinear physical systems, such as Bose-Einstein condensates (BECs) and negative index materials (NIMs). There is a considerable interest to study the dynamics of BECs in the presence of time-varying parameters, such as nonlinearity, gain or loss, and oscillator frequency. The nonlinearity being determined by the s-wave scattering length of interatomic collisions which can be tuned experimentally by utilizing the external magnetic or low-loss optical Feshbach-resonance techniques. Using the isospectral Hamiltonian approach, discussed in Chapter 2, we construct a family of self-similar waves, related through a free parameter, in quasi one-dimension Gross-Pitaevskii equation with time-varying parameters. This approach enables us to control the dynamics of dark and bright similaritons, and first- and second- order self-similar rogue waves in Bose-Einstein condensate through the modulation of time dependent trapping potential [Panigrahi *et al.*, Eur. Phys. J. Special Topics 222 (2013) 655]. NIMs are designed to have exotic and unique properties that cannot be obtained with naturally occurring materials and thus offer entirely new prospects for manipulating light. Recently, much of work has been done on the propagation of electromagnetic waves in NIMs because of the recent experimental realization of NIMs in infrared and optical frequency. We present a detailed analysis for the existence of dark and bright solitary waves for generalized nonlinear Schrödinger equation (GNLSE) model for competing cubicquintic and higher-order nonlinearities with dispersive permittivity and permeability in NIMs [Sharma *et al.*, J. Mod. Opt. 60 (2013) 836]. The evolution of dark solitary waves is shown for a specific range of normalized frequency while the existence of bright solitary waves are possible under some conditions on model parameters which can be achieved through the structural changes in negative index materials. We further explored the fractional-transform solutions, containing

periodic, hyperbolic and cnoidal solitary wave solutions for GNLSE, in the absence of quintic and nonlinear dispersion terms. Parameter domains were delineated in which these ultrashort optical pulses exist in negative-index materials.

The work described in this thesis has led to some important new results in the field of nonlinear optics regarding generalized self-similar waves in tapered graded-index waveguides and chirped optical solitons in the presence of two-photon absorption. These solutions may be useful in communication networks and other optical processes. The exact solutions for inhomogeneous NLRD and CGLE models will be useful to understand the dynamics of various nonlinear physical phenomena.

List of publications

Papers in refereed journals

1. R. Gupta, **A. Goyal**, T. S. Raju and C.N. Kumar, Symbiotic multimode spatial similaritons and rogons in inhomogeneously coupled optical fibers, ***Journal of Modern Optics***, DOI: 10.1080/09500340.2013.842004 (2013).

2. **A. Goyal**, R. Gupta, C. N. Kumar, T. S. Raju and P. K. Panigrahi, Controlling optical similaritons in a graded-index nonlinear waveguide by tailoring of the tapering profile, ***Optics Communications*** 300 (2013) 236.

3. V. K. Sharma, **A. Goyal**, T. S. Raju and C. N. Kumar, Periodic and solitary wave solutions for ultrashort pulses in negative-index materials, ***Journal of Modern Optics*** 60 (2013) 836.

4. **A. Goyal**, R. Gupta, S. Loomba and C. N. Kumar, Riccati parameterized self-similar waves in tapered graded-index waveguides, ***Physics Letters A*** 376 (2012) 3454.

5. C. N. Kumar, R. Gupta, **A. Goyal**, S. Loomba, T. S. Raju and P. K. Panigrahi, Controlled giant rogue waves in nonlinear fiber optics, ***Physical Review A*** 86 (2012) 025802.

6. **A. Goyal**, Alka, T. S. Raju and C. N. Kumar, Lorentzian-type soliton solutions of ac-driven complex Ginzburg-Landau equation, ***Applied Mathematics and Computation*** 218 (2012) 11931.

7. **A. Goyal**, Alka, R. Gupta and C. N. Kumar, Solitary wave solutions for Burgers-Fisher type equations with variable coefficients, ***World Academy of Science Engineering and Technology*** 60 (2011) 1742.

8. W. Alka, **A. Goyal** and C. N. Kumar, Nonlinear dynamics of DNA - Riccati generalized solitary wave solutions, ***Physics Letters A*** 375 (2011) 480.

9. Alka, **A. Goyal**, R. Gupta, C. N. Kumar and T. S. Raju, Chirped femtosecond solitons and double-kink solitons in the cubic-quintic nonlinear Schrödinger equation with self-steepening and self-frequency shift, ***Physical Review A*** 84 (2011) 063830.

10. **A. Goyal**, V. K. Sharma, T. S. Raju and C. N. Kumar, Chirped double-kink and fractional-transform solitons in an optical gain medium with two-photon absorption, Manuscript submitted to ***Journal of Modern Optics***, 2013.

Conference papers in refereed journals

1. P. K. Panigrahi, R. Gupta, **A. Goyal** and C. N. Kumar, Riccati generalization of self-similar solutions of nonautonomous Gross-Pitaevskii equation, ***European Physical Journal Special Topics*** 222 (2013) 655.

2. V. K. Sharma, **A. Goyal**, C. N. Kumar and J. Goswamy, Travelling wave solutions in negative index materials in the presence of external source, ***AIP Conference Proceedings*** 1536 (2013) 717.

3. **A. Goyal**, V. K. Sharma and C. N. Kumar, Optical solitons supported by localized gain in the presence of two-photon absorption, International Conference on Fiber Optics and Photonics, ***OSA Technical Digest*** (online) (Optical Society of America, 2012).

Papers in conferences and workshops

1. **A. Goyal** and C. N. Kumar, Double-kink and Lorentzian-type similaritons in graded-index nonlinear waveguide with cubic-quintic nonlinearity, ***International Workshop on Singularities and Topological Structures of Light***, ICTP, Trieste, Italy, July 8-12, 2013

2. **A. Goyal**, H. Kaur and C. N. Kumar, Controlling optical rogue waves in tapered graded-index waveguides, 7^{th} ***Chandigarh Science Congress***, Panjab University, March 01-03, 2013.

3. **A. Goyal** and C. N. Kumar, Chirped bright and dark solitary wave solutions in nonlinear negative index materials, ***Dynamic Days Asia Pacific*** 7 **-** ***The*** 7^{th} ***International Conference on Nonlinear Science***, Academia Sinica, Taipei, Taiwan, Aug. 05-09, 2012.

4. **A. Goyal**, T. S. Raju and C. N. Kumar, Soliton solutions of complex Ginzburg-Landau equation driven by external force, 7^{th} ***National Conference on Nonlinear Systems and Dynamics***, IISER Pune, July 12-15, 2012.

5. **A. Goyal**, V. Sharma, J. Goswamy and C. N. Kumar, Soliton-like solutions for higher order nonlinear Schrödinger equation, 6^{th} ***Chandigarh Science Congress***, Panjab University, Feb. 26-28, 2012.

6. **A. Goyal**, Alka and C. N. Kumar, Dynamics of a nonlinear model for DNA, 5^{th} ***Chandigarh Science Congress***, Panjab University, Feb. 26-28, 2011.

7. **A. Goyal**, Alka and C. N. Kumar, Solitary wave solutions of nonlinear reaction-diffusion equations with variable coefficients, 6^{th} ***National Conference on Nonlinear Systems and Dynamics***, Bharathidasan University, Jan. 27-30, 2011.

8. **A. Goyal**, Alka and C. N. Kumar, Nonlinear dynamics of elastic roads and application to DNA, 55^{th} ***Congress of Indian Society of Theoretical and Applied Mechanics***, NIT Hamirpur, Dec. 18-21, 2010.

9. **A. Goyal**, S. Loomba and C. N. Kumar, Solutions of sine-Gordon-type equations using algebraic method, 4^{th} ***Chandigarh Science Congress***, Panjab University, March 19-20, 2010.

Selected Reprints